Towards Numerical Hydromechanics Analysis of an Arbitrary Shape Floating Body in Ice-Infested Waters

Hendrikus Yun Fredo Ferdian

MSc Offshore & Dredging Engineering
Bottom Founded Structures, Arctic & Wind

TU Delft

Towards Numerical Hydromechanics Analysis of an Arbitrary Shape Floating Body in Ice-Infested Waters

by

Hendrikus Yun Fredo Ferdian

to obtain the degree of Master of Science
at the Delft University of Technology,
to be defended publicly on Wednesday October 18, 2017 at 14:00 PM.

Student number:	4507312	
Project duration:	November 14, 2016 – October 18, 2017	
Thesis committee:	Prof. Dr. A. V. Metrikine,	TU Delft, Chairman Committee
	Ir. C. Keijdener,	TU Delft, Supervisor
	Dr. Ir. H. J. de Koning Gans	TU Delft, Supervisor

This thesis is confidential and cannot be made public until October 11, 2017.

TU Delft

Abstract

In the last couple of decades, Arctic Engineering has become a topic of interest. There are still plenty rooms of research to understand the unique characteristic of sea ice, especially in relation to offshore engineering. This includes the most fundamental problem in floating body motion analysis: the radiation-diffraction problem. A powerful mathematical concept, - so called Greens Function – is one of the favourable tools to be used for solving this mathematical problem. This is because the radiation-diffraction problem can be formulated as a boundary value problem expressed by partial differential equations. Although the application is already quite advanced for the open water case, the same cannot be said for the vessel operating in ice infested waters. The integral solution of 3D Greens Function for ice-infested waters which has not been studied before, was derived in this thesis. The open water case is also studied to gain more insight in the implementation of an arbitrary floating body thoroughly. As a closure, interpretation about the difference between open and ice-infested waters is discussed.

For Greens Function in the open water case, numerical evaluation of the principal value integral is not straightforward due to the hyperbolic term inside the integrand. This term makes the integrand exceed the limit of floating point number (in MATLAB) and cannot be evaluated into infinity. On the other hand, a numerical integration is quite time consuming (whereas the analytical solution, as far as the writer's concern, is not found yet). A well-known alternative form of the solution which formulated as an infinite series might improve the computation speed. The rate of convergence depends solely on the ratio of horizontal distance between source and field point (R) and water depth (H). Another numerical issue arises in the deep water case. A finite water depth causes a catastrophic cancellation, both for the integral and the infinite series solution, due to the extremely small difference of the wave number between deep water and infinite water depth. This is where the infinite depth solution needs to be used.

In numerical implementation, an influence function at a panel can be approximated by multiplying the potential with panel's surface area. Due to the singularity of the Rankine source term in the integral or the modified Bessel function in the series, this approach fails and the solution need to be integrated over the panel. Although the analytical solution is available, a numerical approach is chosen to simplify the problem. The surface integration procedure can be done by transforming the global arbitrary panel orientation into the local element coordinate system, and subsequently, perform a bilinear mapping to reshape the quadrilateral panel into the desired rectangular panel. This transformation procedure is needed since MATLAB is only capable to handle double numerical integration of a function bounded between four lines perpendicularly each other. This encloses the whole challenge that needs to be addressed and might be re-occur in the ice-infested waters as well.

From the derivation of the Greens Function for ice-infested waters, it is shown that the hyperbolic term inside the integrand is present. This discloses that the obtained solutions cannot be used instantaneously. Another effort to rewrite them in the exponential term might be useful. Moreover, the radiation condition is not satisfied yet in this thesis. However, the suggested approach of the derivation by introducing an imaginary line to represent the source depth location avoids the use of a singular term. Generally speaking, this thesis initiates a promising foundation for further research in the hydromechanics analysis of sea ice.

Hendrikus Yun Fredo Ferdian
Delft, October 2017

Contents

List of Figures

List of Symbols

List of symbols below generally apply for all of the expression present except for certain specified case

g = Acceleration gravity
ρ = Water density
Φ = Psotential
U = Uniform flow
σ = Source / sink elements
k_n = Root of dispersion equation
x = Field point coordinate X at global coordinate system
y = Field point coordinate Y at global coordinate system
z = Field point coordinate Z at global coordinate system
$\hat{x}$ = Source point coordinate X at global coordinate system
$\hat{y}$ = Source point coordinate Y at global coordinate system
$\hat{z}$ = Source point coordinate Z at global coordinate system
$\tilde{x}$ = local (element) x coordinate system
$\tilde{y}$ = local (element) y coordinate system
$\tilde{z}$ = local (element) z coordinate system
R = Horizontal distance between field point and source point
r = Actual distance between field point and source point
r_1 = Actual distance between image of field point below seabed and source point
γ = Horizontal angle between field point and source point
H = Water depth
J_0 = Zeroth order of Bessel function first kind
H_0 = Zeroth order of Hankel function second kind
K_0 = Zeroth order of modified Bessel function second kind
K_1 = First order of modified Bessel function second kind
ω = Wave frequencies
G = Greens/influence function
S_0 = Panel surface area
t = Time
v = Velocity
n = Normal unit vector
a = Added mass coefficient
b = Damping coefficient
c = Restoring coefficient
m = Mass
h = half-thickness of level ice
w = Vertical displacement of level ice
E_i = Modulus Elasticity of the Ice
F = Force
P = Pressure
$\emptyset$ = Higher order terms generated from the series expansion

1 Introduction to Thesis Topic

1.1. Motivation of the Problem

Although it is a relatively young field of research, offshore engineering in Arctic region had to be a hot topic when the demand of hydrocarbons was high due to the fact that 30% estimation of global oil and gas reserves are found in this region. Low oil price in the past few years indeed significantly reduces the attention of offshore companies to consider exploration projects within this region. Nevertheless, it is an undeniable fact that knowledge development in this topic grows. Oil & gas exploration has just become a trigger and prove that engineering job in the Arctic region is feasible, which in the same time open a good path for another field of business opportunity. It is obvious that vessels/floaters always involve in any kind of offshore operation, whether the floater itself as the main utility structure or just become a supporting role such as handling an installation/transportation job. With this in mind, understanding the dynamic behavior of the floater is a crucial issue in any field of offshore engineering job.

As a matter of fact, understanding a floating body motion operating in the sea ice condition has its own uniqueness in terms of challenge. Interaction between a floater and ice, fluid and ice, fluid and the floater are interconnected each other. There are a lot branch hydromechanics analysis of floating bodies in sea-ice condition, whether related to the ice-breaking process when a floater hits the ice or about the hydrodynamic effect (e.g. radiation and diffraction forces) due to the presence of the level ice itself. This thesis will focus on the latter case.

(a) An Example of Positionally-Stationed Floater in Sea Ice (Source: ogj.com)

(b) Loading Ice breaker Crude Oil Tanker at Oil Terminal (Source: pinterest.com)

Figure 1.1: Floater in Sea Ice

On the other hand, analyzing the motion of a vessel in open water has been a quite accustomed task since decades ago. Accurate prediction of the motion, robust calculation in the computational/numerical

model, taking a non-linear phenomenon into account, forward speed consideration, motion coupling effects for several bodies and any other sophisticated analyses to mimic a various real-life offshore project condition are achievable and many researches have been evolved in this field. Many world leading universities, research institutes and companies develop reliable tools to do this kind of analysis which usually described as a boundary value problem based on potential theory. Greens Function is one of powerful mathematical tool to solve partial differential equations which represents this boundary value problem. It can be said that and the Greens Function is the "heart" of most diffraction codes. Even though the Greens Function for "open water" condition has discovered decades ago, research activities to establish an efficient solution are still quite attractive to improve the assumption being used. However, it does not seem that this radiation-diffraction analysis, lean towards into the icy region of the seas. Most of the time, hydromechanics body analysis in the sea ice focuses more on ice breaking processes (interaction of the ice and structure). This thesis tries to fill the gap and provide an initial effort to establish a floating body motion analysis where the occurrence of level ice in the sea surface is taken into account by deriving its Greens Function. The “open water” sea condition analysis is still provided in an extensive manner (in terms of approach) to trigger the awareness about several challenges which might be occur for ice-infested waters as well.

1.2. Historical Remark about Floating Body Analysis

To give a glance idea about research development in this field, some brief historical milestones are presented in a narrative manner. The study about fluid mechanics already established since before the century (around 250 BC) when Archimedes discovered the fundamental principles of hydrostatic and dynamics. However, there are several names that cannot be absent when one is going further in a literature study of modern numerical hydomechanics.

In relation with the fundamental concept being used, Horace Lamb (1879) [13] wrote an important book about classical theory of fluid mechanics. The work done by George Green (1828) about potential theory gave a significant contribution in the implementation of mathematical technique (Greens Theorem) which in fact is applicable in many fields of physics. The Greens Function becomes a powerful tool to solve a boundary element problem represented by partial differential equations. Since floating body analysis can be well formulated by this method (BEM), finding an efficient Greens Function is a pivotal task.

In 1950, John [10] suggested an infinite series form of Greens Function to analyze floating body motion in 3-dimensional domain which derived based on eigen-function expansion method. Wehausen and Laiton (1960) [20] derived the integration solution form from the same physical problem. Hess and Smith (1962, 1964, 1966)[7] [9] [8] worked extensively to calculate potential flows in arbitrary three-dimensional body based on panel method. Even their field of research in the beginning was in aerodynamic, since they worked in both of non-lifting and lifting potential flows, in the end their research can be applied not only in spacecraft design but also in ship/floating structures.

Around two decades later, Newman (1985) [15] gave very important contribution in the development of diffraction tools for analyzing numerical hydromechanics problem. An eigen-function expansion form of the Greens Function which derived by John was used effectively. He distinguished the solution in several regions based on its convergence rate parameters and used a multi-dimensional approximation in economized polynomial. Because of this approach, computation speed to solve a large integral equations could be improved significantly. His works have become an excellent step forward in the development of numerical solution with a certain controlled accuracy. He implemented his works as a subroutine FINGREEN (in the form of 800 lines FORTRAN code) and it became the ’heart’ of a well-known diffraction code called WAMIT supplied by MIT. Up to several decades afterwards, this subroutine was used everywhere and became a benchmarking tool for any other diffraction codes developed anywhere else. Even some research institutes/universities such as DNV GL and TU Delft itself, are still using this FINGREEN subroutine to develop their own diffraction codes. Noblesse and Tesle (1986)[17] gave a contribution into this field of research by providing an efficient method of numerical evaluation for deep water case. Chakrabarti (2001)[4] validated the work done by Noblesse by using several routines: 2 series solutions, 2 integral routines and 2 infinite depth series and in the end, he compared the results to Newman’s solution. The most recent research in the evaluation of three-dimensional open water Green function by Ying Liu (2015)[14] indicates that there is still plenty space of research to improve the robustness of the solutions.

To create an awareness about the implementation of this Greens Function in well-developed diffraction tool nowadays (and its extended capability), there are several numerical tools/software mentioned below.

- **WAMIT Version 6.4, 6.4S (developed by MIT)** In WAMIT, the boundary value problem is solved by using a Greens theorem to derive an integral equation to obtain the radiation and diffraction velocity potentials on the body boundary. This software is capable to implement accurate surface panel discretization by using a higher order panel method (e.g: B-Splines). Second order wave force (wave drift force) also can be considered. Moreover, an analysis of coupling effect between multiple bodies is also possible.

- **AQWA Release 15.0 (developed by ANSYS,Inc)** Since directly evaluating the finite depth Greens Function in frequency domain is time-consuming, in ANSYS AQWA, Greens Function (and its first order derivative) is computed beforehand and stored in a database. The desired solution from certain input parameters can be given efficiently. As a drawback, there is a certain limit of low frequency input, which depends on the gravity and water depth. A second order wave effect also can be considered in this program. In addition, there are many other interesting features to analyze/design a typical offshore structure such as moorings, fenders, tethers, etc.

- **SESAM WADAM version 8.1 (developed by Det Norske Versitas)** Similar with ANSYS, Sesam is an extensive offshore engineering software which has a lot of sub-programs for different analysis, such as Sesam for offshore wind, marine operation, floating structures, moorings and risers, fixed structures, pipelines, and even design optimization. Radiation/diffraction code lies in the Sesam for floating structure and consists of 3 modules, from intact and damaged stability calculation (HydroD module), linear (Wadam), or non-linear (Wasim) hydrodynamic analysis.

  In the user manual of Wadam, it is explicitly stated that a potential theory described in the Newman's work[15] is being used. The actual implementation of this, is based on Wamit by using the 3D panel method to evaluate velocity potentials and hydrodynamic coefficients. However, the method used in Wasim is the Rankine panel method. Rankine method does not satisfy the free surface boundary condition. As a consequence, the integral equation need to be solved will have unknowns both on the hull and free surface. This makes the system of equation become larger. On the other hand, the matrix equation of this system is easier to evaluate than the one solved by the Greens Function method. This program can compute global responses of the structure and local loading on the vessels moving at any forward speed. The simulation is carried out in the time domain, but the results are also transformed into the frequency domain by using Fourier transform.

- **MOSES, 2017 (developed by Bentley)** MOSES is a powerful software devoted for a broad analysis of offshore engineering problem such as mooring design, ballasting, stability, transportation, sea-keeping, launching, upending, lowering, load-out, deck installation and in-place analysis. In its hydrodynamic module, the 3D diffraction theory has been validated with a model test result from Deep Water Construction Vessel (DCV) Balder. Similarly with the other diffraction software, Moses uses a source superposition technique by using the Greens Function solution method. Physically, distribution of the source strength complies the John's description [10] for shallow water case, and also Noblesse [17] for deep water.

- **Others** At the research institutes in the Netherlands, apparently there are plenty of numerical tools exist, such as DIFFRAC, SEAWAY, DELFRAC, SEASCAPE, DELWAVE with their own specialities and different approaches.

However, none of the numerical tools described above are capable to analyze floating body motion in the sea-ice condition. This is obvious because the boundary value problem is different, therefore the Greens Function will also differ. A research focus in hydromechanics of ice-infested waters is still reasonably young. Xu Ji (2016)[22] studied about the ice-induced vibration (due to ice breaking process). Even though it might be applicable in stationary-positioned floater, the actual phenomenon try to be captured is different with the radiation-diffraction problem. Timothy, et al (2017) [21] also studied about the breaking phenomena of the ice, but due to the wave instead of the structure. They also included the calculation of the wave radiation stress.

1.3. Research Objectives

The research objectives of this thesis are formulated as three questions below.

- What is the possible form of the 3D Greens Function to solve radiation-diffraction problem in ice-infested waters boundary value problem?
- What are the challenges of constructing an equation of motion for an arbitrary floating body in 3D open water with finite depth?
- Up to what extend the approach used in open water analysis can be implemented for ice-infested waters?

To answer these specifically, some boundaries are established to define the working scope of the thesis. These boundaries are

- The Greens Function (integral form) for ice-infested waters is derived without being implemented.
- A linear potential theory is used to describe the flow properties. All of boundary conditions, excitation, and any other terms which present in the problem description are truncated into the linear part.
- The analysis is based on the low order panel method. Floating body is meshed into a large number of quadrilateral panels. Considering the small size of the panel, it is quite reasonable to assume that the panels have a flat surface.
- The open water analysis tends to focus on implementation of the approach and obtaining the calculation result, instead of an accurate and robust solution. The approach starts from generating arbitrary shape numerical model and ends until obtaining the equation of motion without evaluating it.
- There is no effort has been done to improve the computation speed of Greens Function evaluation (e.g.: by using economized polynomial /by creating a database). The approach used in this thesis (for open water case) depends on the integral and the infinite series solution form.

2

General Formulation of The Problem

In this chapter, a general approach to construct an equation of motion of floating body is presented. The explanation is made in such a way to cover the whole, but general idea of the approach. Some important mathematics concepts are also recalled. However, no effort has been put to rewrite every derivation of the formulas because the reader is expected to be familiar with the basic theory of hydromechanics.

2.1. Axis Convention

Normally, there are 3 axis conventions used in the analysis of floating body motion: earth bound coordinate system, body bound coordinate system, and steadily translating coordinate system. Since the forward speed is not incorporated in this thesis, only the first two coordinate systems are important. At the global earth bound coordinate system, the X-Y plane lies in the still water surface with the positive X axis pointing towards the bow, positive Y to the starboard side, and positive Z directed upwards. The origin of this coordinate system lies in the center of floatation. The illustration is presented in the following figure.

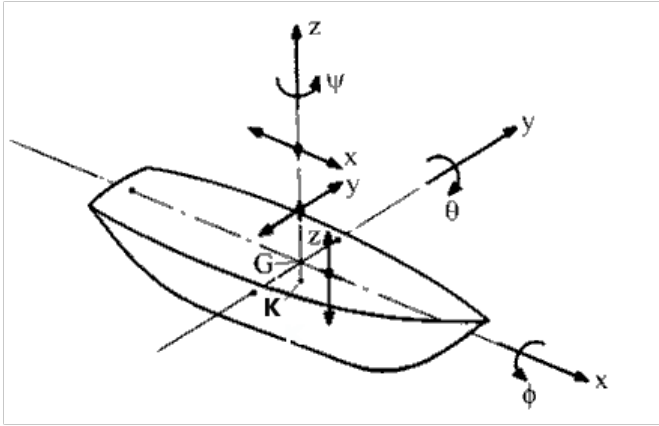

Figure 2.1: Axis Convention (Source: wiki.marin.nl)

In the latter chapter, a local element coordinate system which depends on the panel's orientation is found to be important. This is related to the surface integration procedure. The approach of doing this will be elaborated further in chapter 4.9:*Panel Integration*.

2.2. Problem Formulation

Generally speaking, the behavior of vessel motion can be understood by evaluation of the coupled 6 Degrees of Freedom equation of motion. This matrix equation is generated from the fluid forces. The most common approach to describe these fluid forces is by distinguishing these forces into 4 terms: wave excitation, diffraction, hydrostatic, and hydrodynamic response forces. In terms of linear approach, the excitation and reaction forces are determined separately. The diffraction problem (composed by wave excitation and diffraction

forces) is a condition where the floating body fixed in the certain position and wave excitation is present. In contrast, the radiation problem (contains the hydrodynamic response forces) is a condition where the floating body move and there is no wave excitation present. This radiation condition is used to determine the fluid forces (from potential) at the left hand side of the equation of motion, whereas the diffraction condition is for the right hand side. It means that since the very beginning, a strong assumption has been made because they are determined independently. In reality, this excitation-reaction forces are coupled to each other. However, this assumption is commonly acceptable for linear approach. One only needs to determine the magnitude of these fluid forces to construct the matrix equation of motion.

$$m \cdot \ddot{z} = \sum F$$

$$m \cdot \ddot{z} = F_r + F_w + F_d + F_s$$

$$(m + a) \cdot \ddot{z} + b \cdot \dot{z} + cz = F_w + F_d$$

with
F_r = Radiation force
F_w = Wave excitation (Froude Krylov) force
F_d = Diffraction force
F_d = Hydrostatic Force

At the left hand side of the equation of motion, the hydrostatic force determines the stiffness matrix coefficients (c), whereas the radiation forces influences the added mass coefficient (a) and damping matrix coefficient (b). The wave excitation (Froude Krylov) force (F_w) is an undisturbed wave force regardless the presence of a body. This force needs to be adjusted by another forcing term (diffraction force F_d) to represent the correct physical problem. Roughly speaking, the work done in this thesis is about calculating and quantifying these forces.

In hydromechanics, a complete mathematical description of fluid flow can be derived from the viscous Navier-Stokes equation. One can reproduce the characteristic of compressible and viscous flow from it. Since the result improvement is not really comparable with the degree of complexity which risen, the physical characteristic of the fluid flow such as velocity, acceleration, and forces can be derived based on potential flow theory instead. This means, the fluid is assumed to be irrational, incompressible, having no drag force, non viscous and no circulation is required to generate a lift force. The fundamental quantity must be obtained are these potentials. The readers are expected to be well aware about these assumptions and realize until what extend the same analysis/results can be applied.

A set of boundary equations is composed to determine these potentials. The needs of using this Greens Function is due to the fact that these boundary equations are expressed in partial differential equations. Greens Function is an impulse response of inhomogeneous linear differential equation defined on a domain with specified boundary/initial conditions. For different problem with different set of boundary equations, the Greens Function is going to be different. If one can evaluate this Greens Function, one can determine the physical quantity in the fluid domain, including fluid forces composing the matrix equation of motion. In the case of ice covered sea condition, this Greens Function only affects the added mass, damping coefficients and the diffracted wave force. The incoming wave potential itself need to be redefined from the appropriate surface condition. Several characteristic and identities of the Greens Function is recalled and presented below.

Dimension of the Greens Function

Consider Poisson's equation

$$\nabla^2 \Phi(x) = F(x)$$

Just for the purpose of dimensional analysis, consider Φ as a velocity potential function (unit [m^2/s]). In the same time, this reflects that the right hand side of the equation (F) has a unit [1/s]. The unknown variable Φ can be solved by convolving its Greens Function and the right hand side (F). Expression of the same differential equation problem by using the Greens Function is given by

$$\nabla^2 G(x - \hat{x}) = \delta(x - \hat{x})$$

Recalling the property of delta function

$$\int_{-\infty}^{\infty} \delta(x - \hat{x}) d\hat{x} = 1$$

which indicates that the unit of $\delta(x-\hat{x})$ is [1/m] and in the same time defines that the unit of G is [m]. The solution of Poisson's equation is found by $(G * F)$

$$\Phi(x) = \int_{-\infty}^{\infty} G(x-\hat{x})F(x)\,d\hat{x}$$

with unit [m^2/s = m 1/s m]. This reflects that the dimension of Greens Function depends on the differential operator $\bigtriangledown$ and the delta function defined.

Implementation in Hydromechanics

A short description above shows that the solution of differential equation can be expressed in terms of integration by finding an appropriate form of G. However, the effectiveness of this method in hydromechanics field is shown in the implementation of actual problem. Consider two different potential functions Φ and Ψ between certain closed surface S* with a volume V*. Starting from a divergence theorem and by implementing the Greens second identity, these potential functions can be formulated as

$$\iiint_{V^*} \left(\Phi \bigtriangledown^2 \Psi - \Psi \bigtriangledown^2 \Phi\right) dV^* = \iint_{S*} \left(\Phi \frac{\partial \Psi}{\partial n} - \Psi \frac{\partial \Phi}{\partial n}\right) dS^*$$

When potential function Φ represents velocity potential (satisfying LAPLACE equation), the left hand side of the equation reduces into

$$\iiint_{V^*} \left(\Phi \bigtriangledown^2 \Psi\right) dV^* = \iint_{S*} \left(\Phi \frac{\partial \Psi}{\partial n} - \Psi \frac{\partial \Phi}{\partial n}\right) dS^*$$

By determining the Ψ in such a way, this volume integral can be converted (evaluated) as a double integral represented by right hand side of the equation only. Basically, the Ψ also represents the velocity potential, but this Ψ will be treated in slightly different manner. There are a lot of solutions of the potential function Ψ which satisfy the Laplace equation ($\bigtriangledown^2\Psi = 0$). However, further simplification of the above equation (volume-surface integral) can be acquired by finding the fundamental solution of Ψ instead of assuming an arbitrary solution. Fundamental solution of Ψ satisfies

$$\bigtriangledown^2 \Psi(\overline{x}-\overline{\xi}) = \delta(\overline{x}-\overline{\xi})$$

and given by

$$\Psi = -\frac{1}{4\pi r} + w_{x,y,z,\hat{x},\hat{y},\hat{z}}$$

with $r = \sqrt{x^2+y^2+z^2}$

and (w) is arbitrary regular potential function. It is possible to include this another elementary solution (w) since Laplace equation is linear (superimposing principle can be used). However, since this (w) is assumed to be an additional regular *potential function*, the Laplace operator in the left hand side of the equation (inside the volume integral) gives $\bigtriangledown^2 w = 0$. Only the 1/r need to be evaluated to satisfy $\bigtriangledown^2 \frac{1}{r} = \delta(\overline{x}-\overline{\xi})$. The proof that this form (1/r) is the fundamental solution of Laplace equation can be found in many references and therefore is not going to be discussed further. Some reference derived the Poisson's equation by $-\bigtriangledown^2 \Psi(\overline{x}-\overline{\xi}) = \delta(\overline{x}-\overline{\xi})$ and obtaining the negation of the result above. The other elementary solution (w) is defined based on another boundary equation which must be satisfied (e.g: free surface, seabed, radiation condition). By implementing this fundamental solution, the left hand side of the volume integral becomes

$$\iiint_{V^*} \left(\Phi \bigtriangledown^2 \Psi\right) dV^* = \begin{cases} 0 \text{ if } \overline{x}-\overline{\xi} \neq = 0 \\ \Phi \text{ if } \overline{x}-\overline{\xi} = 0 \end{cases}$$

Therefore

$$p\Phi = \iint_{S*} \left(\Phi \frac{\partial \Psi}{\partial n} - \Psi \frac{\partial \Phi}{\partial n}\right) dS^*$$

$$\text{where p} = \begin{cases} 0 \text{ for P outside fluid domain V} \\ 1 \text{ for P inside fluid domain V} \end{cases}$$

P is the point where the source is situated. Until this point, the source point P can be placed anywhere in the domain of interest. In order to represent that this source point P lies in the body (S), only half of this source is needed to be taken into account (p = 1/2). This is the case because the source point produces a flow that

radiates anywhere in 3D domain. By taking only half the strength of this source, it means only the half side of the point produces the flow (half of the mass is streaming into V) and the other half is not (the other side of the body which is in dry condition). The illustration about this fact can be seen in the following figure

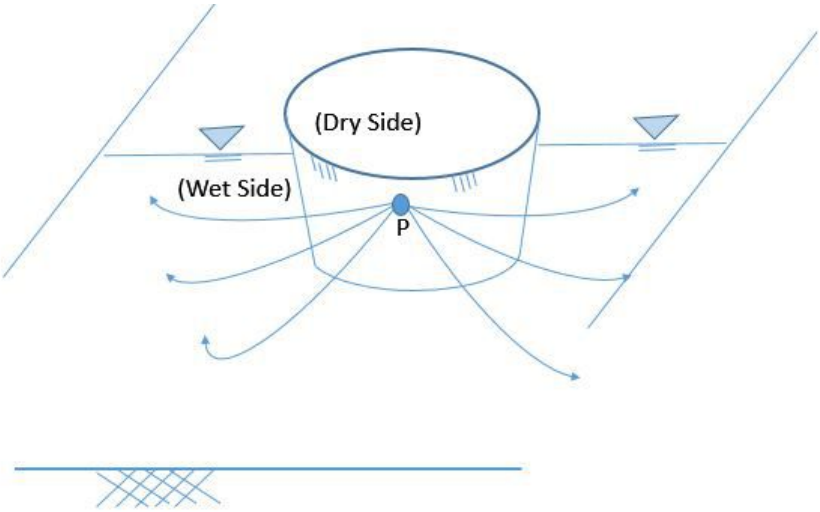

Figure 2.2: Source Potential

As a result, the conversion of volume integral into surface integral is obtained

$$\iint_S \Psi \frac{\partial \Phi}{\partial n} dS = -\frac{1}{2}\Phi + \iint_S \Phi \frac{\partial \Psi}{\partial n} dS$$

$$\iint_S (-\frac{1}{4\pi r} + w_{x,y,z,\hat{x},\hat{y},\hat{z}}) \frac{\partial \Phi}{\partial n} dS = -\frac{1}{2}\Phi + \iint_S \Phi \frac{\partial(-\frac{1}{4\pi r} + w_{x,y,z,\hat{x},\hat{y},\hat{z}})}{\partial n} dS$$

The Ψ is none other than the distribution function (Greens Function) itself (it is derived from the delta function in the right hand side of the equation). Integration of influence function along the whole domain of interest (body surface) where it was distributed, gives an identity (1). This will simplify the left hand side of the equation become $\frac{\partial \Phi}{\partial n}$. On the other hand, the Φ in the right hand side of the equation (in a physical sense) is the strength of the source term itself. At the end, this will give

$$\frac{\partial \Phi}{\partial n} = -\frac{1}{2}\sigma + \iint_S \sigma \frac{\partial G}{\partial n} dS$$

Above form gives a possibility to have a potential function which satisfy the kinematic body boundary condition in the form of double integral operation. Moreover, if the (w) is determined in such a way (to satisfy the other boundary equations), a complete description of potential flow on the surface body is obtained.

2.2.1. Boundary Conditions

Derivation of the potential in a whole domain is based on several boundary conditions expressed below. The discussion about each condition can be found in many hydromechanics books, therefore, no more elaboration is presented.

Continuity Condition

Laplace condition represents a continuity of the fluid. In Cartesian coordinate system, the Laplace equation for inviscid and irrotational flow is

$$\frac{\partial^2 \Phi}{\partial x^2} + \frac{\partial^2 \Phi}{\partial y^2} + \frac{\partial^2 \Phi}{\partial z^2} = 0$$

$$\nabla^2 \Phi = 0$$

holds at the whole domain of the fluid

Sea Bed Boundary Condition (Finite Water Depth)

The seabed is assumed to be flat, located at $-H$ in the global coordinate system. The vertical velocity in this depth must be zero which indicates that there are no fluid going through the seabed.

$$\frac{\partial \Phi}{\partial z} = 0$$

holds at $z = -H$

Far away from the Ship

At distance far away from the ship, there is no disturbances occur due to the ship's presence. This condition can be expressed by

$$\lim_{R \to \infty} \Phi = 0$$

Surface Boundary Condition (Ice-Infested Waters)

For ice-infested waters, the surface boundary condition is not really common to be found in hydromechanics text book. This condition basically can be expressed based on combination of linearized Bernoulli equation and Kirchoff-Love plate theorem and will be shown in chapter 3. *Derivation of 3D Greens Function for Ice-Invested Waters.*

Free Surface Boundary Condition (Open Water)

The water particle cannot leave the free surface (kinematic boundary condition). This can be expressed by a linearized Bernoulli equation below.

$$\frac{\partial^2 \Phi}{\partial t^2} + g \frac{\partial \Phi}{\partial z} = 0$$

holds at $z = 0$

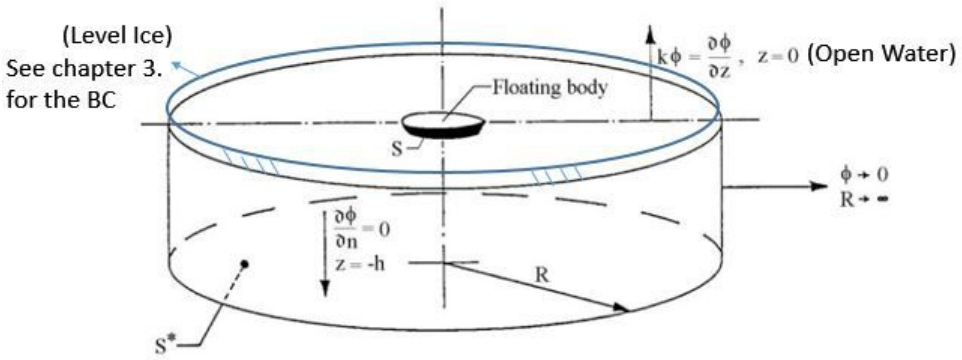

Figure 2.3: Boundary Conditions

2.2.2. Implementation of BEM in Numerical Hydromechanics of Floating Body

The boundary equations written above describe fluid characteristics in the domain. Since the presence of a body disturbs these characteristics, one more boundary condition need to be satisfied which represented by the kinematic condition on the oscillating body.

Kinematic Boundary Condition on The Oscillating Body Surface (Radiation Condition)

This boundary condition is needed to determine the hydrodynamic reaction force (to fill the left hand side of the equation of motion) and represent the water tightness of a body (there is no fluid going through the body). The velocity/displacement of water particle at a point on the surface body is equal to the velocity/displacement of point on the body itself.

$$\frac{\partial \Phi_{j(x,z,t)}}{\partial n} = v_j$$

holds at S_0, with $j = 1, ..., 6$ as mode of the motions

Since To acquire the distribution of this potential along the immersed body, an unknown dummy variable "(source strength σ)" is introduced as a constant multiplier in every panel. The magnitude of this "unknown source strength" is determined by solving the linear system of matrix equation generated by implementation of above kinematic boundary condition for each mode of motion. Therefore, in every mode of motions, the unknown source strength has to be solved by its respective directional mode of equation. Lastly, because the body is described as a panel instead of point, this final form of the potential must be integrated (or multiplied) along the panel surface. As a result, the final form of the potential is given by

$$\Phi_{j(x,y,z)} = \frac{1}{4\pi}\iint_{S_0} \sigma_j(\hat{x},\hat{y},\hat{z})G(x,y,z,\hat{x},\hat{y},\hat{z})dS_0$$

or numerically as

$$\Phi_{j(x,y,z)} = \frac{1}{4\pi}\sigma_j(\hat{x},\hat{y},\hat{z})G(x,y,z,\hat{x},\hat{y},\hat{z})\Delta S_0$$

Kinematic Boundary Condition of The Wave Diffracted Excitation(Diffraction Condition)

Similarly with above approach, one more equation is introduced to represent the water-tightness of the body. Instead for determining hydrodynamic reaction forces, this condition is needed to adjust the undisturbed wave excitation forces and diffract them out of the body. In parallel with radiation condition, the representation about this diffraction condition is about the fact that velocity/displacement of water particle at a point on surface of the body is equal to the velocity/displacement of point on the body itself.

$$\frac{\partial\Phi_{d(x,z,t)}}{\partial n} = \frac{\partial\Phi_{w(x,z,t)}}{\partial n}$$

holds at S_0
where the wave potential can be taken from the linear wave theory and expressed by (complex form)

$$\Phi_{w(t)} = \frac{\zeta_0 g}{\omega}\frac{\cosh(k(z+H))}{\cosh(kH)}e^{ik(x\cos\mu+y\sin\mu)}e^{-i\omega t}$$

and the space dependent part

$$\phi_w = \frac{\zeta_0 g}{\omega}\frac{\cosh(k(z+H))}{\cosh(kH)}e^{ik(x\cos\mu+y\sin\mu)}$$

with μ represents the wave heading as visualized in the following figure

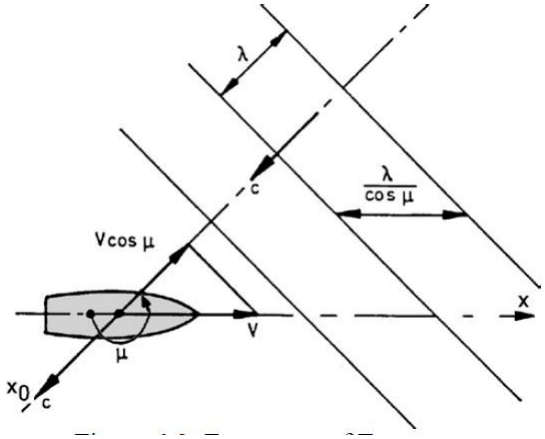

Figure 2.4: Approaching Wave Direction (Source: Offshore Hydromechanics [11])

The magnitude of diffraction potential is determined in the same manner by

$$\Phi_{d(x,y,z)} = \frac{1}{4\pi}\sigma_d(\hat{x},\hat{y},\hat{z})G(x,y,z,\hat{x},\hat{y},\hat{z})\Delta S_0$$

2.3. Mathematics

In the following, several quite uncommon mathematical concepts are being used. These theorems are presented here just as a short reminder to the readers.

2.3.1. Surface Integral

An evaluation of function under a surface integral is easier when it reconstructed as a normal double integral of converted function multiply by its Jacobian.

$$\iint_R f_{(x,y)}\,dA = \iint_S f_{(g_{(u,v)},h_{(u,v)})} \left|\frac{\partial(x,y)}{\partial(u,v)}\right| du\,dv$$

where the Jacobian is calculated by

$$\left|\frac{\partial(x,y)}{\partial(u,v)}\right| = \begin{vmatrix} \frac{\partial x}{\partial u} & \frac{\partial x}{\partial v} \\ \frac{\partial y}{\partial u} & \frac{\partial y}{\partial v} \end{vmatrix}$$

Generally speaking, this implies that the integral operation of a function (x,y) can be expressed in another integral operation of function with different variables $(g_{(x,y)}, h_{(x,y)})$.

2.3.2. Bessel Function

Bessel function are the solutions $y(x)$ of Bessel's differential equation for an arbitrary complex number (α).

$$x^2\frac{d^2y}{dx^2} + x\frac{dy}{dx} + (x^2-\alpha^2)y = 0$$

- **Bessel Function ($\mathbf{J}_\alpha$,$\mathbf{Y}_\alpha$)**

$$J_\alpha(x) = \sum_{m=0}^{\infty} \frac{(-1)^m}{m!\Gamma(m+\alpha+1)}\left(\frac{x}{2}\right)^{(2m+\alpha)}$$

with
α = the *order* of Bessel function
$\Gamma(n) = (n-1)!$
J_α = Bessel Function of the first kind
Y_α = Bessel Function of the second kind

For zeroth order Bessel Function of the first kind, the integral form can be written (Abramowitz and Stegun (1972, p.360)[1]) as

$$J_0(z) = \frac{1}{\pi}\int_0^\pi e^{iz\cos\theta}d\theta$$

- **Hankel Function ($\mathbf{H}_\alpha^{(1)}$, $\mathbf{H}_\alpha^{(2)}$)**

$$H_\alpha^{(1)}(x) = J_\alpha(x) + i\,Y_\alpha(x)$$
$$H_\alpha^{(2)}(x) = J_\alpha(x) - i\,Y_\alpha(x)$$

with
$H_\alpha^{(1)}$ = Hankel Function of the first kind
$H_\alpha^{(2)}$ = Hankel Function of the second kind

- **Modified Bessel Function ($\mathbf{I}_\alpha$, $\mathbf{K}_\alpha$)**

$$I_\alpha(x) = i^{-\alpha}J_\alpha(ix) = \sum_{m=0}^{\infty}\frac{1}{m!\Gamma(m+\alpha+1)}\left(\frac{x}{2}\right)^{2m+\alpha}$$

$$K_\alpha(x) = \frac{\pi}{2}\frac{I_{-\alpha}(x) - I_\alpha(x)}{\sin(\alpha\pi)}$$

with
I_α = Modified Bessel Function of the first kind
K_α = Modified Bessel Function of the second kin

3

Derivation of 3D Greens Function for Ice-Infested Waters

3.1. Source Point on the Free Surface-Level Ice Interface Condition

In order to build up the derivation of Greens Function smoothly, initially, a simple 3D boundary-value problem is formulated. Source points (which represent the discretized floating body/panel) lie in an interface between the free surface and level ice. This problem formulation is not representing the body motion analysis because there is no source point immersed in the water. However, it is still a good example to begin the derivation with.

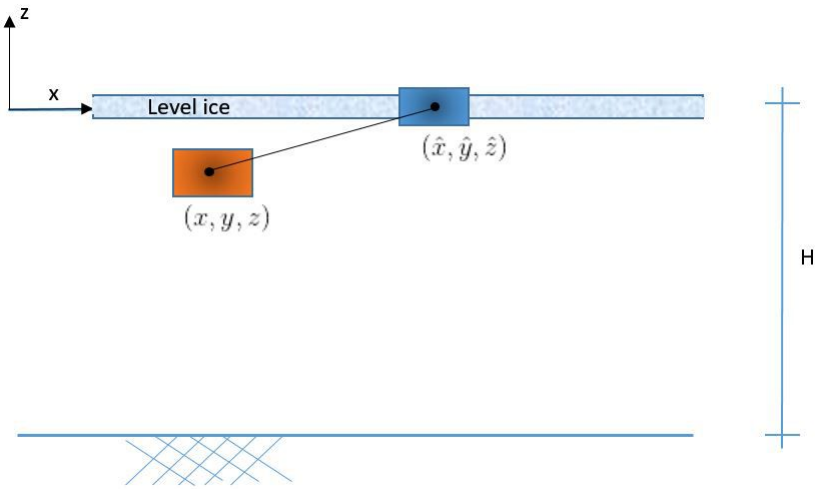

Figure 3.1: Source at Free Surface - Level Ice Interface Condition

3.1.1. Boundary Conditions

The implementation of a panel method is basically based on the pressure integration over the panel. The pressure is obtained from the potential. When deriving the Greens Function, the potential is split as a space dependent and time dependent part. An extensive discussion about this can be seen in the reference written by Journee [11]. To begin with the derivation, an assumed velocity potential is given in the form

$$\Phi_{(x,y,z,t)} = \phi_{(x,y,z,\omega)} e^{-i\omega t}$$

adapting the notation as written in [11]

$$\phi = -i\omega \sum_{j=0}^{7} \widehat{\phi}_j \zeta_j$$

combine the oscillatory motion and the potential into one variable

$$\phi = -i\omega \sum_{j=0}^{7} \tilde{\phi}_j$$

distinguish the diffraction, radiation and wave potentials

$$\phi = -i\omega \left((\tilde{\phi}_0 + \tilde{\phi}_7) + \sum_{j=1}^{6} \tilde{\phi}_j \right)$$

Slightly different from the potential for the open water, the potential for ice-infested waters is derived from the $\tilde{\phi}$ above. Therefore, every unknown potential quantity addressed in this derivation is represented as *displacement* potentials with the unit [m^2]. The boundary equations for this $\tilde{\phi}$ are given in the following. The $\tilde{\phi}$ is expressed directly as a G (The Greens Function) by including the delta function in one of the boundary equations.

Laplace

$$\frac{\partial^2 G_{(x,y,z,t)}}{\partial x^2} + \frac{\partial^2 G_{(x,y,z,t)}}{\partial y^2} + \frac{\partial^2 G_{(x,y,z,t)}}{\partial z^2} = 0$$

Seabed

$$\frac{\partial G_{(x,y,-H,t)}}{\partial z} = 0$$

Free Surface

The boundary condition at the free surface is composed by combination of pressure description based on linearized Bernoulli equation and the equation of motion for Kirchoff-Love plate theorem. The left hand side equation is derived from the linearized Bernoulli equation.

$$-\rho_w \left(\frac{\partial^2 G_{(x,y,z,t)}}{\partial t^2} + g \frac{\partial G_{(x,y,z,t)}}{\partial z} \right) = p_{(x,y,z,t)}$$

The right hand side, an equation of motion for a thin plate is given by

$$p_{(x,y,t)} = D \left(\frac{\partial^4 w_{(x,y,t)}}{\partial x^4} + 2 \frac{\partial^4 w_{(x,y,t)}}{\partial x^2 \partial y^2} + \frac{\partial^4 w_{(x,y,t)}}{\partial y^4} \right) + q_{(x,y,t)} + 2\rho_i h \frac{\partial^2 w_{(x,y,t)}}{\partial t^2}$$

The boundary condition in the absence of external load (q) on top of the ice and taking an infinite source disturbance into account (which is the representation of panel body) can be written as

$$-\rho_w \left(\frac{\partial^2 G_{(x,y,z,t)}}{\partial t^2} + g \frac{\partial G_{(x,y,z,t)}}{\partial z} \right) \Big|_{z=0} = D \left(\frac{\partial^4 w_{(x,y,t)}}{\partial x^4} + 2 \frac{\partial^4 w_{(x,y,t)}}{\partial x^2 \partial y^2} + \frac{\partial^4 w_{(x,y,t)}}{\partial y^4} \right) + 2\rho_i h \frac{\partial^2 w_{(x,y,t)}}{\partial t^2} + \delta(x-\hat{x})\delta(y-\hat{y})$$

since

$$w_{(x,y,t)} = \frac{\partial G_{(x,y,z,t)}}{\partial z} \Big|_{z=0}$$

therefore

$$-\rho_w \left(-\omega^2 G_{(x,y,z,t)} + g \frac{\partial G_{(x,y,z,t)}}{\partial z} \right) \Big|_{z=0} = D \left(k_x^4 \frac{\partial G_{(x,y,z,t)}}{\partial z} + 2k_x^2 k_y^2 \frac{\partial G_{(x,y,z,t)}}{\partial z} + k_y^4 \frac{\partial G_{(x,y,z,t)}}{\partial z} \right) \Big|_{z=0}$$
$$-2\rho_i h \omega^2 \frac{\partial G_{(x,y,z,t)}}{\partial z} \Big|_{z=0} + \delta(x-\hat{x})\delta(y-\hat{y})$$

with
$D = \frac{2h^3 E_i}{3(1-\nu^2)}$
$2h$ =thickness of level ice
E_i =Modulus Elasticity of Level Ice
ν =Poisson's Ratio of Level Ice

In order to raise the awareness about which quantity that the Greens Function really represent to, a dimensional analysis has been carried out. It is already mentioned that the boundary equations are represented by *displacement potential* $\tilde{\phi}$. This means, initially, before implementing the Greens Function, the pressure equation is given by

$$-\rho_w\left(-\omega^2\tilde{\phi}+g\frac{\partial\tilde{\phi}}{\partial z}\right)\Big|_{z=0}-D\left(k_x^4\frac{\partial\tilde{\phi}}{\partial z}+2k_x^2k_y^2\frac{\partial\tilde{\phi}}{\partial z}+k_y^4\frac{\partial\tilde{\phi}}{\partial z}\right)\Big|_{z=0}+2\rho_i h\omega^2\frac{\partial\tilde{\phi}}{\partial z}\Big|_{z=0}=0$$

by taking one expression (e.g.: $\rho_w\omega^2\tilde{\phi}$), it can seen that the units of these terms (excluding the $\tilde{\phi}$) are given by $[\frac{kg}{m^3s^2}=\frac{\text{Pa}}{m^2}]$. When the Greens Function is being implemented

$$[\frac{\text{Pa}}{m^2}][G]=[\delta(x-\hat{x})][\delta(y-\hat{y})]$$

Therefore, the unit [G] = $\frac{1}{\text{Pa}}$

3.1.2. Integral Transformation

Double integral Fourier transform is needed to change the boundary equations into ordinary differential equations with the same differential variable. In this case, the transformation is used to convert the boundary equations from x and y differential variables into the k_x and k_y by

$$\hat{G}_{(k_x,k_y,z)}=\int_{-\infty}^{-\infty}\int_{-\infty}^{-\infty}G_{(x,y,z)}e^{-i(k_xx+k_yy)}dxdy$$

for delta function

$$e^{-i(k_x\hat{x}+k_y\hat{y})}=\int_{-\infty}^{-\infty}\int_{-\infty}^{-\infty}\delta(x-\hat{x})\delta(y-\hat{y})e^{-i(k_xx+k_yy)}dxdy$$

and the inverse transformation is given by

$$G_{(x,y,z)}=\frac{1}{4\pi^2}\int_{-\infty}^{-\infty}\int_{-\infty}^{-\infty}\hat{G}_{(k_x,k_y,z)}e^{i(k_xx+k_yy)}dk_xdk_y$$

$$\delta(x-\hat{x})\delta(y-\hat{y})=\frac{1}{4\pi^2}\int_{-\infty}^{\infty}\int_{-\infty}^{\infty}e^{i(k_x(x-\hat{x})+k_y(y-\hat{y}))}dk_xdk_y$$

Therefore, by applying this integral transformation, the boundary equations change into

Laplace

$$-k_x^2\hat{G}_{(k_x,k_y,z)}-k_y^2\hat{G}_{(k_x,k_y,z)}+\frac{\partial^2\hat{G}_{(k_x,k_y,z)}}{\partial z^2}=0$$

introduce new notation
$k^2=k_x^2+k_y^2$

$$\frac{\partial^2\hat{G}_{(k_x,k_y,z)}}{\partial z^2}-k^2\hat{G}_{(k_x,k_y,z)}=0$$

Seabed

$$\frac{\partial\hat{G}_{(k_x,k_y,z)}}{\partial z}\Big|_{z=-H}=0$$

Free Surface

$$-\rho_w\left(-\omega^2\hat{G}_{(k_x,k_y,z)}+g\frac{\partial\hat{G}_{(k_x,k_y,z)}}{\partial z}\right)\Big|_{z=0}=D\left(k_x^4\frac{\partial\hat{G}_{(k_x,k_y,z)}}{\partial z}+2k_x^2k_y^2\frac{\partial\hat{G}_{(k_x,k_y,z)}}{\partial z}+k_y^4\frac{\partial\hat{G}_{(k_x,k_y,z)}}{\partial z}\right)\Big|_{z=0}$$

$$-2\rho_i h\omega^2\frac{\partial\hat{G}_{(k_x,k_y,z)}}{\partial z}\Big|_{z=0}+e^{-i(k_x\hat{x}+k_y\hat{y})}$$

3.1.3. Solving Differential Equation

In order to obtain a function $\hat{G}$ which satisfy all of above equations, second order homogeneous differential equation from transformed Laplace condition can be solved by assuming a general solution:

$$\hat{G}_{(k_x,k_y,z)} = C_1 \cos(S_n z) + C_2 \sin(S_n z)$$

Fundamentally speaking, this assumed solution can be anything. This form has been chosen due to its flexibility and has a lot of convenience. Substituting this assumed solution into the transformed BC (Laplace), gives

$$-S_n^2 \left(C_1 \cos(S_n z) + C_2 \sin(S_n z)\right) - k^2 \left((C_1 \cos(S_n z) + C_2 \sin(S_n z)\right) = 0$$

and the characteristic equation is

$$S_n^2 = -k^2$$

with, $S_1 = ik$ and $S_2 = -ik$
Therefore, the general solution can be written as:

$$\hat{G}_{(k_x,k_y,z)} = C_1 \cosh(kz) - C_2 \sinh(kz)$$

The subsequent steps afterwards are done by substituting above general solution into the other boundary conditions to determine the unknown coefficients (C_1 and C_2). By substituting above equation into the sea bed boundary condition, the following expression is obtained

$$\frac{\partial \left(C_1 \cosh(kz) - C_2 \sinh(kz)\right)}{\partial z}\Big|_{z=-H} = 0$$

$$C_2 = C_1 \tanh(-kH)$$

Since the unknown constant C_2 is expressed in term of C_1, substitution into the general solution results an equation with only one remaining unknown constant C_1

$$\hat{G}_{(k_x,k_y,z)} = C_1 \cosh(kz) - C_1 \tanh(-kH) \sinh(kz)$$

$$\hat{G}_{(k_x,k_y,z)} = C_1 \left(\cosh(kz) - \tanh(-kH) \sinh(kz)\right)$$

Lastly, C_1 can be obtained from substitution to the free surface boundary condition

$$-\rho_w C_1 \left(-\omega^2 + gk(\tanh(kH))\right) = (k^4 D - 2\rho_i h\omega^2) C_1 k \tanh(kH) + P e^{-i(k_x \hat{x} + k_y \hat{y})}$$

and solving for C_1 gives

$$C_1 = -\frac{e^{-i(k_x \hat{x} + k_y \hat{y})}}{(k^4 D - 2\rho_i h\omega^2 + \rho_w g) k \tanh(kH) - \omega^2 \rho_w}$$

Therefore, all of the unknown constants are defined, and the complete solution becomes

$$\hat{G}_{(k_x,k_y,z)} = -\frac{e^{-i(k_x \hat{x} + k_y \hat{y})} (\sinh(kH) \sinh(kz) + \cosh(kz) \cosh(kH))}{(k^4 D - 2h\rho_i \omega^2 + \rho_w g) k \sinh(kH) - \rho_w \omega^2 \cosh(kH)}$$

which can be rewritten by adjusting the trigonometric function and using an infinite depth wave number $\alpha = \omega^2 / g$

$$\hat{G}_{(k_x,k_y,z)} = \frac{e^{-i(k_x \hat{x} + k_y \hat{y})} (\tanh(kH) \sinh(kz) + \cosh(kz))}{\rho_w \alpha g - (k^4 D - 2h\rho_i \alpha g + \rho_w g) k \tanh(kH)}$$

or

$$\hat{G}_{(k_x,k_y,z)} = \frac{e^{-i(k_x \hat{x} + k_y \hat{y})}}{\rho_w \alpha g - (k^4 D - 2h\rho_i \alpha g + \rho_w g) k \tanh(kH)} \frac{\cosh(k(H+z))}{\cosh(kH)}$$

The final form of the solution is double inverse Fourier transform of above solution (to convert it back in its original domain), expressed in space (x, y, z) domain.

$$G_{(x,y,z,\hat{x},\hat{y},0,\omega)} = \frac{1}{4\pi^2} \int_{-\infty}^{\infty} \int_{-\infty}^{\infty} \frac{e^{i(k_x(\hat{x}-x) + k_y(\hat{y}-y))}}{\rho_w \alpha g - (k^4 D - 2h\rho_i \alpha g + \rho_w g) k \tanh(kH)} \frac{\cosh(k(H+z))}{\cosh(kH)} dk_x dk_y$$

By inputting the correct dimensions of every terms, it can be seen that the unit of G is in $[\frac{1}{\text{Pa}}]$ and agrees with the previous definition. When one omitting the effect of the ice by taking the limit of D and ρ_i into zero, representation of the integral above is similar (extended version) with the one appears in the reference written by Chris[12] for 2-dimensional fluid domain problem without the level ice. The only differences are the exponent term (which reflect the difference dimension), constant denominator ρ_w and g which can be included in the unknown G without changing the integral formulation itself. One need to remember that the radiation condition is not satisfied yet. This is can be done by solving the integral above by using Cauchy's residue Theorem/ applying Sommerfeld radiation condition.

3.2. Source Point on the Fluid Domain

Considering the fact that above derivation is not applicable to analyze a floating body (pulsating source point only lies in the interface between free surface and level ice), a different physical condition is formulated. In the second case, an imaginary line between free surface and the seabed is introduced. The depth location of this imaginary line represents the depth location of the source point ($\hat{z}$). As a consequence, the boundary value problem is split into two parts. There will be two solutions of the function G and the potentials. One describes the fluid characteristic between level ice/free surface into the imaginary line and one for the fluid characteristic between an imaginary line into the seabed. In application, calculation of Greens Function at the field point (panel) also must be distinguished whether it lies above or under imaginary line (source point $\hat{z}$). In this section, all of transformed boundary equations are presented directly after implementing a double integral of Fourier transform.

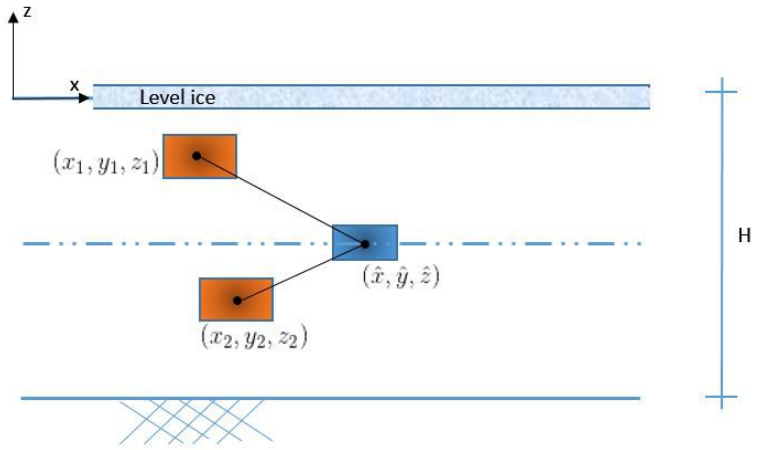

Figure 3.2: Source at Fluid Domain Introduced Interface Condition

3.2.1. Transformed Boundary Conditions

Laplace

Laplace condition is exactly the same with the one occur in the previous derivation (chapter 3.1 *Source Point on the Free Surface-Level Ice Interface Condition*).

$$-k_x^2 \hat{G}_{n(k_x,k_y,z)} - k_y^2 \hat{G}_{n(k_x,k_y,z)} + \frac{\partial^2 \hat{G}_{n(k_x,k_y,z)}}{\partial z^2} = 0$$

with index $n = 1, 2$.
Index 1 is used to derive the solution of field points located between the level ice-free surface and imaginary line, whereas index 2 is used for field points lay between the imaginary line and seabed. The other boundary equations also remain the same.

Free Surface Condition

$$-\rho_w \left(-\omega^2 \hat{G}_{1(k_x,k_y,z)} + g \frac{\partial \hat{G}_{1(k_x,k_y,z)}}{\partial z} \right) \Big|_{z=0} = D \left(k_x^4 \frac{\partial \hat{G}_{1(k_x,k_y,z)}}{\partial z} + 2k_x^2 k_y^2 \frac{\partial \hat{G}_{1(k_x,k_y,z)}}{\partial z} + k_y^4 \frac{\partial \hat{G}_{1(k_x,k_y,z)}}{\partial z} \right) \Big|_{z=0}$$

$$-2\rho_i h\omega^2 \frac{\partial \hat{G}_{1(k_x,k_y,z)}}{\partial z}\Big|_{z=0}$$

Seabed Boundary Condition

$$\frac{\partial \hat{G}_{2(k_x,k_y,z)}}{\partial z}\Big|_{z=-H} = 0$$

Interface Condition

In addition to the boundary equations above, two interface conditions (dynamic and kinematic conditions) must be specified in the imaginary line. These conditions are expressed by an equal displacement and pressure fields.
Displacement:

$$\frac{\partial \hat{G}_{1(k_x,k_y,z)}}{\partial z}\Big|_{z=\hat{z}} = \frac{\partial \hat{G}_{2(k_x,k_y,z)}}{\partial z}\Big|_{z=\hat{z}}$$

Pressure:

$$\left(P_{1(k_x,k_y,z)} - P_{2(k_x,k_y,z)}\right)\Big|_{z=\hat{z}} = e^{-i(k_x\hat{x}+k_y)}$$

$$\left(-\rho_w\left(-\omega^2\hat{G}_{1(k_x,k_y,z)} + g\frac{\partial \hat{G}_{1(k_x,k_y,z)}}{\partial z}\right) + \rho_w\left(-\omega^2\hat{G}_{2(k_x,k_y,z)} + g\frac{\partial \hat{G}_{2(k_x,k_y,z)}}{\partial z}\right)\right)\Big|_{z=\hat{z}} = e^{-i(k_x\hat{x}+k_y\hat{y})}$$

The right hand side of the pressure equation comes from double integral Fourier transform of the delta function which represent the infinite source pressure disturbance.

3.2.2. Solving Differential Equation

From previous discussion, it is known that the general solution of transformed Laplace equation can be found in the form

$$\hat{G}_{n(k_x,k_y,z)} = C_{1,n}\cos(S_n z) + C_{2,n}\sin(S_n z)$$

Substitute this assumed solution into conditions:
The first potential ($\hat{G}_1$) with the free surface-level ice boundary condition, gives

$$-\rho_w(-gkC_{21} - \omega^2 C_{11}) = D(-kC_{21}k_x^4 - 2kC_{21}k_x^2k_y^2 - kC_{21}k_y^4) + 2\rho_i h\omega^2 kC_{21}$$

solve for $C_{2,1}$

$$C_{2,1} = -\frac{\rho_w\omega^2 C_{11}}{(k^4 D - 2\rho_i h\omega^2 + g\rho_w)k}$$

Substituted back to the assumed solution for $\hat{G}_{1(k_x,k_y,z)}$

$$\hat{G}_{1(k_x,k_y,z)} = \frac{((k^4 D - 2\rho_i h\omega^2 + g\rho_w)k\cosh(kz) + \rho_w\omega^2\sinh(kz))C_{11}}{(k^4 D - 2\rho_i h\omega^2 + g\rho_w)k}$$

Substitute the assumed solution of Laplace equation into seabed boundary condition for the second potential ($\hat{G}_2$), gives

$$-C_{12}k\sinh(kH) - C_{22}k\cosh(kH) = 0$$

solve for $C_{2,2}$

$$C_{2,2} = -\tanh(kH)C_{12}$$

Substituted back to the assumed solution for $\hat{G}_{2(k_x,k_y,z)}$

$$\hat{G}_{2(k_x,k_y,z)} = C_{12}(\tanh(kH)\sinh(kz) + \cosh(kz))$$

The expression of $\hat{G}_{1(k_x,k_y,z)}$ and $\hat{G}_{2(k_x,k_y,z)}$ have unknown constants ($C_{1,1}$ and $C_{1,2}$) respectively. These constants can be determined by using 2 interface conditions.
Displacement:

$$\frac{\partial \hat{G}_{1(k_x,k_y,z)}}{\partial z}\Big|_{z=\hat{z}} = \frac{\partial \hat{G}_{2(k_x,k_y,z)}}{\partial z}\Big|_{z=\hat{z}}$$

Pressures:

$$\left(-\rho_w\left(-\omega^2\hat{G}_{1(k_x,k_y,z)}+g\frac{\partial\hat{G}_{1(k_x,k_y,z)}}{\partial z}\right)+\rho_w\left(-\omega^2\hat{G}_{2(k_x,k_y,z)}+g\frac{\partial\hat{G}_{2(k_x,k_y,z)}}{\partial z}\right)\right)\Big|_{z=\hat{z}}=e^{-i(k_x\hat{x}+k_y\hat{y})}$$

At the very end, the expression of $\hat{G}_{n(k_x,k_y,z)}$ are given by:

$$\hat{G}_{1(k_x,k_y,z)}=\frac{e^{-i(\hat{x}k_x+\hat{y}k_y)}\left(\sinh(kH)\cosh(k\hat{z})+\cosh(kH)\sinh(k\hat{z})\right)\left((k^4D-2h\rho_i\omega^2+g\rho_w)k\cosh(kz)+\rho_w\omega^2\sinh(kz)\right)}{\rho_w\omega^2\left((k^4D-2h\rho_i\omega^2+g\rho_w)k\sinh(kH)-\rho_w\omega^2\cosh(kH)\right)}$$
$$\hat{G}_{2(k_x,k_y,z)}=\frac{e^{-i(\hat{x}k_x+\hat{y}k_y)}\left(\sinh(kH)\sinh(kz)+\cosh(kH)\cosh(kz)\right)\left((k^4D-2h\rho_i\omega^2+g\rho_w)k\sinh(k\hat{z})+\rho_w\omega^2\cosh(k\hat{z})\right)}{\rho_w\omega^2\left((k^4D-2h\rho_i\omega^2+g\rho_w)k\sinh(kH)-\rho_w\omega^2\cosh(kH)\right)}$$

and also can be rewritten by adjusting the trigonometric function and an infinite depth wave number

$$\hat{G}_{1(k_x,k_y,z)}=\frac{e^{-i(\hat{x}k_x+\hat{y}k_y)}\left(\tanh(kH)\cosh(k\hat{z})+\sinh(k\hat{z})\right)\left((k^4D-2h\rho_i g\alpha+g\rho_w)k\cosh(kz)+\rho_w g\alpha\sinh(kz)\right)}{\rho_w g\alpha\left((k^4D-2h\rho_i g\alpha+g\rho_w)k\tanh(kH)-\rho_w g\alpha\right)}$$

$$\hat{G}_{2(k_x,k_y,z)}=\frac{e^{-i(\hat{x}k_x+\hat{y}k_y)}\left(\tanh(kH)\sinh(kz)+\cosh(kz)\right)\left((k^4D-2h\rho_i g\alpha+g\rho_w)k\sinh(k\hat{z})+\rho_w g\alpha\cosh(k\hat{z})\right)}{\rho_w g\alpha\left((k^4D-2h\rho_i g\alpha+g\rho_w)k\tanh(kH)-\rho_w g\alpha\right)}$$

or

$$\hat{G}_{1(k_x,k_y,z)}=\frac{e^{-i(\hat{x}k_x+\hat{y}k_y)}\left((k^4D-2h\rho_i g\alpha+g\rho_w)k\cosh(kz)+\rho_w g\alpha\sinh(kz)\right)}{\rho_w g\alpha\left((k^4D-2h\rho_i g\alpha+g\rho_w)k\tanh(kH)-\rho_w g\alpha\right)}\frac{\cosh(k(H+\hat{z}))}{\cosh(kH)}$$

$$\hat{G}_{2(k_x,k_y,z)}=\frac{e^{-i(\hat{x}k_x+\hat{y}k_y)}\left((k^4D-2h\rho_i g\alpha+g\rho_w)k\sinh(k\hat{z})+\rho_w g\alpha\cosh(k\hat{z})\right)}{\rho_w g\alpha\left((k^4D-2h\rho_i g\alpha+g\rho_w)k\tanh(kH)-\rho_w g\alpha\right)}\frac{\cosh(k(H+z))}{\cosh(kH)}$$

The final expression of the Greens Functions are double inverse Fourier transform of these solutions.

$$G_{1(x,y,z,\hat{x},\hat{y},\hat{z})}=\frac{1}{4\pi^2}\int_{-\infty}^{\infty}\int_{-\infty}^{\infty}\frac{e^{i(k_x(\hat{x}-x)+k_y(\hat{y}-y))}\left((k^4D-2h\rho_i g\alpha+g\rho_w)k\cosh(kz)+\rho_w g\alpha\sinh(kz)\right)}{\rho_w g\alpha\left((k^4D-2h\rho_i g\alpha+g\rho_w)k\tanh(kH)-\rho_w g\alpha\right)}\frac{\cosh(k(H+\hat{z}))}{\cosh(kH)}dk_xdk_y$$
$$G_{2(x,y,z,\hat{x},\hat{y},\hat{z})}=\frac{1}{4\pi^2}\int_{-\infty}^{\infty}\int_{-\infty}^{\infty}\frac{e^{i(k_x(\hat{x}-x)+k_y(\hat{y}-y))}\left((k^4D-2h\rho_i g\alpha+g\rho_w)k\sinh(k\hat{z})+\rho_w g\alpha\cosh(k\hat{z})\right)}{\rho_w g\alpha\left((k^4D-2h\rho_i g\alpha+g\rho_w)k\tanh(kH)-\rho_w g\alpha\right)}\frac{\cosh(k(H+z))}{\cosh(kH)}dk_xdk_y$$

Similarly, these integral can be solved by using Cauchy's residue Theorem and applying the Sommerfeld radiation condition. The poles of the integrand depend on some sort of modified dispersion equation and containing one propagating root and infinitely many evanescence roots.

3.3. Further Favourable Form

From above derivation, it is shown that the obtained solutions are not really simple and quite cumbersome to evaluate because of the double integral. This issue can be avoided by using Bessel function. Basically, the effort is about expressing the spatial Cartesian dimension into the radial form to change a partial differential equation into an ordinary differential equation. This can be done by combining wave number in each horizontal direction (x and y axis) into one as shown in the figure below.

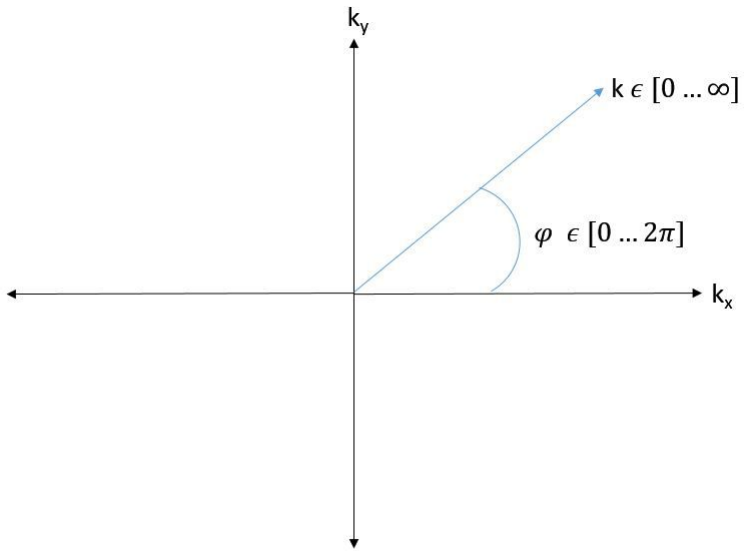

Figure 3.3: Combined Wave Number

Therefore,

$$k_x = k\cos\varphi$$
$$k_y = k\sin\varphi$$

where k is the modulus of wave number and agree with the introduced notation in section 3.2.1.*Integral Transformation.* Rewriting the obtained solution of the first problem (source point on the free surface-level ice interface condition) by implementing above adjustment and assuming

$$f_{(k)} = \frac{1}{\rho_w \alpha g - (k^4 D - 2h\rho_i \alpha g + \rho_w g)k\tanh(kH)} \frac{\cosh(k(H+z))}{\cosh(kH)}$$

gives

$$G_{(x,y,z,\hat{x},\hat{y},0,\omega)} = \frac{1}{4\pi^2}\int_0^\infty \int_0^{2\pi} f_{(k)} e^{i(k\cos\varphi(\hat{x}-x)+k\sin\varphi(\hat{y}-y))} d_\varphi d\,k$$

Since $f_{(k)}$ does not depend on φ, it can be excluded from the first integrand. Horizontal distance between source and field point also can be written in a polar coordinate system as shown in the following figure

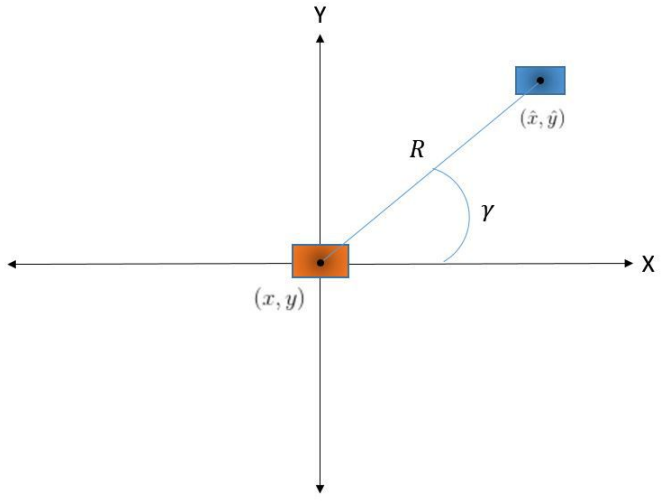

Figure 3.4: Plan View of Source and Field Points

with,

$$\hat{x} - x = R\cos\gamma$$

$$\hat{y} - y = R\sin\gamma$$

One must be aware that the horizontal distance is not inside the cosines term. This fact gives

$$G_{(x,y,z,\hat{x},\hat{y},0,\omega)} = \frac{1}{4\pi^2}\int_0^{\infty} f_{(k)} \int_0^{2\pi} e^{ikR(\cos\varphi\cos\gamma+\sin\varphi\sin\gamma)}\, d_\varphi\, dk$$

Implement some trigonometric identities gives

$$G_{(x,y,z,\hat{x},\hat{y},0,\omega)} = \frac{1}{2\pi^2}\int_0^{\infty} f_{(k)} \int_0^{\pi} e^{ikR\cos(\varphi-\gamma)}\, d_\varphi\, dk$$

The integrand with respect to φ can be represented by zeroth order Bessel function of the first kind (see chapter 2.3.3. *Bessel Function*) and gives

$$G_{(x,y,z,\hat{x},\hat{y},0,\omega)} = \frac{1}{2\pi}\int_0^{\infty} f_{(k)} J_0(kR)\, dk$$

Therefore, the final simplified solution appears as a single integral evaluation

$$G_{(x,y,z,\hat{x},\hat{y},0,\omega)} = \frac{1}{2\pi}\int_0^{\infty} \frac{1}{\rho_w\alpha g - (k^4 D - 2h\rho_i\alpha g + \rho_w g)k\tanh(kH)} \frac{\cosh(k(H+z))}{\cosh(kH)} J_0(kR)\, dk$$

For the second problem (source point on the fluid domain), above adjustment also can be implemented in the exactly the same manner. The difference is only about the term f(k) which given by

$$f_{1(k)} = \frac{\left((k^4 D - 2h\rho_i g\alpha + g\rho_w)k\cosh(kz) + \rho_w g\alpha\sinh(kz)\right)}{\rho_w g\alpha\left((k^4 D - 2h\rho_i g\alpha + g\rho_w)k\tanh(kH) - \rho_w g\alpha\right)} \frac{\cosh(k(H+\hat{z}))}{\cosh(kH)}$$

$$f_{2(k)} = \frac{\left((k^4 D - 2h\rho_i g\alpha + g\rho_w)k\sinh(k\hat{z}) + \rho_w g\alpha\cosh(k\hat{z})\right)}{\rho_w g\alpha\left((k^4 D - 2h\rho_i g\alpha + g\rho_w)k\tanh(kH) - \rho_w g\alpha\right)} \frac{\cosh(k(H+z))}{\cosh(kH)}$$

In the end, the final solutions are given by

$$G_{1(x,y,z,\hat{x},\hat{y},\hat{z})} = \frac{1}{2\pi}\int_0^{\infty} \frac{\left((k^4 D - 2h\rho_i g\alpha + g\rho_w)k\cosh(kz) + \rho_w g\alpha\sinh(kz)\right)}{\rho_w g\alpha\left((k^4 D - 2h\rho_i g\alpha + g\rho_w)k\tanh(kH) - \rho_w g\alpha\right)} \frac{\cosh(k(H+\hat{z}))}{\cosh(kH)} J_0(kR)\, dk$$

$$G_{2(x,y,z,\hat{x},\hat{y},\hat{z})} = \frac{1}{2\pi}\int_0^{\infty} \frac{\left((k^4 D - 2h\rho_i g\alpha + g\rho_w)k\sinh(k\hat{z}) + \rho_w g\alpha\cosh(k\hat{z})\right)}{\rho_w g\alpha\left((k^4 D - 2h\rho_i g\alpha + g\rho_w)k\tanh(kH) - \rho_w g\alpha\right)} \frac{\cosh(k(H+z))}{\cosh(kH)} J_0(kR)\, dk$$

The implementation of this Greens Function in a floating body analysis is not going to be done in this thesis. This is the case considering a reason that the radiation condition is not satisfied yet. Nevertheless, to address the whole possible challenges of analyzing arbitrary shape floating body, the open water solution is used instead.

4

Numerical Hydromechanics Approach for Open Water Condition

This chapter is intended to discuss about the implementation of the theory, to construct a matrix equation of motion for an arbitrary shape floating body in the open water sea condition. The discussion is presented in a narrative manner, in line with the code/function need to be generated in the programming tool being used (MATLAB). Every restrictions and concerns are mentioned in each respective section.

4.1. Numerical Model Generation

Regardless conducting an analysis for rigid body or solely analysis of the fluid motion itself (without body), a point coordinate information is needed. For the case of floating body analysis, one needs to build a numerical model and discretize it into a large number of panels. In this thesis, it must become a concern that the generated panel's shape has to be a quadrilateral. The developed MATLAB code will fail when any other type of polygons are present (e.g: triangular, hexagonal, etc.). As long as the panel has four corners (vertices), the analysis can proceed smoothly. For a panel with an extremely short distance between its corners, some problem about the accuracy of the solution raises. Generally speaking, the accurate and robust calculation time will be achieved when the element shape is not deviate too much from a rectangular shape. This is due to the reason that in the end, one of the term inside the Greens Function need to be integrated numerically over the panel area by MATLAB. These generated panels are assumed to be flat and have a constant source term over the surface (except specific case when the Greens Function gives an infinite solution/singular). This constant source lies in the center point of the panel.

There are two types of data input being used: one is generated from ANSYS, and one uses the standardized hydrodynamic software format so called "International Marine Software Associates (IMSA) format" and provided as an interface definition file (Idf.). The motivation of generating these two types of input is because by using ANSYS, one can "draw" the body by defining its dimensions, such as the width, length, depth, etc. In contrast, sometimes, describing the coordinates of 3D geometric object such as sphere, ellipsoid, wigley hull, etc. is much simpler by using a mathematical function. In both input, the center of floatation must be placed in the global origin coordinate system $(0,0,0)$. Both of the input formats are explained in the following sub-section. Basically, this section explains how to generate the mesh properly in order to get a 'read-able information (by the MATLAB code being created)' about the panel coordinates (vertices) of the floating body.

4.1.1. Input generated from ANSYS

A body geometric data generated from ANSYS must contain the whole shape of the wetted body (the immersed part), even though the body is symmetric. There are several things must present in the ANSYS output data:

- List of Nodes
  A list of nodes represents the vertices of panels which generated from the meshed body. In ANSYS mechanical APDL, one only needs to type NLIST, , , ,COORD before writing the /OUTPUT command to get this information.

- Element Data
  An element data represents the connectivity of the generated nodes. Apparently, the element data label generated by ANSYS contains more information, such as element numbers, materials, types, rel, esy, sec and nodes. Only the element number and the nodes are treated in the developed MATLAB codes. Any other information about element parameter are neglected. ELIST is the command need to be written.

- List of Key-points
  The meshing procedure by ANSYS is determined by key-points. The nodes are generated between these points. Moreover, the ordering number of these key-points needs to be done in a clockwise direction to obtain unit vectors pointing outward direction, otherwise the panel faces the inner-side (the dry-side) of the body. Basically, this can be done while defining the plane area between those points. KLIST is the command need to be written.

- List of Lines
  A list of lines provides an information to calculate the water plane area which becomes an important key to determine hydrostatic coefficient automatically. LLIST is the command need to be written.

A complete example of the input command in ANSYS including the generated output format which going to be used for analysis are provided in Attachment 1. Example ANSYS Mechanical APDL Command to Generate The Geometric Model & Attachment 2. Example Geometric Input Generated FROM ANSYS. The following figure visualizes the information listed above.

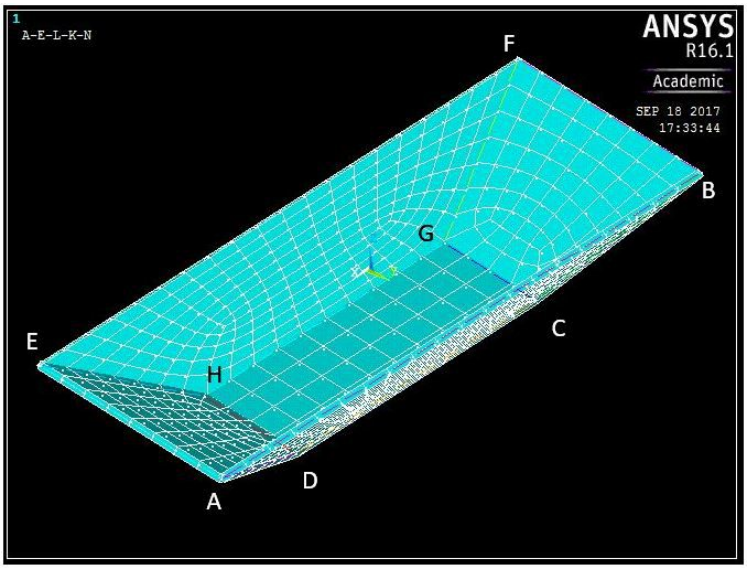

Figure 4.1: Example ANSYS Model

Point A,B,C,D,E,F,G,H are the key-points. To generate the appropriate direction of normal unit vectors in the starboard side, the plane area must be defined from ABCD /BCDA /CDAB/ DABC instead of ADCB,etc. Same goes for the other sides (BFGC,FEHG,AEHD,GCDH). Every line connecting these key-points has to be selected before being exported in ANSYS.out.

4.1.2. International Marine Software Associates [IMSA]Input Format

In contrast with the input format generated from ANSYS, when the IMSA input format is chosen, one needs to be aware that this format only capable to handle a symmetric shape floating body. Only half of the wetted body needs to be modelled from the bow to the aft. A crucial information about this input format is about the number of grids in the X and Y directions. They must be input correctly and represent a correct number of the generated node coordinate data which calculated beforehand. If the number of grids and the generated nodes do not match, an error message will appear.

On the other hand, the order of coordinate data also becomes a crucial input. It must be assured that the coordinate data is sorted in ascending order from the same X, Y, then Z respectively. If the input is not provided in this way, the whole calculation will give completely incorrect results. This is because the MATLAB

script developed in this thesis reads the geometric output in *"slice by slice"* manner, from the coordinate which has the same lowest X (and does not necessarily have the same Y and Z at the same time), until the highest X coordinates. It is similar to grouping the stern coordinates and move discretely to the bow. In addition, the geometric meshing in the vertical (Z) direction is not possible. It means, every perfectly vertical panel cannot be modelled (discretized) by using this input format. When one needs to model a ship with transoms, or any other un-ship-shaped structure with large vertical walls (e.g: Barge, Semi-submersible, etc.), the ANSYS input format is the one must be used.

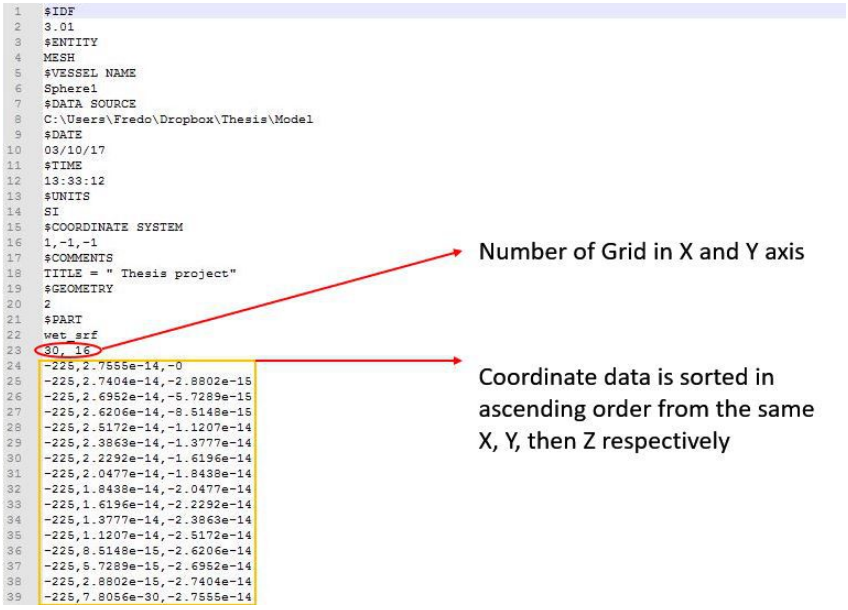

Figure 4.2: Example IMSA Format Input

A complete example of the IMSA input format is provided in Attachment 3. Example Geometric Input Generated in IMSA Format.

4.2. Dispersion Relation

The dispersion relation is one of the most important equations in the linear wave theory. The derivation of the expression can be found in many reference. The final form of the equation is given by

$$k\tan(kH) = -\alpha$$

The above equation is a transcendental equation. The roots (k) depends whether the solution is proportional to $\exp(-i\omega t)$ or $\exp(i\omega t)$. When one assumes that all variables are proportional to $\exp(-i\omega t)$, the solution in complex plane consists a pair of imaginary roots (propagating roots) and infinitely many real roots (evanescence roots). In contrast, when the variables are assumed to be proportional to $\exp(i\omega t)$, the solution is given by a pair of real roots (propagating roots) and infinitely many imaginary roots (evanescence roots). To give more insight about the occurrence of these roots, the following figures illustrate the obtained values for different water depths and frequencies. All of variables are assumed proportional to $\exp(-i\omega t)$.

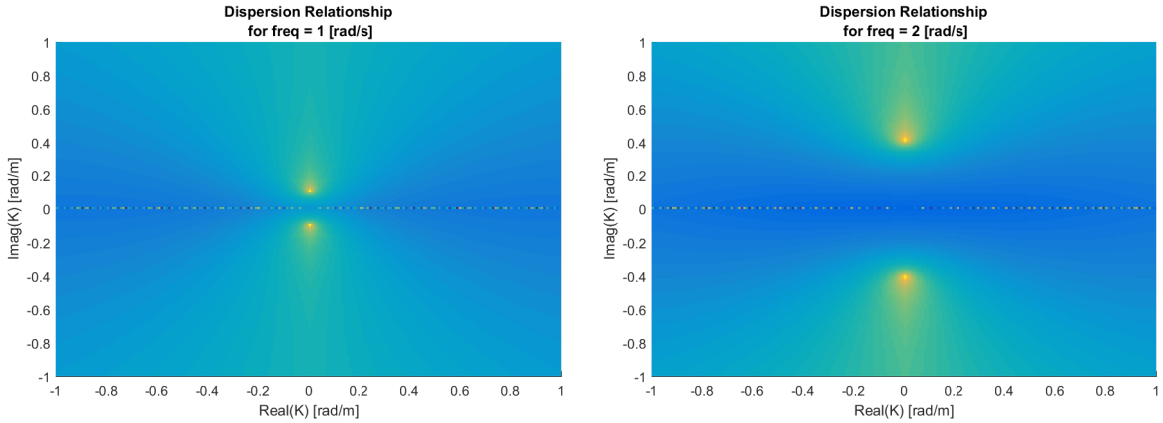

Figure 4.3: Dispersion Equation at 200 m Water Depth

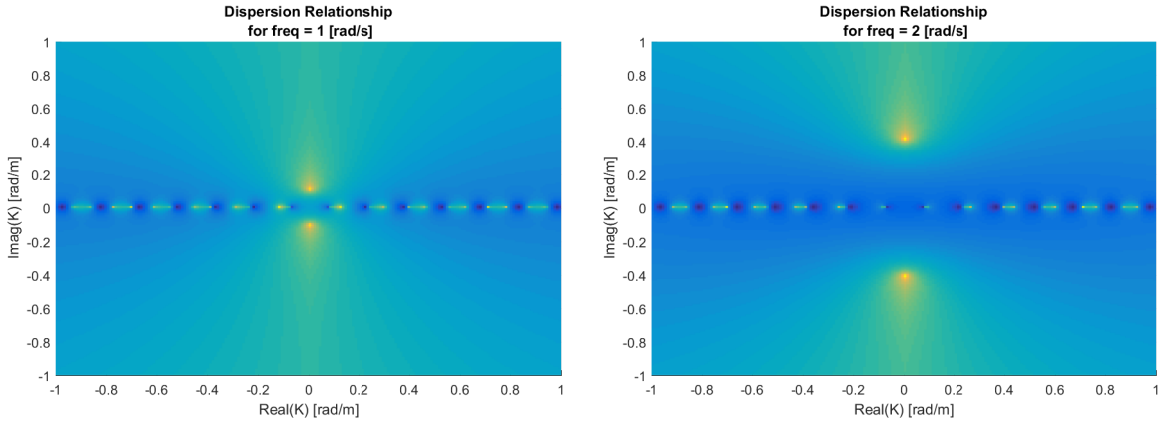

Figure 4.3: Dispersion Equation at 20 m Water Depth

The figures given above are the plot of $(|1/(k\tan(kH)+\alpha)|)$ in a complex plane. When the dispersion relation is satisfied, the plot gives an infinite value represented by the singular points. It can be seen that for the same water depth, the propagating root is higher (the shorter the wavelength) for a higher frequency. On the other hand, it can be seen that the deeper the water, there are a lot more evanescence roots occurring in the same wave number range, compare to the shallow water case.

4.3. Greens Function (Integral Solution Form)

It is already mentioned that the fundamental property must be obtained is the potential. These potentials are derived based on several boundary equations mentioned in chapter 2:*General Formulation of The Problem*. As one can see, these boundary equations relate physical quantities of the flow and presented as a partial differential equation. The solution of potentials can be reformulated as an integral equation by using Greens Theorem. The whole formulation specified in the following are derived based on point sources with strength -4π reside at the point $(\hat{x}_n, \hat{y}_n, \hat{z}_n)$.

The characteristic of fluid in the real life basically is irregular, both in space and time. The potential which can fully describe the fluid behavior can be expressed in the function of time. In order to account this time dependency, the potential is expressed in a harmonic function. As one already knows that any arbitrary function can be represented as a superposition of infinitely many harmonic functions with different frequencies and amplitudes, it is always a good start to express the time dependency as a simple harmonic function in one frequency.

$$\Phi_{(x,y,z,t)} = \bar{\phi}_{(x,y,z)} e^{i\omega t}$$

In order to derive the Greens Function, a written expression as given in the reference [11] is adopted

$$\bar{\phi} = -i\omega \sum_{j=0}^{7} \phi_j \zeta_j$$

$$\bar{\phi} = -i\omega \left((\phi_0 + \phi_7)\zeta_0 + \sum_{j=1}^{6} \bar{\phi}_j \zeta_j \right)$$

with index $i = 0, 1-6, 7$ for wave,radiation, and diffraction potential respectively.

From above notation, it is clear that the unit of potential changes. Φ expresses the complete dependency (time and space) of a *velocity* potential (unit = [m^2/s]) and the $\bar{\phi}$ is its complex magnitude of the oscillation (space dependent part). One must be aware that the assumed form of the potential is proportional to $\exp(i\omega t)$ which gives pair of real propagating root and infinitely many evanescence roots. The introduced notation ϕ is another expression of the potential (sort of magnitude base for *displacement* potential, with unit [m] in the physical sense). The derivation of Greens Function is based on this potential ϕ. Even though the derivation of Greens Function for the open water case is not extensively explained in this thesis (the solution is taken from the work done by Wehausen,J.V. and Laitone,E.V. [20]), above explanation about the unit is a good way to keep in track with the physical meaning behind it. Wehausen,J.V. and Laitone,E.V. [20] expressed the source disturbance in the Laplace Boundary Condition. They assumed the solution of this partial differential equation in the form of

$$G_{(x,y,z,\hat{x},\hat{y},\hat{z},t)} = G_{1(x,y,z,\hat{x},\hat{y},\hat{z},\omega)} \cos(\omega t) + G_{2(x,y,z,\hat{x},\hat{y},\hat{z},\omega)} \sin(\omega t)$$

With $G_1 = \frac{1}{r} + w$ as shown in chapter 2.2. *Problem Formulation.* It can be shown that by implementing point source with strength -4π, above solution is exactly agree with fundamental solution of Laplace equation superimposed by another assumed potential (w). Basically one can assume a solution in any kind of form for the same boundary value problem. The imaginary part ($G_{2(x,y,z)}$) is determined in such a way to satisfy the radiation boundary condition at infinity. By implementing the Greens Function, a set of boundary equations can be rewritten in the forms

- Continuity condition
  $\nabla^2 G_i = \delta(\hat{x} - x)\delta(\hat{y} - y)\delta(\hat{z} - z)$, for $i = 1, 2$
- Free surface boundary condition
  $\frac{\partial G_{i(x,y,0)}}{\partial z} - \alpha G_{i(x,y,0)} = 0$, for $i = 1, 2$
- Far away from the ship (Sommerfeld Radiation Condition)
  $\lim_{R\to\infty} \sqrt{R}\left(\frac{\partial G_1}{\partial R} + \alpha G_2\right) = 0$ and $\lim_{R\to\infty} \sqrt{R}\left(\frac{\partial G_2}{\partial R} - \alpha G_1\right) = 0$
- Sea bed boundary condition
  $\frac{\partial G_{i(x,y,-H)}}{\partial z} = 0$, for $i = 1, 2$

Above equations are the boundary equations mentioned in chapter 2.2.1. *Boundary Conditions* rewritten in the G form. The positive sign inside Sommerfeld Radiation Condition also reflects that the time dependence is assumed in the form $\exp(i\omega t)$. First of all, those boundary equations are transformed into the wave number frequency domain. The solution of Greens Function is obtained by substitution of the assumed solution into transformed partial differential equations one by one as done in chapter 3. *Derivation of 3D Greens Function for Ice-Infested Waters.* The delta functions in the first condition are automatically satisfied by term (1/r), therefore the other assumed potential (w) only needs to satisfy a Laplace equation instead. For the other conditions, both of (1/r) and (w) must be substituted simultaneously. After the unknown constants are obtained, the solution is transformed back to the space coordinate and time domain. The final solution is given in the form:

$$G_{(x,y,z,\hat{x},\hat{y},\hat{z},t)} = \left[\frac{1}{r} + \frac{1}{r_1} + PV \int_0^\infty \frac{2(\xi + \alpha) e^{-\xi H} . \cosh \xi(H + \hat{z}) . \cosh \xi(H + z)}{\xi \sinh \xi H - \alpha \cosh \xi H} . J_0(\xi R) d\xi \right] \cos(\omega t)$$

$$+ i \left[2\pi \frac{(k^2 - \alpha^2)}{(k^2 - \alpha^2)H + \alpha} . \cosh k(H + \hat{z}) . \cosh k(H + z) . J_0(kR) \right] \sin(\omega t)$$

or summarized as

$$G_{(x,y,z,\hat{x},\hat{y},\hat{z},t)} = [G_a + G_b + G_c]\cos(\omega t) + i[G_d]\sin(\omega t)$$

with
$G_a = \frac{1}{r} = \frac{1}{\sqrt{(x-\hat{x})^2+(y-\hat{y})^2+(z-\hat{z})^2}}$
$G_b = \frac{1}{r_1} = \frac{1}{\sqrt{(x-\hat{x})^2+(y-\hat{y})^2+(z+2H+\hat{z})^2}}$
$G_c = PV\int_0^\infty \frac{2(\xi+\alpha)e^{-\xi H}.\cosh\xi(H+\hat{z}).\cosh\xi(H+z)}{\xi\sinh\xi H-\alpha\cosh\xi H}.J_0(\xi R)d\xi$
$G_d = \frac{2\pi(k^2-\alpha^2)}{(k^2-\alpha^2)H+\alpha}.\cosh k(H+\hat{z}).\cosh k(H+z).J_0(kR)$
and
$R = \sqrt{(x-\hat{x})^2+(y-\hat{y})^2}$

It is quite clear that every term has the unit [1/m]. Several terms expressed above are discussed separately in the following chapter. The G_a is addressed as the fundamental Rankine source term, G_b is its image below the seabed, G_c and G_d represent the wave source terms. In case of infinite water depth, the G_b is not present and substituted by the image of Rankinse source term above the free surface instead. Moreover, the wave source term part (G_c and G_d) will has much simpler expression. This difference is not going to be discussed any further because this thesis only cover the finite water depth problem. Roughly speaking, infinite depth is particular case of finite depth problem.

4.3.1. Fundamental Rankine Source Term $[G_a]$ (Real Part)

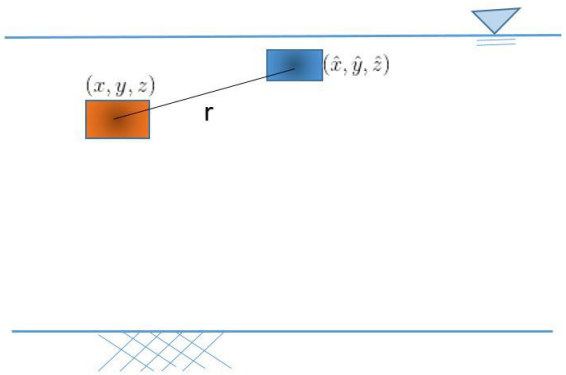

Figure 4.4: Fundamental Rankine Source Term

The Fundamental Rankine source term represents the influence at field point (x,y,z) due to source point at $(\hat{x},\hat{y},\hat{z})$ as visualized in above figure. This term is originally derived as a fundamental solution of the Laplace equation in 3D domain. It goes to infinity (singular) for evaluation at its own point. Since only at an infinitely small point the magnitude is infinite, total influence over the panel will be finite. Therefore, by doing surface/double integration over the panel, the magnitude of influence function can be determined. Detail of the integration approach over a quadrilateral panel is elaborated further in the section 4.9. *Panel Integration*. To give an idea about a distribution of the influence over a panel, the following figure illustrates a field panel influence due to its own source, over a rectangular panel.

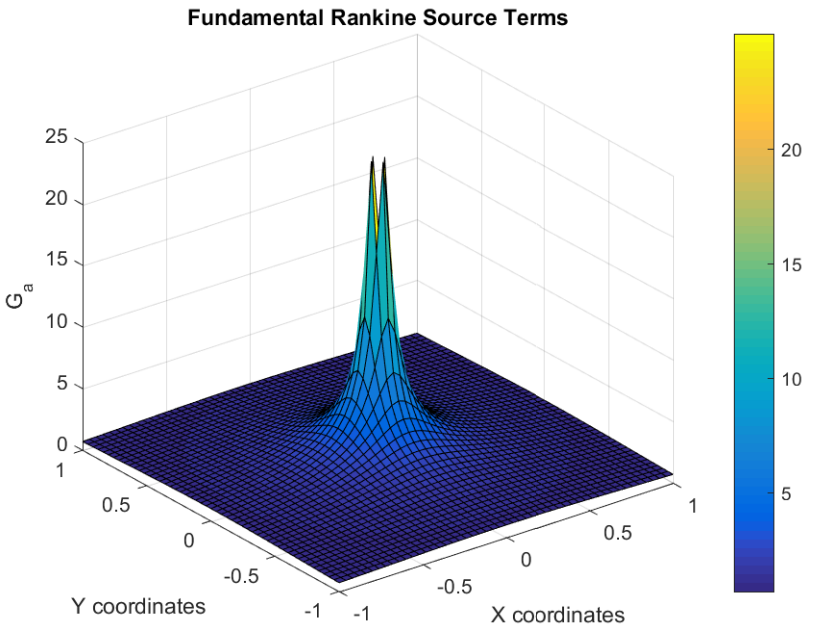

Figure 4.5: Fundamental Rankine Source Term Over Rectangular Panel Due to Its Own Source

4.3.2. Rankine Image Source Below Seabed $[G_b]$ (Real Part)

Together with the fundamental Rankine source term, the source image below seabed reproduces a similar physical characteristic of the seabed line. This term will never be singular. The illustration about this term is given in the following figure.

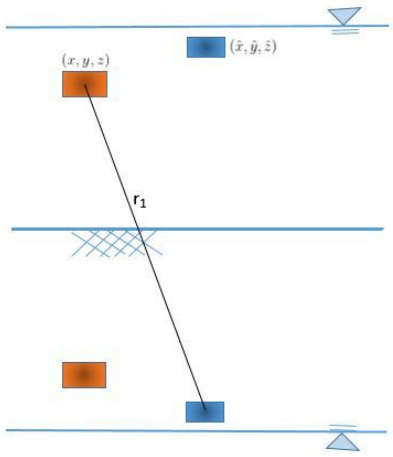

Figure 4.6: Rankine Image Source Below Seabed

About its distribution over the panel, the calculation is approximated by an evaluation of the influence at the panel's center point and multiply by panel area. The following figures represent the distribution. Figure (a) shows the distribution when the field and source points are close to the seabed whereas figure (b) visualizes the distribution as the distance grows. As one can see, for the case (b), the approximation by multiplying the influence at center point with panel area is a relatively good approximation since as long as the distance r_1 is far enough, there is no big difference of the influence over the panel surface/sides.

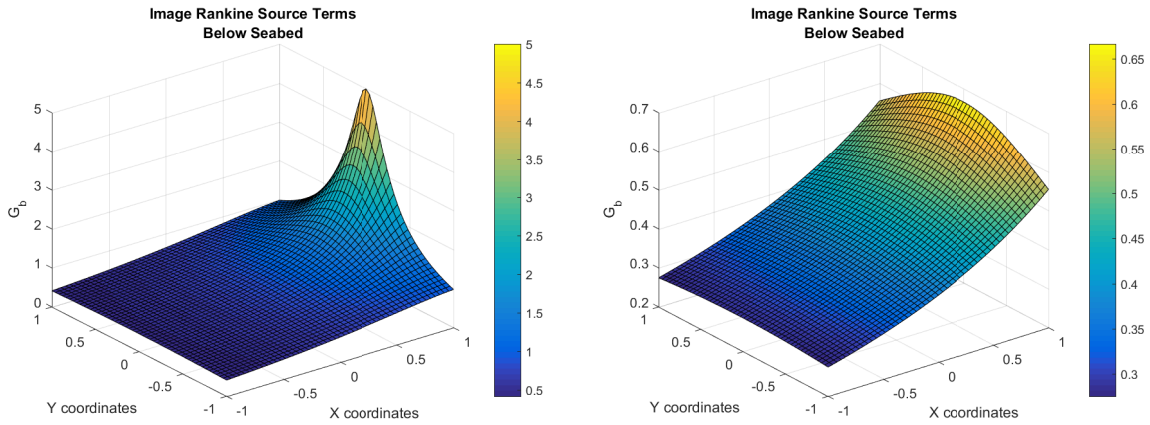

(a) (b)

Figure 4.7: Rankine Image Source Below Seabed Over The Panel

4.3.3. Wave Source Term (Real and Imaginary Part)

G_c **(Real Part)**

The real part of the wave source term evaluation is relatively cumbersome. The denominator of the G_c is a dispersion relationship itself, which means that the poles of integrand are just a propagating root and an infinitely many evanescence root. The principal value of the integral can be calculated by contour integration method over a complex number domain or by omitting the pole, then integrate it in its axis of integration. The latter one is chosen because it is relatively easy to be done. This means that the integrand is evaluated along the propagating root axis by excluding the positive real root of dispersion equation.

Even the pole location is evident, some numerical issue arises during evaluation of the integrand. Two cosines hyperbolic terms in the nominator and denominator easily overshoots the results into a number bigger than maximum double precision floating point that MATLAB can handle (overflow computation). This is an undesirable process of numerical integration since above integrand is finite (visualized by the following figures). This issue gives a NaN output when the ξ goes higher, and never reach $\xi = \infty$. Apparently, a subroutine can be made in such a way that the numerical integration process is stopped just before the hyperbolic terms result in infinite values. As a consequence of doing this, a lot of precision will lost during numerical integration (figure (a)). To encounter this problem, the integrand is rewritten as an exponential form. It is known that $\sinh(x) = (e^x - e^{-x})/2$ and $\cosh(x) = (e^x + e^{-x})/2$. By implementing these identities, an alternative form of the same integrand can be written as:

$$G_c = PV \int_0^\infty \frac{(\xi+\alpha)e^{\xi(\hat{z}+z)}.\left(1+e^{-2\xi(H+\hat{z})}\right).\left(1+e^{-2\xi(H+z)}\right)}{\xi.\left(1-e^{-2(\xi H)}\right)-\alpha.\left(1+e^{-2(\xi H)}\right)} J_0(\xi R)d\xi$$

Above form ensures that overflow computation will not happen. The exponents terms on both nominator and the denominator are always negative (therefore it converges) as long as $z \neq \hat{z} \neq 0$, which physically means, there should not be any panel's center point lies exactly on the free surface line. Two figures below represent the behavior of integrand after and before the modification into an exponential form.

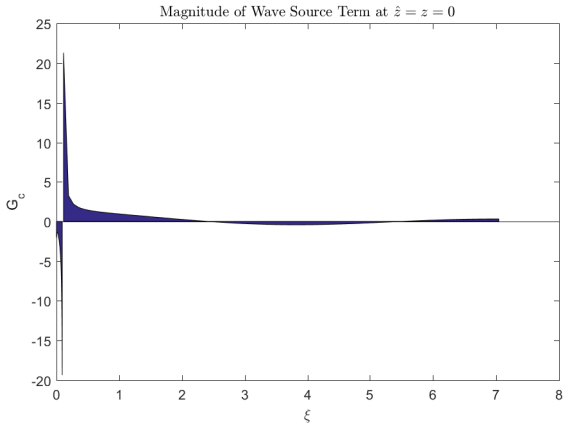

(a) Original integrand of wave source term

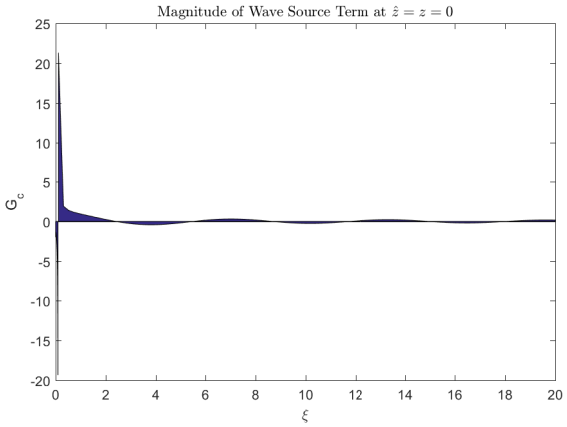

(b) Modified integrand of wave source term

As one can see from the above figures, propagating root of the dispersion equation lies in $\xi_p = 0.1019$ based on a certain specific input example. This is the value of ξ where G_c goes to infinity (the pole). After ξ goes around 7 (figure (a)), the nominator of integrand exceeds the extreme floating point number and therefore, the G_c results in NaN and cannot be evaluated (represented by the discontinuity of the tail). Even the integrand clearly converges, behavior of the tail can not be captured. After rewriting the equation in an exponential form, this undesired behavior can be avoided (figure (b)), and the integrand can be evaluated until infinity. From $\xi = 0$ up to slightly below the pole ($\xi_p - 10^{-8}$), the integrand is evaluated along the real axis. Around the pole, the integration path is shifted in complex-number domain with the same tolerance ($\xi_p \pm i10^{-8}$). In the end, from $\xi_p + 10^{-8}$ into infinity, the integrand can be evaluated back in its propagating root axis (see the following figure). Since G_c is a real function, the integration along the real axis gives a real result. In contrast, the integration paths around the pole which going to the (positive and negative) imaginary plane give the imaginary results. However, these results compensate each other and the whole integration process gives an exact real result which is in agreement with what expected (real part of the wave source term).

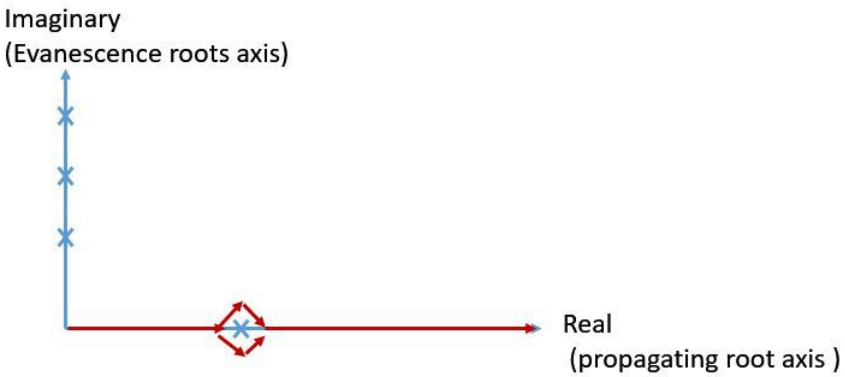

Figure 4.9: Path of Integration

G_d (Imaginary Part)

An evaluation the imaginary part of the wave source term has a different computational issue. There is no singularity problem arise. The nominator is always positive and the zeroth order Bessel function of the first kind never gives an infinite result. However, when the water depth (H) is quite deep, the propagating root of dispersion equation (k) is very close to the wave number of infinite water depth (α). If this difference cannot be captured (if the evaluation of the dispersion equation cannot give a high precision propagating root), this term gives a zero value. The resulting damping coefficient in the end will be zero as well. This phenomenon is illogical because it means physically, there is no energy being dissipated by the system. Basically, this problem can be encountered by using an infinite depth solution of the Greens Function. Another effort to rewrite the equation in slightly different form might work as well.

Further discussion about this is elaborated together with the alternative solution (infinite series) form in the following section. For visualization purposes, the distribution of these wave influence sources (real and imaginary part) is plotted in the following figures. It is shown that an approximation of influence function over the panel by multiplication with panel area will overestimate the result. However, the workload to improve accuracy of the results is rising quite significantly and generating an accurate result itself is not really the aim of this thesis, therefore, it is going to be neglected for a time being.

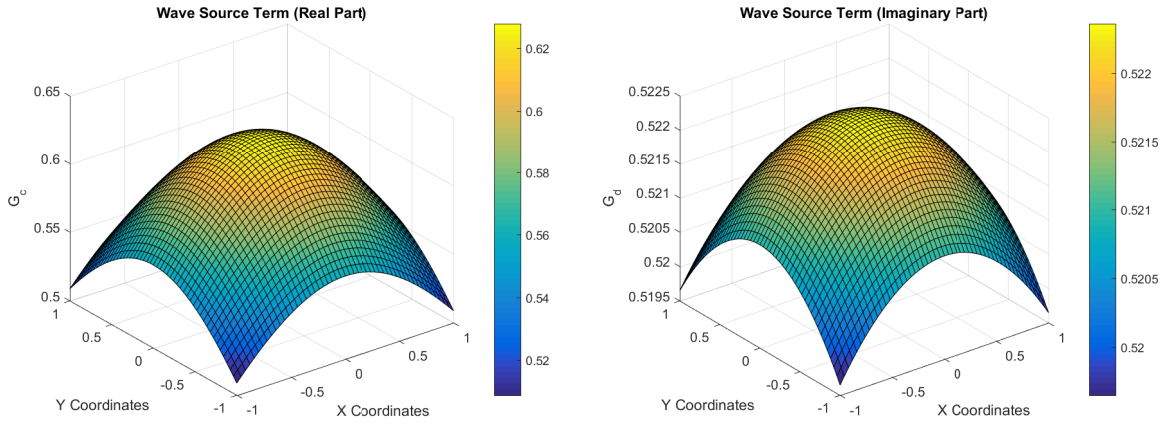

(a) Wave Source Term Over The Panel (Real)

(b) Wave Source Term Over The Panel (Imaginary)

4.4. Numerical Efficiency of the Greens Function (Infinite Series Form)

From the previous section, it is known that in order to acquire a single influence function in a point, one needs to do a numerical evaluation of wave source term (real part) which cannot be done instantaneously. This is a relatively unfavorable issue considering the number of points (panels) which must be evaluated is in order hundreds-thousands. In addition, to understand the dynamic characteristic of a system, one needs to evaluate the matrix equation of motion from different excitation (wave) frequencies. Moreover, even though an analytical solution related to *surface* integral of fundamental Rankine source term (1/r) over an arbitrary quadrilateral panel has been found, in this thesis (for simplicity purpose and establish a more generic method to integrate an arbitrary function: e.g. Greens Function for ice-infested waters), this distribution is also integrated numerically instead. This fact also adds quite a large amount of computational time. This means, that the evaluation of the Greens Function by using the original integral equation is not really efficient. An alternative form which can give more robust solution might be used for. Based on the eigenfunction expansion method, a solution of the same boundary value problem derived by John (1950)[10] is given as

$$G(x,y,z,\hat{x},\hat{y},\hat{z},t) = [G_1]\cos(\omega t) + i\,[G_2]\sin(\omega t)$$

with

$$G_1 = \left(4\sum_{n=1}^{\infty}\frac{k_n^2+\alpha^2}{(k_n^2+\alpha^2)H-\alpha}\cos k_n(z+H)\cos k_n(\hat{z}+H)K_0(k_nR)\right) - \left(2\pi\frac{k^2-\alpha^2}{(k^2-\alpha^2)H+\alpha}\cosh k(z+H)\cosh k(\hat{z}+H)Y_0(kR)\right)$$

$$G_2 = \left[2\pi\frac{k^2-\alpha^2}{(k^2-\alpha^2)H+\alpha}\cosh k(z+H)\cosh k(\hat{z}+H)J_0(kR)\right]$$

and
$\alpha = \frac{\omega^2}{g}$ (infinite water depth wave number)
$R = 1/\sqrt{(x-\hat{x})^2+(y-\hat{y})^2}$
$K_0 = \text{zero}^{th}$ order modified Bessel Function of the second kind
$Y_0 = \text{zero}^{th}$ order Bessel Function of the second kind
$J_0 = \text{zero}^{th}$ order Bessel Function of the first kind

It is completely clear that the above formula is somewhat become an alternative solution to avoid the principal value integration of the original integral solution. The imaginary part (G_d) from integral solution is exactly the same with the (G_2) above. From a computational point of view, this alternative solution is much

more convenient rather than the original integral solution. Generally speaking, this infinite series form is applicable in any region, except for the case when the horizontal distance between source and field point (R) is zero. John [10] explicitly stated that this alternative form of the Greens Function is valid only when $R > 0$. The modified Bessel Function of the second kind (K_0) gives ∞ for $R = 0$. It means, this alternative approach fails and the original integral solution need to be used. This case is present in the determination of diagonal values inside the Greens Function matrix, which represent the influence of field points due to their own source ($x = \hat{x}, y = \hat{y}, z = \hat{z}$), and also in the case when field point is straight above/under source points ($x = \hat{x}, y = \hat{y}$). The latter case occurs when the floating body has perfectly vertical meshed sides/transoms.

Fundamentally speaking, for evaluation of an influence function at the field point due to its own source, the original integral equation fails as well. Fundamental Rankine source term (G_a) goes to infinity. However, since it is already discussed that the surface integration result of (G_a) over the panel is finite, the solution still can be found. It is obvious that integrating (over surface area) the fundamental Rankine source term (1/r) from the integral solution is much more convenient rather than integrating the whole infinite series solution.

To understand about the effectiveness of this alternative solution, study about the convergence rate has been conducted. From the equation given above, it is clear that only magnitude proportional to the cosines part (real part) needs to be evaluated until converge using the *evanescence roots (k_n)*. The magnitude of the sinus part (imaginary part) is calculated based on a *propagating root (k)* of dispersion equation. However, the *propagating root (k)* also influences the real part in expression inside the right bracket. It has a similar expression to the imaginary part, except for the Bessel function (Y_0 and J_0). However, since it does not influence the rate of convergence, but some sort of giving an amplitude base for the real part, the study is focussed for the left bracket part of the real solution (G_1).

In order to study about the behavior of the summation in every *evanescence root* (k_n), initially, left bracket expression of the real part is distinguished into four terms as

$$G_{(x,y,z,\hat{x},\hat{y},\hat{z},t)} = 4\sum_{n=1}^{\infty} G_a G_b G_c G d$$

with
$G_a = \frac{k_n^2+\alpha^2}{(k_n^2+\alpha^2)H-\alpha}$
$G_b = \cos k_n(z+H)$
$G_c = \cos k_n(\hat{z}+H)$
$G_d = K_0(k_n R)$

Above terms are plotted separately for particular input of ($x, y, z, \hat{x}, \hat{y}, \hat{z}$, and H) with respect to the evanescence roots (k_n) obtained. The results depicted below are G_a, G_b, G_c and G_d plotted from around 650 evanescence roots.

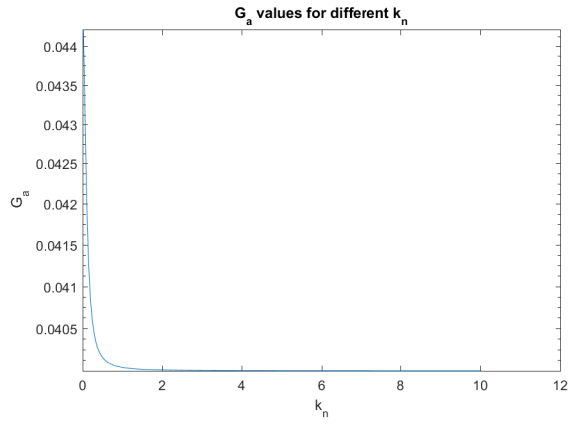

(a) First Term of the G

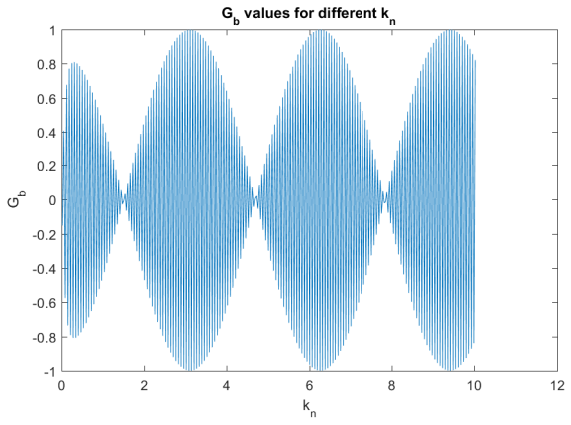

(b) Second and Third Term of the G

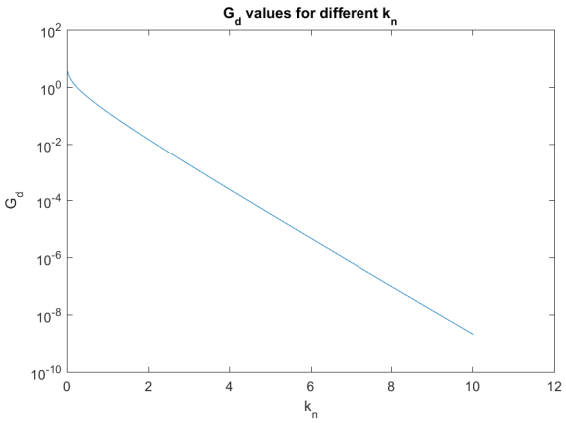

(c) Forth Term of the G

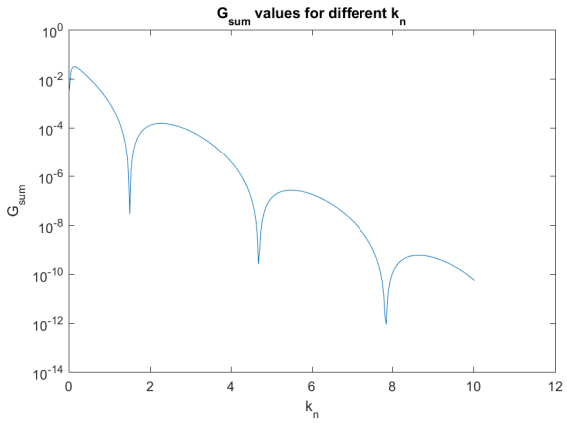

(d) Greens Function (Infinite Series Solution)

The first three graphs above (a,b,c) show the behavior of distinguished terms of the real part which evaluated using the evanescence roots. Figure (a),(c) and (d) are plotted in a semi-logarithmic scale. It must be noted that those terms must be multiplied each other. Figure (d) shows the result of multiplication ($G_{\text{sum}} = G_a G_b G_c G_d$) which represent the whole summation of the terms for every evanescence root that need to be summed up.

If one looks the behavior separately in each term, the first contribution (G_a) shows that after using several numbers of root, it converges into some constant value. Theoretically, this never be a zero value because the squared summation of an evanescence root and an infinite depth wave number ($k_n^2 + \alpha^2$) never be zero. The second and third contributions (G_b and G_c) are simply a sinusoidal behavior, which can be represented by the second graph (b). This means that they do not affect the rate of convergence. The last term (G_d) represented by the third graph (c). It is shown that G_d is converging exponentially (since it is semi-logarithmic scale) to zero constant value. When these terms are multiplied each other, term G_d is the one that governing the rate of convergence of the summation. This can be clearly seen in figure (d). The first term (G_a) initially contributes to tilt the slope of figure (d) until $k_n = 2$. Afterwards the prevailing slope of the figure (d) is kind of equal with slope (G_d) at the figure (c). It can be concluded that when G_d is extremely small, adding more roots will not give any significant difference. For a large number of modes (after G_a become constant), the rate of convergence solely depends on ($k_n R$).

However, it is obvious that an infinitely many evanescence root (k_n) is obtained from the dispersion equation $k_n \tan(k_n H) = -\alpha$. This dispersion relation is plotted in the following figures to give some idea about the characteristic of the roots.

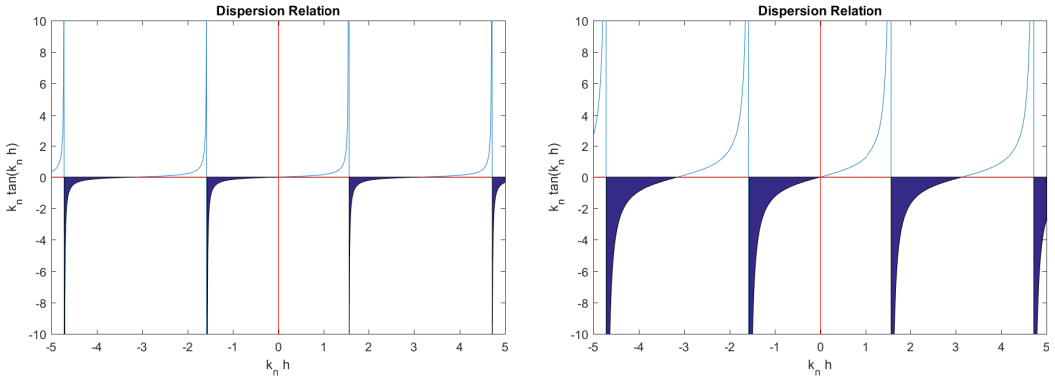

Figure 4.12: Dispersion Relation

The x axis in the above graphs is the ($k_n H$) which define the tangent, and the y axis is the dispersion equation. It is quite clear that the dispersion relation is satisfied when it gives a negative value ($-\alpha$) which occur in the blue hatched area. It can be concluded that the satisfying roots (k_n) appear in certain periodic function. The root k_n in front of the tangent term only affects the graph's curvature and does not affect the

periodical occurrence of the roots. Therefore, the occurrence of these roots can be formulated as

$$\pi(n-\frac{1}{2}) \leq k_n H \leq \pi n$$

with
$n = 1, 2, ..., \infty$
which depends on π, integer n and H. Recalling $G_d = K_0(k_n R)$ as the only governing term for the rate of convergence, the term inside zeroth order modified Bessel Function of the second kind can be represented by

$$\pi n R/H$$

Since π and integer n are just constant values, the rate of convergence in the end will solely depend on R/H. The number of roots needed to obtain a converge solution is calculated by

$$N = \hat{N} H/R$$

with
N = number of roots
$\hat{N}$ = dummy constant
and the $\hat{N}$ is determined based on a numerical test and specified degree of accuracy about the G compared to the integral solution.

In order to compare the effectiveness of series and integral solution, the influence function is calculated for different region of R/H. Those regions are:
– Region 1: $0 \leq$ R/H ≤ 0.0005
– Region 2: $0.0005 \leq$ R/H ≤ 0.05
– Region 3: $0.05 \leq$ R/H ≤ 0.5
– Region 4: $0.5 \leq$ R/H
On those regions, the influence functions are distinguished again in another 4 different value of R/H and also plotted in different normalized depth location. Results for the first region are shown in 4 graphs below.

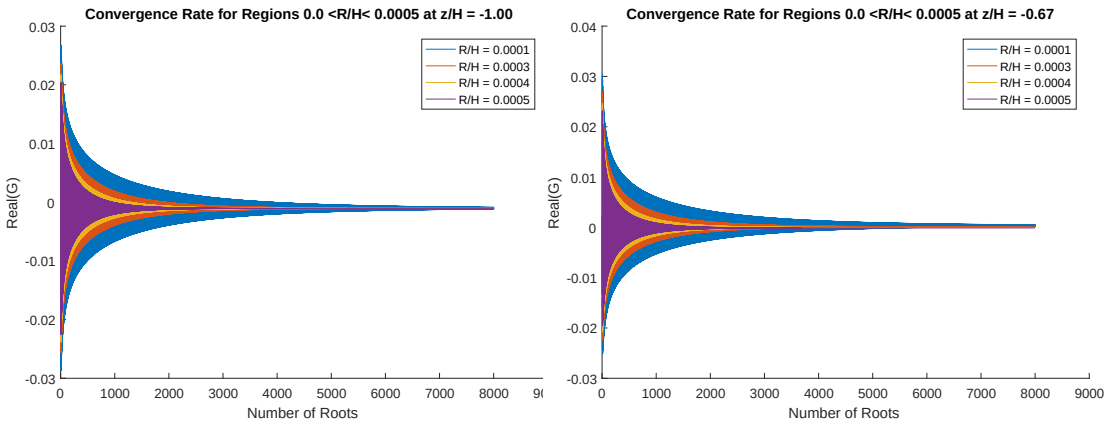

(a) Convergence of the series at seabed

(b) Convergence of the series at 2/3 water depth

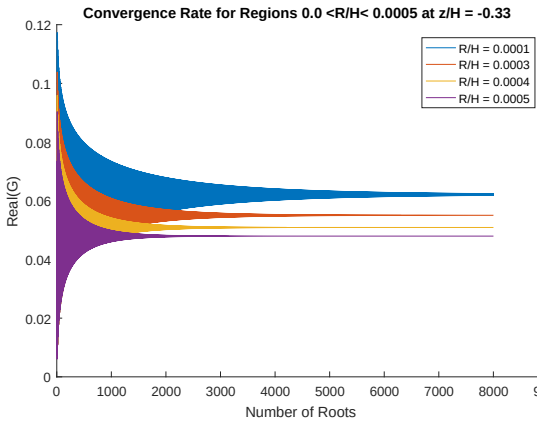

(c) Convergence of the series at 1/3 water depth

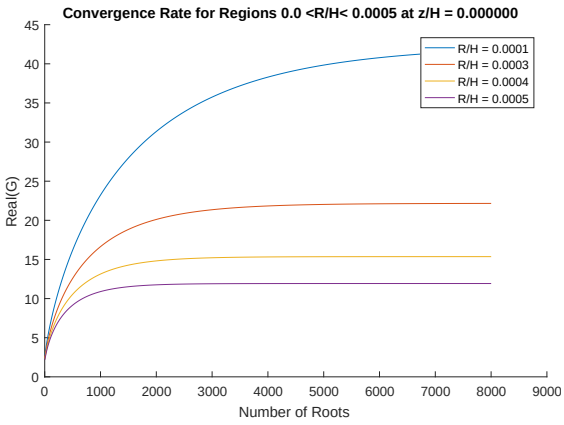

(d) Convergence of the series on the free surface

Figure 4.13: Real(G) Region $0 \leq R/H \leq 0.0005$

One general conclusion which could be taken from those graphs is the fact that in this region, the influence function needs a large number of roots to converge (up to 8000 evanescence roots). On the graph (a), the influence function converge to zero, which is in line with the fact that on the seabed, the influence is vanish (theoretically, it is not necessarily zero, but its derivative with respect to z instead). The R/H locations at each graph above (blue, red, yellow and purple lines) also determined in such a way in which they are proportional to the wave number. Each different line represents the same oscillating location of the trough/peak of the wave at an instantaneous moment in time. From graph (c) and (d), one can clearly see that as R/H goes larger, which means the examined field point is going further from the source point, the influence function also goes smaller (satisfying radiation boundary condition at infinity).

Generally, the behavior of influence functions in the other regions is the same with above. The only difference is the fact that the bigger the ratio R/H, the smaller number of evanescence roots need to be used to acquire converged solution. This is actually can already be seen from the graph (d) above. The blue line is the shortest distance between field and source point compared to the other lines (red, yellow and purple). It is shown that the blue line converged after around 8000 evanescence roots whereas for the other locations already converged before around 2000 roots.

However, to clearly see the difference, several graphs are provided in the following to visualize this behavior. Another 3 regions of R/H are presented together with four different locations of normalized depths in each region. The figures below are visualization of influence function for region 2: $0.0005 \leq R/H \leq 0.05$.

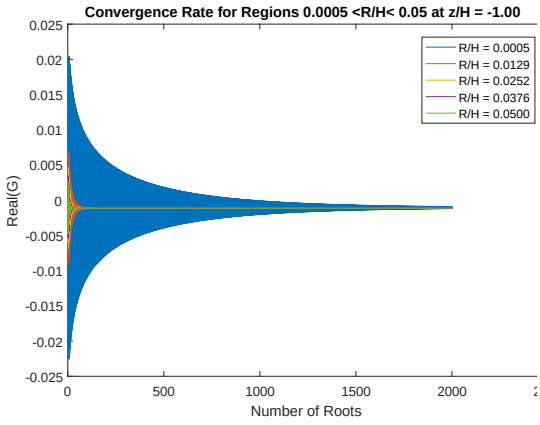

(a) Convergence of the series at seabed

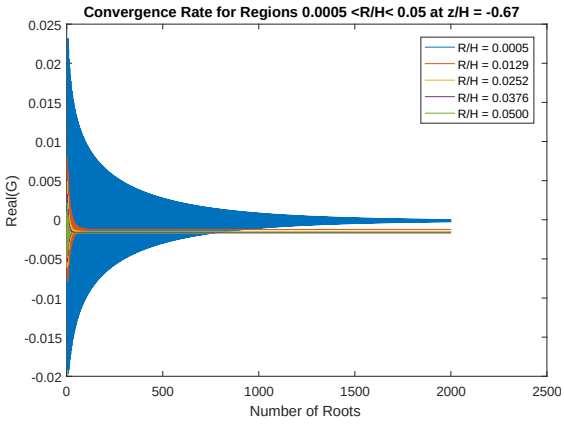

(b) Convergence of the series at 2/3 water depth

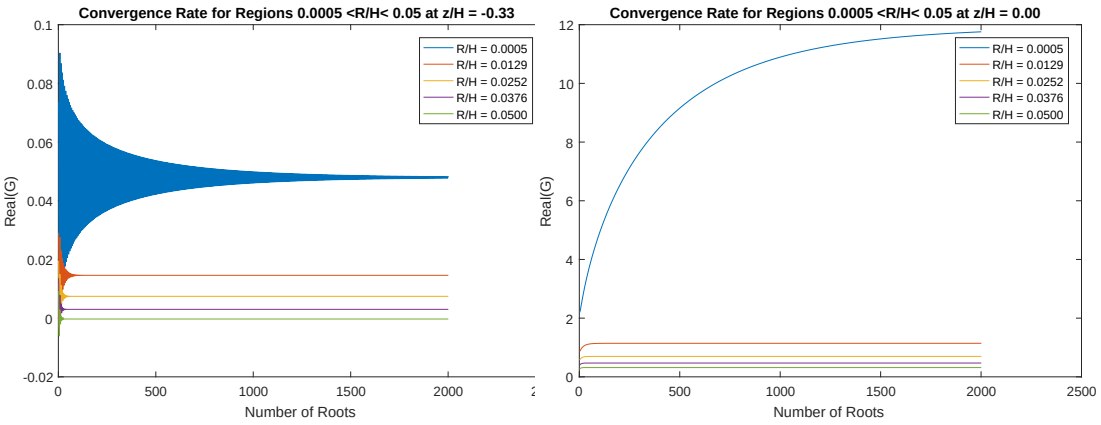

(c) Convergence of the series at 1/3 water depth (d) Convergence of the series on the free surface

Figure 4.14: Real(G) Region $0.0005 < R/h \leq 0.05$

It can be seen that after 2000 roots (does not necessarily need until 8000 roots), the smallest ratio of R/H, or can be said as the shortest distance to the source point (line blue, clearly seen in figure (d)), the influence function is already converge. The order of magnitude is also in agreement with the representative distance as discussed in previous region.

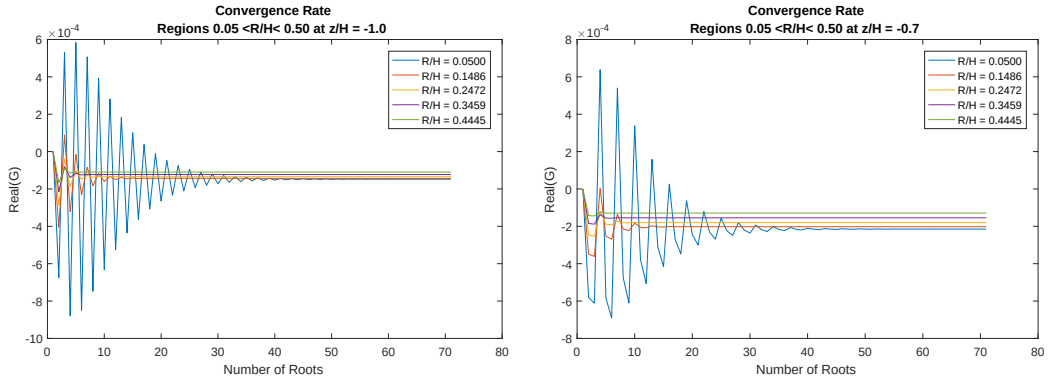

(a) Convergence of the series at seabed (b) Convergence of the series at 2/3 water depth

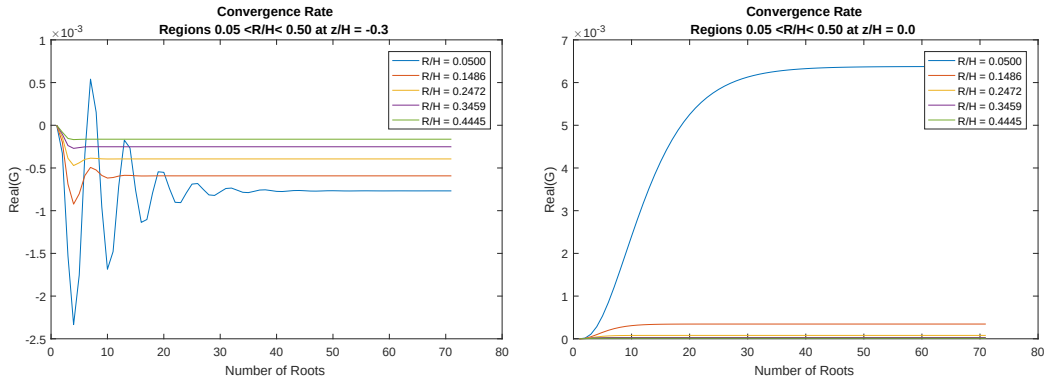

(c) Convergence of the series at 1/3 water depth (d) Convergence of the series on the free surface

Figure 4.15: Real(G) Region $0.05 < R/h \leq 0.5$

For region 3: $0.05 \leq R/H \leq 0.5$, the influence function converges quite soon. Less than hundred numbers of root are needed to obtain a converged solution.

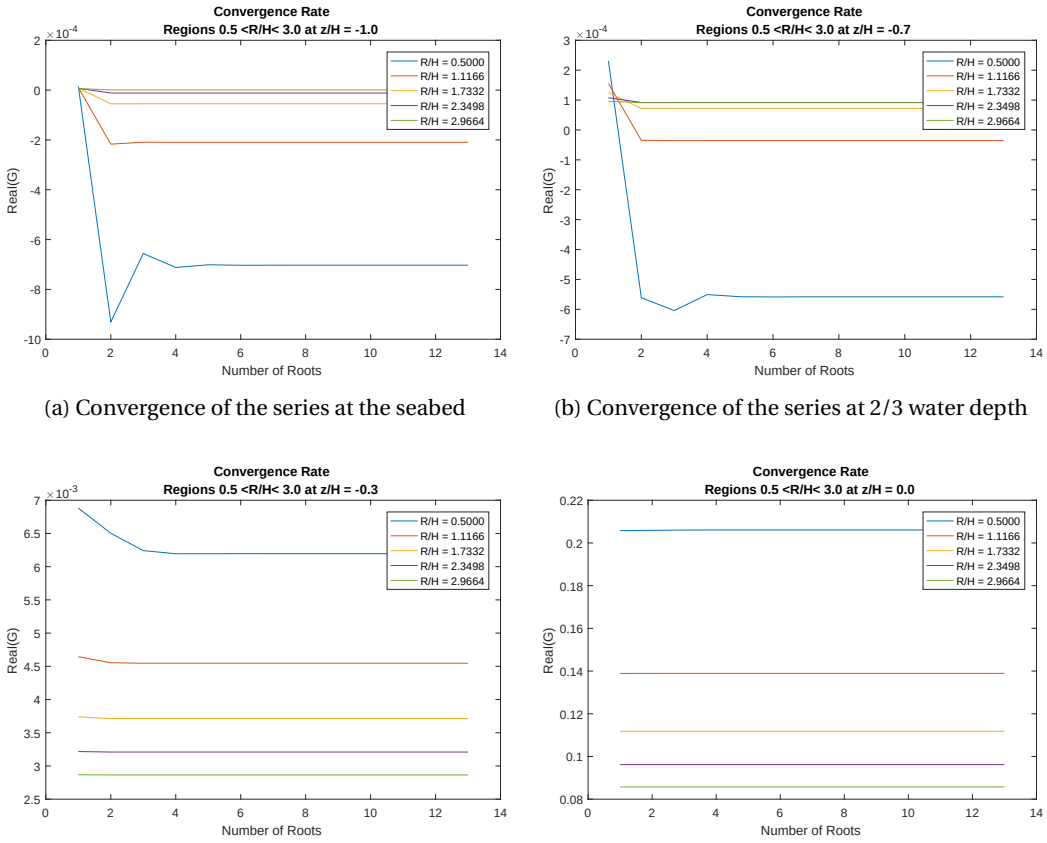

(a) Convergence of the series at the seabed

(b) Convergence of the series at 2/3 water depth

(c) Convergence of the series at 1/3 water depth

(d) Convergence of the series on the free surface

Figure 4.16: Real(G) Region 0.5 < R/h ≤ 3

Lastly, for region 4: 0.5 ≤ R/H, the influence function converges immediately by only using several numbers of evanescence root. It means that in this region, the infinite series solution is capable to improve the computation speed significantly compared to the integral solution. Based on several graphs above, previously plotted G_{sum} with respect to k_n and some numerical test, which is also stated in the work done by Newman (1984) [15], infinite series form can give an accurate solution (10^{-6} precision) when $N = 6H/R$ (obtained $\hat{N} = 6$). In order to quantify the effectiveness of this series solution based this specified accuracy, computation times between the infinite series and the integral solution are compared. This comparison is done in 4 different regions above and the results are summarized in the following figures.

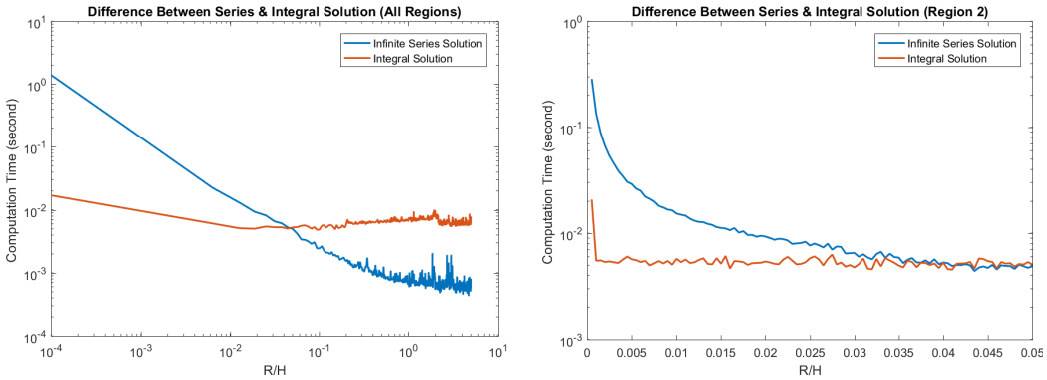

(a) Comparison of Computational Speed in All Region (b) Comparison of Computational Speed in Region 2

Figure 4.17: Computation Speed Difference Between Series and Integral Solution

From above figure, it is quite clear that for a small ratio of R/H, infinite series form is useless to provide a

more robust solution. This is where Newman [15] gave a significant contribution by introducing a "polynomial expansion" form (Chebhyshev polynomial) of the Greens Function. He implemented the infinite series only for region R/H > 0.5 , and using the polynomial expansion form for the other region. A recent research by Yingyi Liu [14] even make a great improvement of Newman's work by distinguishing the region into four, and using an epsilon algorithm to propose another approximation solution of Greens Function. This robustness issue is not going to be discussed any further. However, the evaluation at $R = 0$ still become a crucial thing which discussed in the latter chapter.

On the other hand, considering the fact that both of integral and the infinite series solution will be used together, it must be ensured that they really represent the correct evaluation of the problem. The graphs depicted below show a comparison of influence function at a field point, between infinite series and integral solution for different water depth and frequencies at a certain distance from the source point. These values are only the real part of the solution since the imaginary part from both forms are the same.

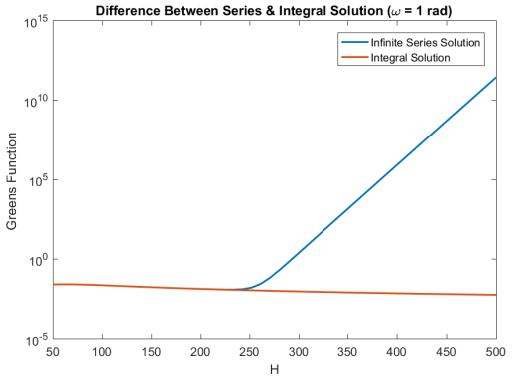

(a) Series vs Integral Solution for Different Water Depth

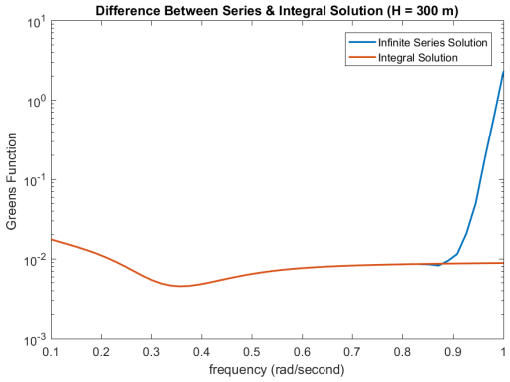

(b) Series vs Integral Solution for Different Wave Frequencies

From two graphs above, it can be seen that the integral and the infinite series solution initially are in a good agreement (give the same results). After reaching a specific water depth/frequencies, the difference between integral and the infinite series solution grows exponentially. Careful examination concludes that this issue is related to the wave number/propagating root. As soon as the deep water condition has been reached, the propagating root and an infinite depth wave number are indistinguishable. This issue can clearly be seen in the following figures.

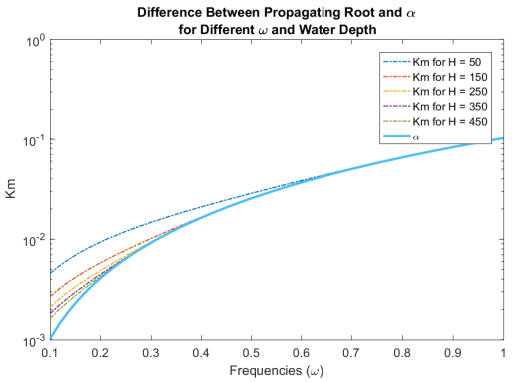

(a) K_m

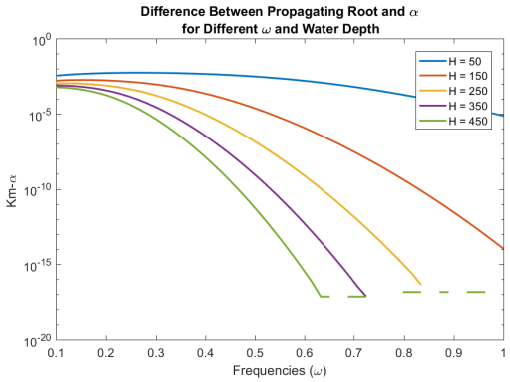

(b) $K_m - \omega^2/g$

Figure 4.19: Propagating Root and Infinite Depth Wave Number

Figure (a) shows the propagating roots and infinite depth wave number for different frequencies and water depth, whereas figure (b) shows the difference between them. It is clear that after 10^{-16}, the difference $(K_m - \alpha)$ cannot be captured. The reason behind it is because maximum number of decimal digits can be captured for double precision is 10^{-16}. Therefore, when this condition happens, the expression in the right

bracket of the infinite series solution (G_1) is become zero ($k^2-\alpha^2=0$). However, even though above comparison is only between the real part of both solutions and integral solution does not have this kind of issue, the imaginary part of both solutions have the same formulation except for the Bessel Function. This means, as long as the deep water condition being reached, the imaginary part of the Greens Function is zero as mentioned in chapter 4.3.3. *Wave Source Term (Imaginary Part).* Based on this restriction, by using the same form of Greens Function, one needs to specify the range of frequencies of interest based on water depth or vice versa. For example, from figure (b) above, for frequency range $0-1$ radian/second (maximum wave period 6.2 seconds), the maximum water depth can be evaluated is just slightly deeper than 150 meters (red line). Since this is quite undesirable limitation, another effort seems necessary to be done. An infinite depth solution of Greens Function (which has been discovered as well) can be implemented in this condition. Another alternative is by rewriting the integral solution in a slightly different manner as

$$G_{(x,y,z,\hat{x},\hat{y},\hat{z},t)} = \left[\frac{1}{r}+\frac{1}{r_1}+PV\int_0^\infty \frac{(\xi+\alpha)e^{\xi(\hat{z}+z)}.\left(1+e^{-2\xi(H+\hat{z})}\right).\left(1+e^{-2\xi(H+z)}\right)}{\xi.\left(1-e^{-2(\xi H)}\right)-\alpha.\left(1+e^{-2(\xi H)}\right)}J_0(\xi R)d\xi\right]\cos(\omega t)$$

$$+i\left[2\pi\frac{(k+\alpha)e^{-kH}\sinh(kH)}{\alpha H+\sinh^2(kH)}\cosh(k(\hat{z}+H))\cosh(k(z+H))J_0(kR)\right]\sin\omega t$$

Even though there is no ($k^2-\alpha^2$) present, the denominator ($\sinh^2$) term is also easily reach a value larger than the maximum double precision for a large value of H. Another effort to rewrite it in exponential form might help, but this is not going to be discussed any further. Up to this point, the evaluation of influence function still cannot assure to be correct. Above explanation so far, only gives a fact that the integral and the infinite series solution have the same results. One needs to validate them by checking all of boundary equations.

4.5. Validation of Greens Function

The boundary equations must be satisfied by the Greens Function are: continuity, seabed, free surface, and radiation conditions. In order to validate these conditions, one needs to determine the first and second derivative of Greens Function with respect to global direction (x,y,z). Since it is already checked that the integral and infinite series solution give reasonable the same results, the validation is done based on the infinite series solution. In this form, terms x and y only appear inside the Bessel function: $K_0(k_nR)$, $Y_0(k_nR)$ and $J_0(k_nR)$ with ($R=\sqrt{x^2+y^2}$) whereas the z term appears on the third term ($\cos(k_mz)$) with ($m=0-\infty$) and $k_0=ik$. Derivation of the Bessel Function is easily obtained by using the symbolic toolbox in MATLAB (MATLAB is provisioned with Bessel Functions) / Maple or any other similar program. The first derivatives of the infinite series solutions are given in equations below.

$$\frac{\partial G}{\partial m}=\frac{\partial G_1}{\partial m}\cos(\omega t)+\frac{\partial G_2}{\partial m}\sin(\omega t)$$

with $m=x,y,z$
and respectively, those expressions are given by

$$\frac{\partial G_1}{\partial x}=\left[4\sum_{n=1}^{\infty}\frac{k_n^2+\alpha^2}{(k_n^2+\alpha^2)H-\alpha}\cos k_n(z+H)\cos k_n(\hat{z}+H)\frac{k_nK_0(k_nR)(2x-2\hat{x})}{2R}\right]-\left[2\pi\frac{k^2-\alpha^2}{(k^2-\alpha^2)H+\alpha}\cosh k(z+H)\cosh k(\hat{z}+H)\frac{kY_0(kR)(2x-2\hat{x})}{2R}\right]$$

$$\frac{\partial G_2}{\partial x}=\left[2\pi\frac{k^2-\alpha^2}{(k^2-\alpha^2)H+\alpha}\cosh k(z+H)\cosh k(\hat{z}+H)\frac{kJ_0(kR)(2x-2\hat{x})}{2R}\right]$$

$$\frac{\partial G_1}{\partial y}=\left[4\sum_{n=1}^{\infty}\frac{k_n^2+\alpha^2}{(k_n^2+\alpha^2)H-\alpha}\cos k_n(z+H)\cos k_n(\hat{z}+H)\frac{k_nK_0(k_nR)(2y-2\hat{y})}{2R}\right]-\left[2\pi\frac{k^2-\alpha^2}{(k^2-\alpha^2)H+\alpha}\cosh k(z+H)\cosh k(\hat{z}+H)\frac{kY_0(kR)(2y-2\hat{y})}{2R}\right]$$

$$\frac{\partial G_2}{\partial y}=\left[2\pi\frac{k^2-\alpha^2}{(k^2-\alpha^2)H+\alpha}\cosh k(z+H)\cosh k(\hat{z}+H)\frac{kJ_0(kR)(2y-2\hat{y})}{2R}\right]$$

$$\frac{\partial G_1}{\partial z}=\left(4\sum_{n=1}^{\infty}\frac{k_n^2+\alpha^2}{(k_n^2+\alpha^2)H-\alpha}(-k_n)\sin k_n(z+H)\cos k_n(\hat{z}+H)K_0(k_nR)\right)-\left[2\pi\frac{k^2-\alpha^2}{(k^2-\alpha^2)H+\alpha}k\sinh k(z+H)\cosh k(\hat{z}+H)Y_0(kR)\right]$$

$$\frac{\partial G_2}{\partial z}=\left[2\pi\frac{k^2-\alpha^2}{(k^2-\alpha^2)H+\alpha}k\sinh k(z+H)\cosh k(\hat{z}+H)J_0(kR)\right]$$

The second order derivatives of the Greens Function are determined in the same manner by

$$\frac{\partial^2 G}{\partial^2 m} = \frac{\partial^2 G_1}{\partial^2 m}\cos(\omega t) + \frac{\partial^2 G_2}{\partial^2 m}\sin(\omega t)$$

with $m = x, y, z$
and respectively

$$\frac{\partial^2 G_1}{\partial x^2} = \left[4\sum_{n=1}^{\infty}\frac{k_n^2+\alpha^2}{(k_n^2+\alpha^2)H-\alpha}\cos k_n(z+H)\cos k_n(\hat{z}+H)\frac{\partial^2 K_0(k_nR)}{\partial x^2}\right] - \left[2\pi\frac{k^2-\alpha^2}{(k^2-\alpha^2)H+\alpha}\cosh k(z+H)\cosh k(\hat{z}+H)\frac{\partial^2 Y_0(kR)}{\partial x^2}\right]$$

$$\frac{\partial^2 G_2}{\partial x^2} = \left[2\pi\frac{k^2-\alpha^2}{(k^2-\alpha^2)H+\alpha}\cosh k(z+H)\cosh k(\hat{z}+H)\frac{\partial^2 J_0(kR)}{\partial x^2}\right]$$

$$\frac{\partial^2 G_1}{\partial y^2} = \left[4\sum_{n=1}^{\infty}\frac{k_n^2+\alpha^2}{(k_n^2+\alpha^2)H-\alpha}\cos k_n(z+H)\cos k_n(\hat{z}+H)\frac{\partial^2 K_0(k_nR)}{\partial y^2}\right] - \left[2\pi\frac{k^2-\alpha^2}{(k^2-\alpha^2)H+\alpha}\cosh k(z+H)\cosh k(\hat{z}+H)\frac{\partial^2 Y_0(kR)}{\partial y^2}\right]$$

$$\frac{\partial^2 G_2}{\partial y^2} = \left[2\pi\frac{k^2-\alpha^2}{(k^2-\alpha^2)H+\alpha}\cosh k(z+H)\cosh k(\hat{z}+H)\frac{\partial^2 J_0(kR)}{\partial y^2}\right]$$

$$\frac{\partial^2 G_1}{\partial z^2} = \left[4\sum_{n=1}^{\infty}\frac{k_n^2+\alpha^2}{(k_n^2+\alpha^2)H-\alpha}(-k_n^2)\cos k_n(z+H)\cos k_n(\hat{z}+H)K_0(k_nR)\right] - \left[2\pi\frac{k^2-\alpha^2}{(k^2-\alpha^2)H+\alpha}k^2\cosh k(z+H)\cosh k(\hat{z}+H)Y_0(kR)\right]$$

$$\frac{\partial^2 G_2}{\partial z^2} = \left[2\pi\frac{k^2-\alpha^2}{(k^2-\alpha^2)H+\alpha}k^2\cosh k(z+H)\cosh k(\hat{z}+H)J_0(kR)\right]$$

with

$$\frac{\partial^2 K_0(k_nR)}{\partial x^2} = \left(\frac{k_n\left(\frac{K_1(k_nR)(2x-2\hat{x})}{2((x-\hat{x})^2+(y-\hat{y})^2)} + \frac{k_nK_0(k_nR)(2x-2\hat{x})}{2R}\right)(2x-2\hat{x})}{2R} - \frac{k_nK_1(k_nR)}{R} + \frac{k_nK_1(k_nR)(2x-2\hat{x})^2}{4((x-\hat{x})^2+(y-\hat{y})^2)^{3/2}}\right)$$

$$\frac{\partial^2 K_0(k_nR)}{\partial y^2} = \left(\frac{k_n\left(\frac{K_1(k_nR)(2y-2\hat{y})}{2((x-\hat{x})^2+(y-\hat{y})^2)} + \frac{k_nK_0(k_nR)(2y-2\hat{y})}{2R}\right)(2y-2\hat{y})}{2R} - \frac{k_nK_1(k_nR)}{R} + \frac{k_nK_1(k_nR)(2y-2\hat{y})^2}{4((x-\hat{x})^2+(y-\hat{y})^2)^{3/2}}\right)$$

The same expressions are also valid for the other Bessel Functions (Y_0, J_0) by simply changing the (K_0).

Apparently, another singularity problem also appears in those expressions. The modified zeroth order Bessel Function of the second kind (K_0) still there and is singular when $R = 0$. This is also the case for the firstth order Bessel Function of the second kind (K_1) which occur in the second order derivatives. However, since in the beginning, the infinite series solution form is never going to be used for ($R = 0$), the derivative expression for the integral solution is also needed (only the real part due to the fact that the imaginary part is the same and not singular). These expressions are given in the following

$$\frac{\partial G}{\partial x} = \left[\frac{\partial}{\partial x}\frac{1}{r} + \frac{\partial}{\partial x}\frac{1}{r_1} + PV\int_0^{\infty}\frac{(\xi+\alpha)e^{\xi(\hat{z}+z)}.\left(1+e^{-2\xi(H+\hat{z})}\right).\left(1+e^{-2\xi(H+z)}\right)}{\xi.\left(1-e^{-2(\xi H)}\right)-\alpha.\left(1+e^{-2(\xi H)}\right)}.\frac{\xi J_0(\xi R)(2x-2\hat{x})}{2R}d\xi\right]\cos(\omega t)$$

$$\frac{\partial G}{\partial y} = \left[\frac{\partial}{\partial y}\frac{1}{r} + \frac{\partial}{\partial y}\frac{1}{r_1} + PV\int_0^{\infty}\frac{(\xi+\alpha)e^{\xi(\hat{z}+z)}.\left(1+e^{-2\xi(H+\hat{z})}\right).\left(1+e^{-2\xi(H+z)}\right)}{\xi.\left(1-e^{-2(\xi H)}\right)-\alpha.\left(1+e^{-2(\xi H)}\right)}.\frac{\xi J_0(\xi R)(2y-2\hat{y})}{2R}d\xi\right]\cos(\omega t)$$

$$\frac{\partial G}{\partial z} = \left[\frac{\partial}{\partial z}\frac{1}{r} + \frac{\partial}{\partial z}\frac{1}{r_1} + PV\int_0^{\infty}\frac{\xi.(\xi+\alpha)e^{\xi(\hat{z}+z)}.\left(1+e^{-2\xi(H+\hat{z})}\right).\left(1-e^{-2\xi(H+z)}\right)}{\xi.\left(1-e^{-2(\xi H)}\right)-\alpha.\left(1+e^{-2(\xi H)}\right)}.J_0(\xi R)d\xi\right]\cos(\omega t)$$

with
$\frac{\partial}{\partial x}\frac{1}{r} = \frac{-(2x-2\hat{x})}{2((x-\hat{x})^2+(y-\hat{y})^2+(z-\hat{z})^2)^{3/2}}$
$\frac{\partial}{\partial y}\frac{1}{r} = \frac{-(2y-2\hat{y})}{2((x-\hat{x})^2+(y-\hat{y})^2+(z-\hat{z})^2)^{3/2}}$
$\frac{\partial}{\partial z}\frac{1}{r} = \frac{-(2z-2\hat{z})}{2((x-\hat{x})^2+(y-\hat{y})^2+(z-\hat{z})^2)^{3/2}}$
$\frac{\partial}{\partial x}\frac{1}{r_1} = \frac{-(2x-2\hat{x})}{2((x-\hat{x})^2+(y-\hat{y})^2+(z+2H+\hat{z})^2)^{3/2}}$

$$\frac{\partial}{\partial y}\frac{1}{r_1} = \frac{-(2y-2\hat{y})}{2((x-\hat{x})^2+(y-\hat{y})^2+(z+2H+\hat{z})^2)^{3/2}}$$
$$\frac{\partial}{\partial z}\frac{1}{r_1} = \frac{-(4H+2z+2\hat{z})}{2((x-\hat{x})^2+(y-\hat{y})^2+(z+2H+\hat{z})^2)^{3/2}}$$

Only the first order derivative forms are given above. The exponential form of the wave source term is already implemented to avoid an overflow computation as occur in the original expression. However, for x and y derivatives, it seems that the expressions given above contain some terms which having $2R$ as the denominator. Even this seems to be singular, the nominator of this term is always related to the horizontal distance between source and field point ($x-\hat{x}$ or $y-\hat{y}$), which is zero (for $R=0$). This means, the result of this expression is zero instead of singular. This is reasonable when one sees this characteristic from the physical sense. The case of $R=0$ occurs for a field point's evaluation due to the source at straight above or under the source point, or due to its own source point. In the first case, a perfectly vertical panel will give no horizontal kinematic contribution to the panel straight above or below it. This is represented by $x-\hat{x}$ or $y-\hat{y}=0$ which discussed above. This reflects that a singularity issue occur solely due to the modified zeroth order Bessel Function of the second kind (K_0), not the other Bessel Function (Y_0 or J_0). The zero(th) order Bessel Function of the first kind (J_0) on the imaginary part and zero(^{t}h) order Bessel function of the second kind (Y_0) from propagating root of the real part will just give one instead of infinity for $R=0$.

In terms of the implementation, the second order derivative is not really needed because in order to calculate unknown source strength distribution by solving matrix linear equation, only a normal derivative of the Greens Function is required. The second order derivative is only used to validate the Laplace boundary equation. As long as the validation does not include the evaluation of field point due to its own source or any other location which is exactly below/above it, the derivative expression of the infinite series solution can be used without any issue. Due to this reason, for validation purpose, only a single source point is determined in the origin of the global coordinate system $(\hat{x},\hat{y},\hat{z})=(0,0,0)$. The boundary conditions are evaluated in the 3-Dimensional domain and plotted as a sliced 3D cube. Water depth for this validation is chosen to be 100 m without any conceptual reason. Initially the Laplace (continuity) boundary condition is checked. Basically, both for the real and the imaginary part must satisfy all of the boundary condition independently since they are just representing a time dependency (when $\cos(\omega t)$ is zero, only the real part determines the magnitude of the G and vice versa). But it is true that the combination of both also needs to satisfy the boundary conditions. The result of the continuity (Laplace) condition ($\nabla^2 G$) is given in the following figures.

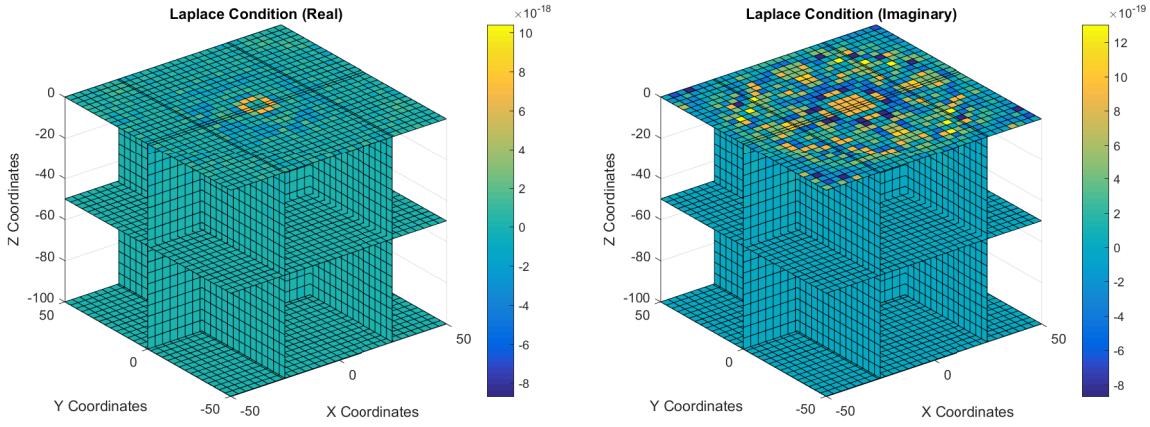

(a) Real Part (b) Imaginary Part

Figure 4.20: Continuity Check Due to Point Source at The Origin

From above graphs, it can be seen that even the result is not completely zero anywhere, the magnitude is extremely small (in order 10^{-18}). It can be concluded that the continuity condition is satisfied. Subsequently, $\frac{\partial G}{\partial z}$ is calculated and plotted in the same domain which represent the vertical velocity of the fluid particle. The seabed boundary condition is satisfied when the magnitude is zero, which is indeed represented by the following figures.

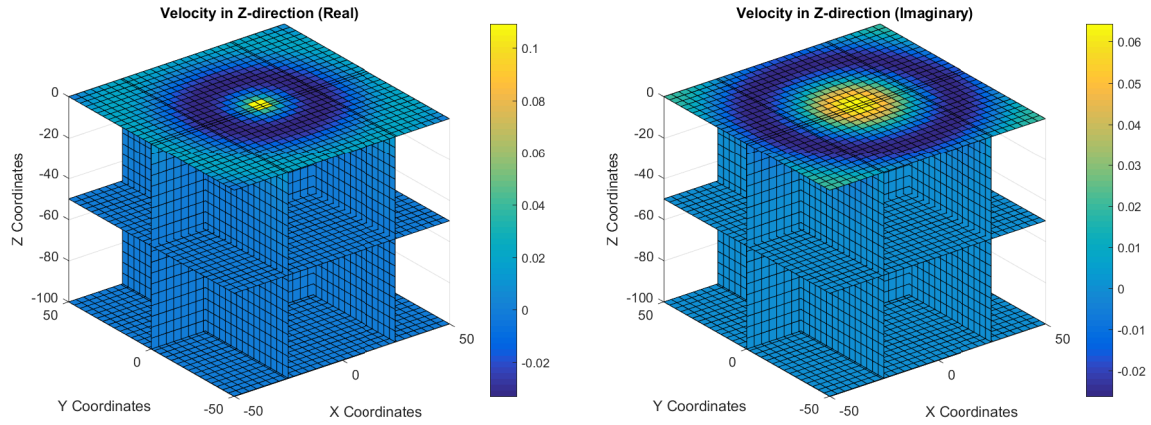

(a) Real Part (b) Imaginary Part

Figure 4.21: Vertical Velocity ($\partial G/\partial z$) Due to Point Source at The Origin

From above graph, it is shown that the vertical velocities at the seabed ($z = -100$) are zero. The velocities at the surface radiate from source point which also makes sense. On the other hand, just for visualization purpose, the velocity in the horizontal direction (x and y) also calculated and presented in the following figures

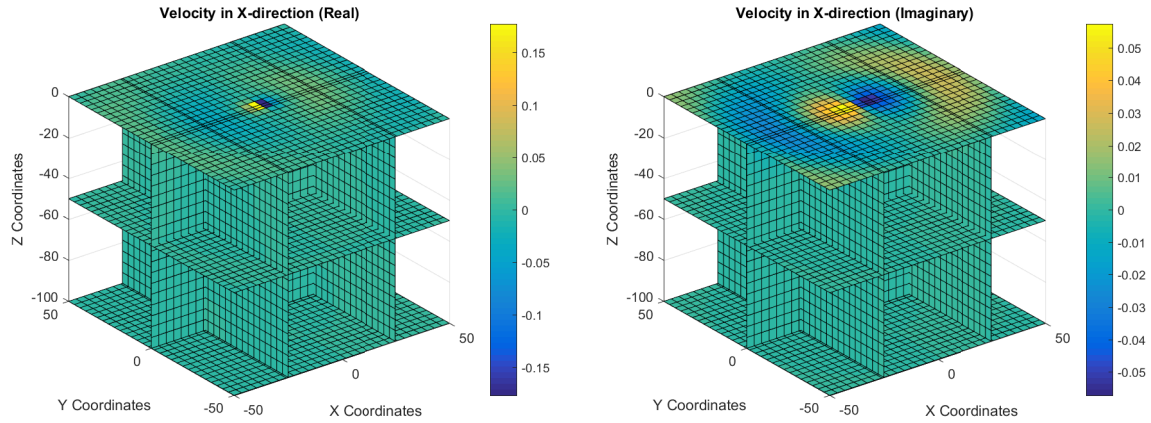

(a) Real ($\partial G/\partial x$) (b) Imaginary ($\partial G/\partial x$)

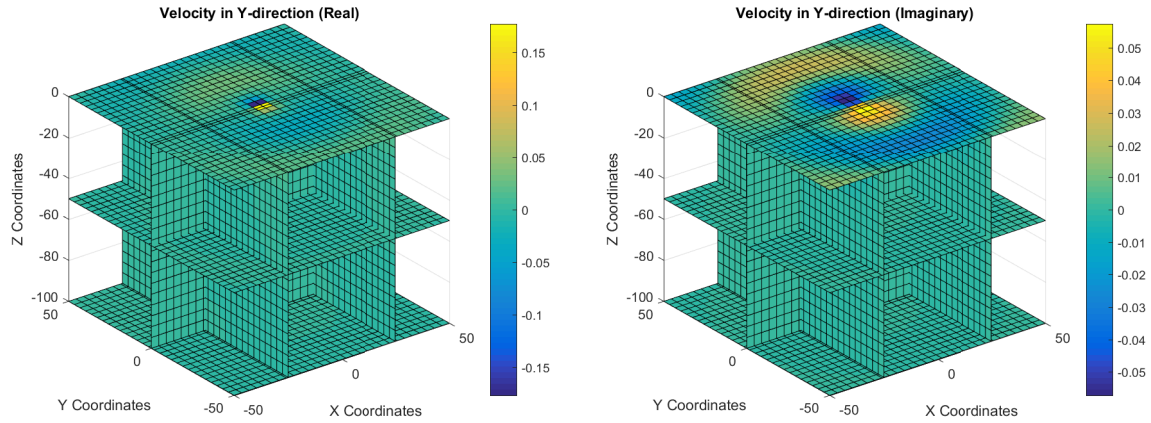

(c) Real ($\partial G/\partial y$) (d) Imaginary ($\partial G/\partial y$)

Figure 4.22: Horizontal Velocity due to point source at the origin

Above graphs visualize that for water particles situated close to the source point, they have much higher velocity magnitude, and diminishing when they go further from the source point. Direction of the propagation is also illustrated in an intuitively correct manner. For the radiation boundary condition, validation is confirmed by the Greens Function itself. There must be zero influence in the distance infinitely far away from the source point. This condition is visualized on the same 3D fluid domain since it is can already be seen that from the distance 50 m from a source point, the pattern of influence is vanishing.

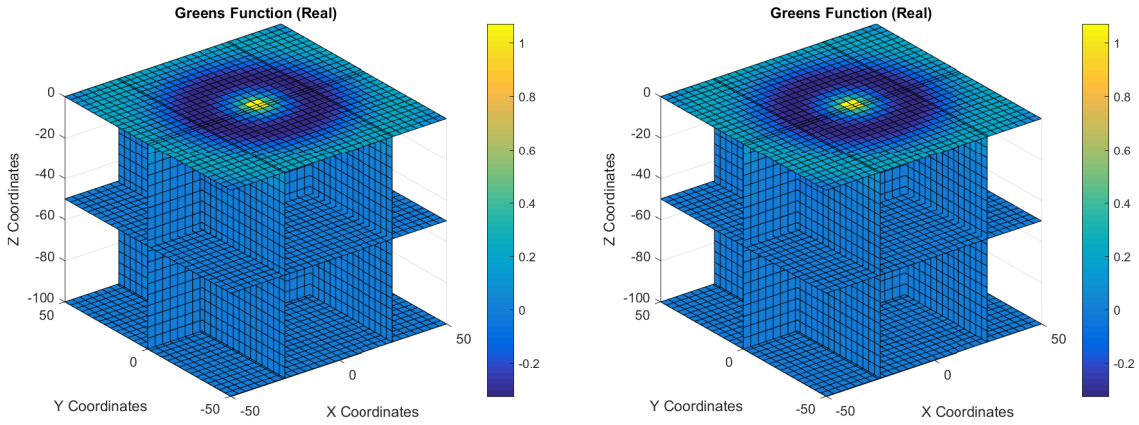

(a) Real part (b) Imaginary part

Figure 4.23: Greens Function due to point source at the origin

From above graph, it is clear that the influence concentrates in the source point location. However, if the excitation frequencies or the discretization size is changed, the plotting gives a quite different behavior. This is the case because all above graphs cannot really capture the fluid particle continuously. It is clear that some peak/trough of the wave (at an instantaneous moment in time) might miss from specified discretization size. Lastly, the pressure boundary condition is calculated based on $\frac{\partial^2 \Phi_{w(x,z,t)}}{\partial t^2} + g\frac{\partial \Phi_w}{\partial z}$. Apparently, both for real and imaginary part give the same results, therefore, only one figure is presented below. It is clearly shown that in the surface condition, there will be no pressure, and as it goes deeper, it simply increases as hydrostatic pressures.

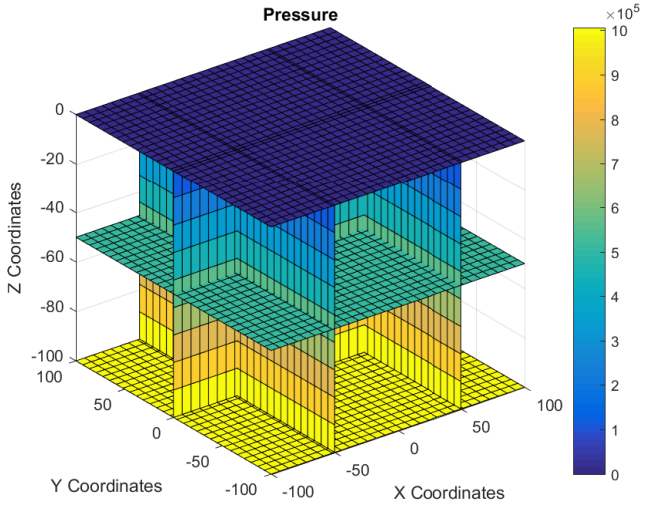

Figure 4.24: Pressure Condition

Up to this point, it is quite reasonable to conclude that the Greens Function and its derivatives are calculated correctly, including the fact that the integral and the infinite series solutions are interchangeable with each other. In the following section, the discussion moves to the implementation of the whole approach by considering the presence of a floating body.

4.6. Directional Derivative of Greens Function

In order to implement the kinematic body boundary condition (the last boundary condition must be satisfied), every panel orientation is determined. This orientation is represented by unit vector. Due to the difference of input format between the ANSYS output model and the IMSA input format, the determination of unit vector on both formats is treated in a slightly different manner. One only needs to choose which input format being used, then, the following subroutines in MATLAB code already programmed automatically to calculate them.

From a theoretical point of view , there is no difference between those input formats. A calculation of unit vector is based on cross product operation between two vectors . The difference between two points (which can be seen as two vertices) generates one vector. Since the panels are assumed to be flat, three vertices give 2 vectors lying in the same plane. Even though these two vectors are not necessarily perpendicular, a cross product operation between those vectors gives a normal vector. By normalizing this generated vector, the normal unit vector is obtained. For the given corner points of the panel $\left(p_{1(x_1,y_1,z_1)}; p_{2(x_2,y_2,z_2)}; p_{3(x_3,y_3,z_3)}\right)$, the unit normal vector is calculated by

$$T_1 = \left((x_2 - x_1), (y_2 - y_1), (z_2 - z_1)\right)$$
$$T_2 = \left((x_3 - x_1), (y_3 - y_1), (z_3 - z_1)\right)$$

$$N = \frac{(T_1 \otimes T_2)}{|T_1 \otimes T_2|}$$

In the ANSYS input format, the discretization technique being used to generate the mesh must comply the specification stated in the *"list of key point"*. This is to make sure that the unit vector generated is pointing outward to the fluid domain from the surface body instead of the other way around. In the IMSA input format, this kind of thing is not an issue as long as the ordering number of coordinate data is already complying with the specification discussed in chapter 4.1.2. *IMSA input format*. One thing must be kept in mind is the fact that the IMSA input format is only capable to handle a symmetric body (in X axis global coordinate). The determination of these unit vectors is only by calculating the unit vector from half part of the body (since there is only half part of the structure must be generated), then the results are being mirrored with the X axis together with the panel coordinates. Script to plot these generated unit vectors follows directly afterwards to ensure that the input of discretization technique is correct and gives an appropriate direction of the unit vector. This is can be considered as an error prevention/detection before going further into the sophisticated calculation which require a quite significant amount of time. Four figures depicted below are some illustrations of the unit vectors generated from these two types of input format.

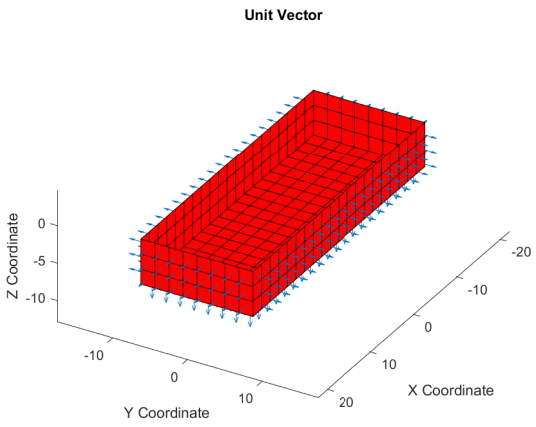

(a) 3D Rectangular

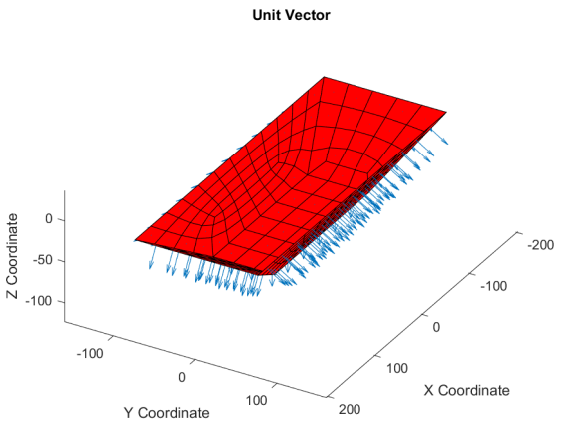

(b) 3D Trapezoid

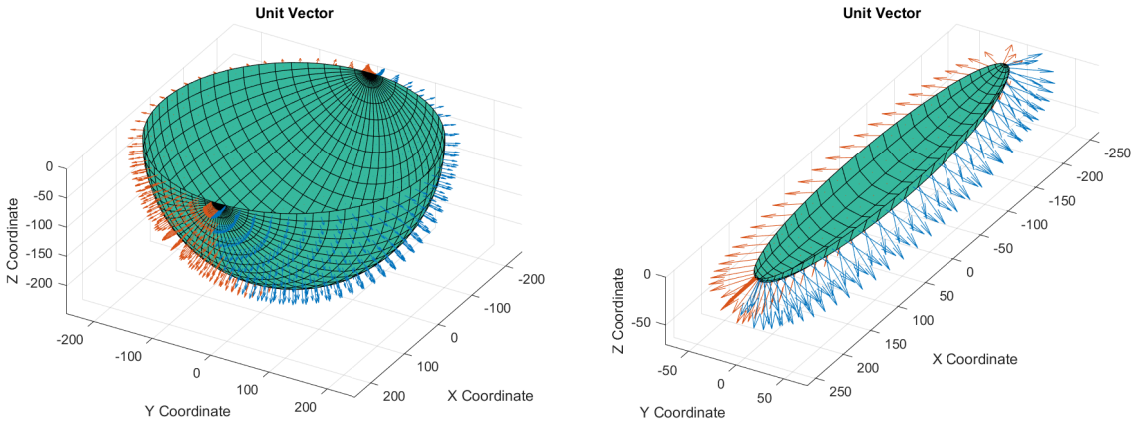

(c) Sphere (d) Spheroid

Figure 4.25: Example Generated Unit Vector

When the normal unit vectors of the panels are acquired, one can calculate the normal derivative of Greens Function. This directional derivative is necessary to obtain the source strength distribution of each panel which calculated by solving a matrix linear system from the kinematic body boundary condition. For unit vector $N = (n_1, n_2, n_3)$, a normal derivative of the Greens Function (unit $[1/\mathrm{m}^2]$) is calculated by

$$\frac{\partial G}{\partial n} = \left(\frac{\partial G}{\partial x} n_1\right) + \left(\frac{\partial G}{\partial y} n_2\right) + \left(\frac{\partial G}{\partial z} n_3\right)$$

4.7. Determining Distributed Source Term

The last step of calculating fluid forces in the matrix equation of motion is by solving the unknown distributed source strength (σ).

Kinematic Boundary Condition on The Oscillating Body Surface (Radiation Condition)

$$\frac{\partial \phi_j}{\partial n} = v_j$$

with ($j = 1, ..., 6$) represent the mode motions of the body (surge, sway, heave, roll, pitch and yaw)

$$\frac{\partial \phi_j}{\partial n} = -\frac{1}{2}\sigma_{j(x,y,z)} + \frac{1}{4\pi}\iint_{S_0} \sigma_{j(\hat{x},\hat{y},\hat{z})} \cdot \frac{\partial G_{(x,y,z,\hat{x},\hat{y},\hat{z})}}{\partial n} dS_0$$

$$-\frac{1}{2}\sigma_{j(m)} + \frac{1}{4\pi}\sum_{n=1}^{N} \sigma_{j(n)} \frac{\partial G_{mn}}{\partial n} \Delta S_n = \frac{\partial \phi_{j(m)}}{\partial n}$$

for $m = 1, ..., N$ and $n \neq m$ which can be solved in a matrix equation as

$$\begin{bmatrix} A_{11} & \dots & \dots & \dots & A_{1N} \\ \dots & A_{22} & \dots & \dots & \dots \\ \dots & \dots & A_{33} & \dots & \dots \\ \dots & \dots & \dots & \dots & \dots \\ A_{N1} & \dots & \dots & \dots & A_{NN} \end{bmatrix} \begin{bmatrix} \sigma_{j,1} \\ \dots \\ \dots \\ \dots \\ \sigma_{j,N} \end{bmatrix} = \begin{bmatrix} v_{j,1} \\ \dots \\ \dots \\ \dots \\ v_{j,N} \end{bmatrix}$$

with;
$A_{nn} = -\frac{1}{2}$
$A_{nm} = \frac{1}{4\pi}\frac{\partial G_{mn}}{\partial n}\Delta S_n$
$\sigma_{n,j}$ = unknown source strength
$n_{n,j}$ = directional cosines of the oscillating body
Index (n) up to (N) is the index of the receiver panel (field point). Index (m) is for the pulsating panel

(source point), whereas index (j) is an index of the motion. The direction cosines which describe the motions are given as

$$surge: n_1 = \cos(n,x)$$
$$sway: n_1 = \cos(n,y)$$
$$heave: n_3 = \cos(n,z)$$
$$roll: n_4 = y\cos(n,z) - z\cos(n,y) = (\overline{r}\otimes\overline{n})_1$$
$$pitch: n_5 = z\cos(n,x) - x\cos(n,z) = (\overline{r}\otimes\overline{n})_2$$
$$yaw: n_6 = x\cos(n,y) - y\cos(n,x) = (\overline{r}\otimes\overline{n})_3$$

Above explanation shows that the normal derivative of ϕ is unit-less $[m/m = 1]$ and agrees with the right hand side of the equation. Source strength magnitude (σ) is unit-less, the expression inside surface integration also gives no unit $[1/m^2.m^2 = 1]$.

Kinematic Boundary Condition of The Wave Diffracted Excitation(Diffraction Condition)

Similarly, the source strength of a diffraction potential can be obtained in the exactly the same manner with radiation source strength, by changing the index 1 to 6 becomes 7 and substitute the right hand side equation with the normal derivative kinematic component of the wave potential.

$$\frac{\partial\phi_0}{\partial n} + \frac{\partial\phi_7}{\partial n} = 0$$

$$-\frac{1}{2}\sigma_{7(m)} + \frac{1}{4\pi}\sum_{n=1}^{N}\sigma_{7(m)}\frac{\partial G_{mn}}{\partial n}\Delta S_n = -\frac{\partial\phi_{0(m)}}{\partial n}$$

$$\begin{bmatrix} A_{11} & \dots & \dots & \dots & A_{1N} \\ \dots & A_{22} & \dots & \dots & \dots \\ \dots & \dots & A_{33} & \dots & \dots \\ \dots & \dots & \dots & \dots & \dots \\ A_{N1} & \dots & \dots & \dots & A_{NN} \end{bmatrix} \begin{bmatrix} \sigma_{7,1} \\ \dots \\ \dots \\ \dots \\ \sigma_{7,N} \end{bmatrix} = \begin{bmatrix} v_{7,1} \\ \dots \\ \dots \\ \dots \\ v_{7,N} \end{bmatrix}$$

This right hand side of the equation represents the directional relation of the wave and the panel's orientation. This normal derivative of wave potential is given by

$$\frac{\partial\Phi_0}{\partial n} = \left(\frac{\partial\Phi_0}{\partial x}n_1\right) + \left(\frac{\partial\Phi_0}{\partial y}n_2\right) + \left(\frac{\partial\Phi_0}{\partial z}n_3\right)$$

with

$\frac{\partial\Phi_0}{\partial x} = \frac{ik\zeta_0 g}{\omega}\frac{\cosh(k(H+z))}{\cosh(Hk)}e^{(ik(x\cos\mu+y\sin\mu))}\cos\mu$

$\frac{\partial\Phi_0}{\partial x} = \frac{ik\zeta_0 g}{\omega}\frac{\cosh(k(H+z))}{\cosh(Hk)}e^{(ik(x\cos\mu+y\sin\mu))}\sin\mu$

$\frac{\partial\Phi_0}{\partial z} = \frac{k\zeta_0 g}{\omega}\frac{\sinh(k(H+z))}{\cosh(Hk)}e^{(ik(x\cos\mu+y\sin\mu))}\cos\mu$

Fundamentally speaking, the unit of ϕ_0 and ϕ_7 must be equal to ϕ_{1-6} [m]. In contrast, the wave potential above is taken from well-known *velocity* potential of linear wave theory (unit [m^2/s]). Apparently, this is not an important issue as long as when the pressure is being calculated, this potential does not re-multiplied by the wave frequency ω and amplitude ζ_0 as shown in the third equation of chapter 3.3, or in other word, these potentials (ϕ_0 and ϕ_7) are no longer magnitude base of *displacement* potential like the radiation potentials, but already the *velocity* potentials. The other alternative approach to keep a generic condition of the unit, is by multiplying wave potential above with $(1/(\zeta_0\omega))$.

Procedure explained above reveals that the determination of source strength can be summarized as procedure of solving matrix linear system

$$[A][\sigma_j] = [v_j]$$
$$[\sigma_j] = [A]^{-1}[v_j]$$

for $j = 1,...,7$

Accuracy of the solution depends on the condition number of the matrix $[A]$. Apparently, for certain input excitation frequencies, this condition number is quite high and give inaccurate results. This phenomenon is called irregular frequencies and occur when the determinant of matrix $[A]$ is close to zero, and the inverse operation cannot be calculated properly. Discussion about this issue is outside the scope of this thesis.

Finally, when all of the source strength distribution is acquired, the potentials which satisfy all of five boundary conditions can be obtained easily by

$$\phi_{j(x,y,z)} = \frac{1}{4\pi}\iint_{S_0} \sigma_j(\hat{x},\hat{y},\hat{z})G(x,y,z,\hat{x},\hat{y},\hat{z})dS_0$$

with [m] as the unit of the ϕ. Since (G) is complex in time ($G = G_1\cos(\omega t) + iG_2\sin(\omega t)$), the obtained potentials (ϕ) are also complex. For the sake of computational effort, the double integral operation can be approximated numerically (multiplication with panel area) as

$$\phi_{j(x,y,z)} = \frac{1}{4\pi}\sigma_j(\hat{x},\hat{y},\hat{z})G(x,y,z,\hat{x},\hat{y},\hat{z})\Delta S_0$$

which can be rewritten in a vector - matrix operation.

$$\left[\Phi_{j(1\ldots m)}\right] = \begin{bmatrix} \frac{1}{4\pi}\sigma_{j(1)} & \frac{1}{4\pi}\sigma_{j(2)} & \ldots & \frac{1}{4\pi}\sigma_{j(m)} \end{bmatrix} \begin{bmatrix} G_{1,1}\Delta S_0 & \ldots & \ldots & \ldots \\ \ldots & G_{2,2}\Delta S_0 & \ldots & \ldots \\ \ldots & \ldots & \ldots & \ldots \\ \ldots & \ldots & \ldots & G_{N,N}\Delta S_0 \end{bmatrix}$$

Above vector-matrix operation is used when the evaluation of Green's Function is done without doing surface numerical integration over the panel. The assumption of constant source strength over the panel is implemented here. For the elements inside matrix G where the series solution fails (the diagonal term and some other location where $x = \hat{x}$ and $y = \hat{y}$), ΔS_0 is excluded and the element of this matrix G is integrated over the area. The procedure of integration is elaborated further in chapter 4.9: *Panel Integration*. Roughly speaking, every physical characteristic of the fluid (in the hydrodynamic sense) such as pressure, acceleration, force and displacement are within one's grasp.

4.8. Equation of Motion

Once all of the potentials needed are obtained, the final coupled 6 Degrees of Freedom equation of motion can be constructed as

$$(m+a)\cdot\ddot{z} + b\cdot\dot{z} + cz = F_w + F_d$$

with
F_r = Radiation force
F_w = Wave excitation (Froude Krylov) force
F_d = Diffraction force
F_d = Hydrostatic Force
These forces are calculated based on pressure integration. It is known that the pressure can be obtained from original *velocity* potential (Φ)

$$p_{(x,y,z,t)} = -\rho\frac{\partial\Phi}{\partial t}$$

which can be expressed in terms of magnitude base of *displacement* potential (ϕ_{0-7})

$$p_{(x,y,z,t)} = \rho\omega^2\left((\phi_0+\phi_7)\zeta_0 + \sum_{j=1}^{6}\phi_j\zeta_j\right)e^{-i\omega t}$$

Therefore, the final forces are calculated by integrating these pressures over the panel area for each respective mode of motion

$$F_k = -\iint_{S_0} pn_k dS_0$$

4.8.1. Hydrodynamic Coefficients

Hydrodynamic coefficients which represent the motion of the body consists of added mass and damping coefficients. These coefficients are determined by distinguishing the generic pressure integration above for radiation potential only.

$$F_k = -\rho\omega^2\sum_{j=1}^{6}\zeta_j e^{-i\omega t}\iint_{S_0}\phi_j n_k dS_0$$

Since above forces are written in the frequency domain, it is quite clear that coefficients for the left hand side equation of motions can be calculated by
Added mass coefficient:

$$a_{kj} = -Re\left[\rho \iint_{S_0} \phi_j n_k dS_0\right]$$

Damping coefficient:

$$b_{kj} = -Im\left[\rho\omega \iint_{S_0} \phi_j n_k dS_0\right]$$

for j and $k = 1,..,6$ Recalling the unit of magnitude base *displacement* potential (ϕ_{0-7}) is [m], the added mass coefficient above has unit [kg] whereas for the added damping coefficient is [kg/s] which is absolutely correct.

4.8.2. Inertia and Restoring Force Coefficients

The inertia forces of the body are characterized by the mass matrix. The added mass coefficients obtained from the hydrodynamic reaction forces above, need to be added to the original mass of the system which described by 6x6 matrix below.

$$\text{Mass} = \begin{bmatrix} \rho_w \nabla & 0 & 0 & 0 & 0 & 0 \\ 0 & \rho_W \nabla & 0 & 0 & 0 & 0 \\ 0 & 0 & \rho_W \nabla & 0 & 0 & 0 \\ 0 & 0 & 0 & I_{xx} & 0 & -I_{xz} \\ 0 & 0 & 0 & 0 & I_{yy} & 0 \\ 0 & 0 & 0 & -I_{zx} & 0 & I_{zz} \end{bmatrix}$$

with
$I_{xx} = k_{xx}^2 \rho_W \nabla$
$I_{yy} = k_{yy}^2 \rho_W \nabla$
$I_{zz} = k_{zz}^2 \rho_W \nabla$

The developed MATLAB code is capable to calculate the mass automatically from discretized convex hull body input. The AlphaShape command in MATLAB is used to create a bounding volume that envelops a set of 3-D points (vertices). For arbitrary (non-convex) hull shape (e.g. semi submersible, TLP, etc.), one needs to calculate and assign the mass matrix manually. This is due to the fact that the determination of a displaced volume (∇) still needs to be improved for an arbitrary coordinate input. A manipulation of the alphaShape command such as tightening/loosing/add/remove the points might useful to create a generic subroutine to calculate an arbitrary displaced volume. Since this already deviates from the subject of interest of the thesis, no more effort has been put. Moreover, for calculating the mass moment of inertia (I_{xx}, I_{yy}, I_{zz}), one still needs to specify the radii of inertia manually even for convex hull shape. However, based on the reference written by Journee [11], radii of inertia (for ship-shaped structure) can be approximated by
$k_{xx} = 0.3B$ to $0.4B$
$k_{yy} = 0.22L$ to $0.28L$
$k_{zz} = 0.22L$ to $0.28L$
the coupling terms I_{xz} and I_{zx} are generally small and most of the time can be neglected.

The last term in the left hand side equation of motion which must be calculated is the stiffness matrix, which determined as shown below

$$\text{Stiffness} = \begin{bmatrix} 0 & 0 & 0 & 0 & 0 & 0 \\ 0 & 0 & 0 & 0 & 0 & 0 \\ 0 & 0 & C_{33} & C_{34} & C_{35} & 0 \\ 0 & 0 & C_{43} & C_{44} & C_{45} & 0 \\ 0 & 0 & C_{53} & C_{54} & C_{55} & 0 \\ 0 & 0 & 0 & 0 & 0 & 0 \end{bmatrix}$$

with
$C_{33} = \rho_W g A_w$
$C_{44} = \rho_W g \nabla GM_{\text{roll}}$

$C_{55} = \rho_W g \bigtriangledown GM_{\text{pitch}}$

This matrix represents the restoring coefficient due to the hydrostatic force. One must be aware that any elements do not correspond to the upward force (buoyant force) will have zero coefficients. It means, for a certain degree of freedom, the equation of motions is *mass - damping (without stiffness)* system. These restoring force coefficients depend on several inputs, such as the water plane area (A_w), displaced volume ($\bigtriangledown$) and distance of center of gravity to the metacenter (GM). The developed MATLAB code is capable to calculate those parameters automatically. The water plane area (A_W) is determined by calculating the *polyarea* of the coordinates situated at the free surface. The displaced volume is already obtained from the calculation of the mass matrix, whereas for (GM), it can be calculated based on location of the center of gravity (input), center of buoyancy, and also radii of inertia mentioned in the previous subsection. In the end, the GM is calculated by

$BM_{\text{roll}} = I_{xx}/\bigtriangledown$
$BM_{\text{pitch}} = I_{yy}/\bigtriangledown$
$GM_{\text{roll}} = KB + BM_{\text{roll}} - KG$
$GM_{\text{pitch}} = KB + BM_{\text{pitch}} - KG$
with visualization of the parameters are shown in the figure below.

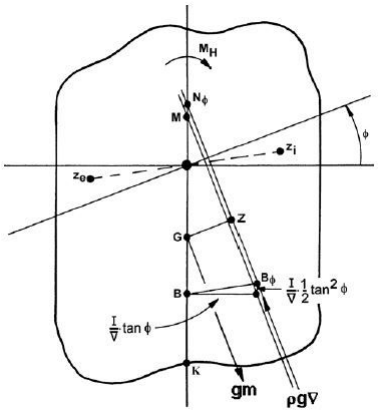

Figure 4.26: Hydrostatic Stability (Source: Offshore Hydromechanics [11])

4.8.3. Excitation

The determination of excitation forces can be done in the same manner with hydrodynamic reaction forces by pressure integration from the appropriate potentials (wave and diffraction).

$$F_k = -\rho\omega^2\zeta_0 e^{-i\omega t} \iint_{S_0} \left(\phi_0 + \phi_7\right) n_k dS_0$$

One must be aware that the potential written above is magnitude base *displacement* potential. As mentioned in chapter 3.7, if the determination of the wave and the diffraction potential above is based on original *velocity* potential taken from the linear wave theory, integration above must be divided by the wave amplitude (ζ_0) and frequency (ω).

Another thing must be underlined is the fact that the diffraction potential above is derived from an influence function (G) which is in a complex form ($G = G_1\cos(\omega t) + iG_2\sin(\omega t)$). It means that the excitation force will also remain in a complex form.

4.9. Panel Integration

In regards to the evaluation of field point due to its own source, the evaluation of influence function and its derivative is always need to be integrated. This is the only case where the following approach needs to be used. The surface integration procedure is done based on the integral solution instead of the infinite series. This is due to the reason that the integral solution has distinguishable terms (fundamental Rankine source term, its image below the seabed, and the wave source term) which can be derived first, then being (surface) integrated later on. Due to the fact that any other terms than fundamental Rankine source (G_a) are not singular in any possible condition, their influence function over the panel can be approximated by

multiplying by panel area. It is possible to integrate image Rankine source below seabed (G_b) and imaginary part of the wave source term (G_d) and obtained more accurate results. However, this is not really the case for the real part of the wave source term (G_c). Evaluation of the principal value integral numerically needs one integration variable (ξ). In order to integrate it over the area, one will need another two more integration variables. It means, in exchange for an accurate solution, a function of three variables must be integrated to give another function of two variables. This is not possible to be done in a numerical program such as MATLAB. Only a symbolic toolbox is having the ability to do this. Therefore, for this thesis, any other terms rather than (G_a) and their first derivatives are not going to be integrated. The second order derivatives also do not need to be calculated because only the normal derivative of the G is needed.

Basically, the following approach is needed only to cover a single problem: Numerically integrating a 3-Dimensionally arbitrary orientated function (1/r) over a quadrilateral panel. An analytical solution of this problem has been formulated decades ago. It is obvious that analytical solution is much better than a numerical approximation. However, since the main motivation of this thesis is to evaluate the Greens Function for ice-infested waters which has a different form from the open water solution, it is better to provide a generic method of surface integration for any kind of 3-dimensional arbitrarily orientated function (not only 1/r).

4.9.1. Implementation: Transformation to Local Coordinate System

Principally, the magnitude of an influence function depends on the distance between the source and field points. There is a certain distribution apply over the panel surface. Due to the flat panel assumption, the surface integration of quadrilateral panel could be calculated based on a standard double integration. However, the arbitrariness of panel's orientation in 3D domain raises a generic problem of the integration procedure. Such an effort can be made to untangle this problem by transforming the vertices information to the local panel coordinate system. The singular point becomes the origin of the local element coordinate system, and the panel located in the same z local element coordinate system.

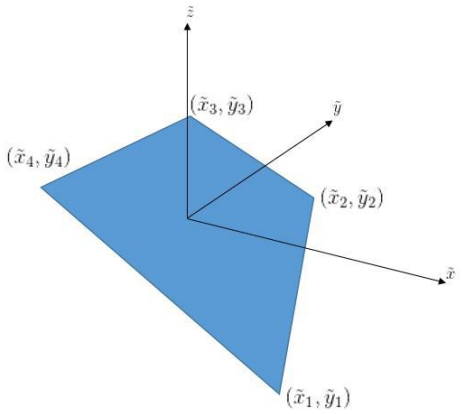

Figure 4.27: Element Local Coordinate System

This method of transformation adapts the work done by Hess and Smith [7] and can be implemented by using 3 unit vectors perpendicularly each other. These vectors can be generated from the vertices data. The determination of a normal unit vector pointing outward of the panel is already discussed in the previous chapter. This unit vector (N) is assigned to be a local Z ($\tilde{z}$) axis in the element coordinate system $\left(\tilde{z} = n_{\tilde{x}_3}, n_{\tilde{y}_3}, n_{\tilde{z}_3}\right)$. The unit vector which assigned as local X axis the element coordinate system ($\tilde{x}$) is calculated from the difference between the first and third nodes of the panel, and then being normalized afterwards $\left(\tilde{x} = n_{\tilde{x}_1}, n_{\tilde{y}_1}, n_{\tilde{z}_1}\right)$. These two unit vectors ($\tilde{x}$ and $\tilde{z}$) are obviously perpendicular each other. Finally, the least unit vector which assigned as the local Y axis the element coordinate system $\left(\tilde{y} = n_{\tilde{x}2}, n_{\tilde{y}2}, n_{\tilde{z}2}\right)$ is calculated by normalizing the resulting cross product between those two unit vectors. These three unit vectors are becoming the tool (a transformation matrix) to express an arbitrary vertices information and orientation, into their own local coordinate system. One must be aware that this transformation procedure has to be done in every single panel of the body. The transformation matrix is given by:

$$T = \begin{bmatrix} n_{\tilde{x}_1} & n_{\tilde{y}_1} & n_{\tilde{z}_1} \\ n_{\tilde{x}_2} & n_{\tilde{y}_2} & n_{\tilde{z}_2} \\ n_{\tilde{x}_3} & n_{\tilde{y}_3} & n_{\tilde{z}_3} \end{bmatrix}$$

A quadrilateral panel bounded by 4 vertices $\left(p_{1(x_1,y_1,z_1)}, p_{2(x_2,y_2,z_2)}, p_{3(x_3,y_3,z_3)}, p_{4(x_4,y_4,z_4)}\right)$ in global coordinate system can be transformed into the same quadrilateral panel which having a local element coordinate system given by $\left(\tilde{p}_{1(\tilde{x}_1,\tilde{y}_1,\tilde{z}_1)}, \tilde{p}_{2(\tilde{x}_2,\tilde{y}_2,\tilde{z}_2)}, \tilde{p}_{3(\tilde{x}_3,\tilde{y}_3,\tilde{z}_3)}, \tilde{p}_{4(\tilde{x}_4,\tilde{y}_4,\tilde{z}_4)}\right)$ by:

$$\begin{aligned}
\tilde{x}_k &= n_{\tilde{x}_1} \cdot (x_k - x_0) + n_{\tilde{y}_1} \cdot \left(y_k - y_0\right) + n_{\tilde{z}_1} \cdot (z_k - z_0) \\
\tilde{y}_k &= n_{\tilde{x}_2} \cdot (x_k - x_0) + n_{\tilde{y}_2} \cdot \left(y_k - y_0\right) + n_{\tilde{z}_2} \cdot (z_k - z_0) \\
\tilde{z}_k &= n_{\tilde{x}_3} \cdot (x_k - x_0) + n_{\tilde{y}_3} \cdot \left(y_k - y_0\right) + n_{\tilde{z}_3} \cdot (z_k - z_0)
\end{aligned}$$

with $k = 1,2,3,4$. In above equation, x_0, y_0, z_0 are the center point of the panel p_0 which calculated by averaging the vertices.

$$\begin{aligned}
x_0 &= \tfrac{1}{4}\left(x_1 + x_2 + x_3 + x_4\right) \\
y_0 &= \tfrac{1}{4}\left(y_1 + y_2 + y_3 + y_4\right) \\
z_0 &= \tfrac{1}{4}\left(z_1 + z_2 + z_3 + z_4\right)
\end{aligned}$$

This approach makes sure that the values of $\tilde{z}$ will always be zero because this axis is no other than a unit vector pointing outward of the panel itself, with the origin is the center point of the panel.

4.9.2. Implementation: Bilinear Mapping

Even though the flat panel assumption and the element local coordinate system transformation resolve the surface integration problem, the fact that panel's shapes are completely random (depends on the meshing technique) elevates another issue. Generating subroutine to integrate a quadrilateral panel from arbitrary four vertices still become a challenging task to do. MATLAB is only capable to do a numerical double integration for the perfect rectangular limit (even though not necessarily square) of the function. In order to encounter this problem, some transformation technique which commonly applied in digital image processing, -so called *Bilinear Mapping*- is implemented. This mapping is some sort of a manipulation technique to find a linear relation (combination) of two vector spaces to yield an element of another vector space. Easy interpretation about this mapping is like finding the linear mathematical function (operation) when one needs to re-scale/fitting a not-rectangular image into a square image as illustrated in the following figure.

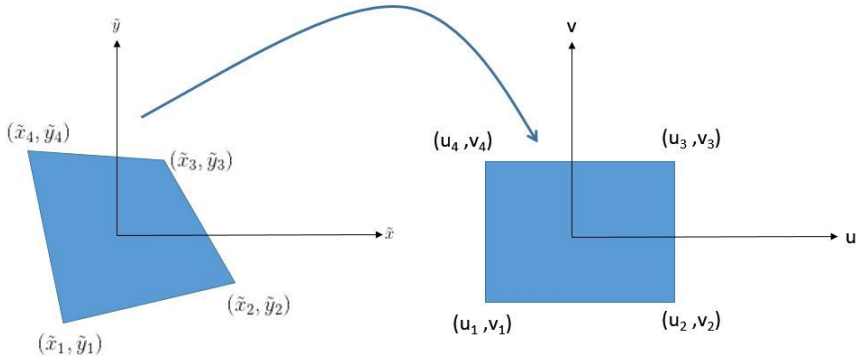

Figure 4.28: Bilinear Mapping

This technique makes the integration procedure become much simpler. The function bounded by the quadrilateral panel $f(\tilde{x}, \tilde{y})$ is transformed into a function bounded by a rectangular panel $f(u, v)$. It means, the distribution function inside the panel (the fundamental Rankine source term) which initially in the function of $(\tilde{x}, \tilde{y})$ needs to be expressed in the function of (u, v). Additionally, the transformed rectangular panel can be specified to lay in the desired coordinates location. This transformed coordinate location is chosen in such a way to make the integration procedure become easier (e.g: located between 0 and 1). For an arbitrary quadrilateral panel with vertices $\left(p_{1(\tilde{x}_1,\tilde{y}_1)}; p_{2(\tilde{x}_2,\tilde{y}_2)}; p_{3(\tilde{x}_3,\tilde{y}_3)}; p_{4(\tilde{x}_4,\tilde{y}_4)}\right)$, the bilinear mapping transforms these vertices into $\left(q_{1(u_1,v_1)}; q_{2(u_2,v_2)}; q_{3(u_3,v_3)}; q_{4(u_4,v_4)}\right)$ with

$$\begin{aligned}
q_1 &= (0,0) \\
q_2 &= (1,0) \\
q_3 &= (1,1) \\
q_4 &= (0,1)
\end{aligned}$$

To obtain the transformation constants, both linear operations below are being used

$$\tilde{x} = a + bu + cv + duv$$

$$\tilde{y} = e + fu + gv + huv$$

Those equations can be expressed in a matrix operation

$$\begin{bmatrix} \tilde{x}_{(u,v)} \\ \tilde{y}_{(u,v)} \end{bmatrix} = \begin{bmatrix} a & b & c & d \\ e & f & g & h \end{bmatrix} \begin{bmatrix} 1 \\ u \\ v \\ uv \end{bmatrix}$$

$$\begin{bmatrix} \tilde{x}_{1(u,v)} & \tilde{x}_{2(u,v)} & \tilde{x}_{3(u,v)} & \tilde{x}_{4(u,v)} \\ \tilde{y}_{1(u,v)} & \tilde{y}_{2(u,v)} & \tilde{y}_{3(u,v)} & \tilde{y}_{4(u,v)} \end{bmatrix} = \begin{bmatrix} a & b & c & d \\ e & f & g & h \end{bmatrix} \begin{bmatrix} 1 & 1 & 1 & 1 \\ 0 & 1 & 1 & 0 \\ 0 & 0 & 1 & 1 \\ 0 & 0 & 1 & 0 \end{bmatrix}$$

Introduce new notations

$$[M] = [T][N]$$

$$[T] = [M]^{-1}[N]$$

where $[T]$ is the transformation matrix needs to be obtained in every panel. Above matrix operation solves 8 unknown constants which used to express the $(\tilde{x})$ and $(\tilde{y})$ in terms of (u) and (v). At this point, the original Greens Function solution encounters two transformation procedures.

$$G(x, y, z, \hat{x}, \hat{y}, \hat{z}) \mapsto G(\tilde{x}, \tilde{y}, 0, x_0, y_0, z_0) \mapsto G(u, v, 0, x_0, y_0, z_0)$$

Basically, the second transformation procedure encloses any problems related to the surface integration of a Greens Function along the panel. Since the variable of integration changes, some calculus technique -so called *"change of variables"*- need to be implemented. This technique is given in the expression below

$$\iint_R G_{(\tilde{x},\tilde{y})}\, dA = \iint_S G_{(g_{(u,v)},h_{(u,v)})} \left| \frac{\partial(\tilde{x},\tilde{y})}{\partial(u,v)} \right| du\, dv$$

with the expression inside vertical brackets is the Jacobian determinant which can be calculated by

$$\left| \frac{\partial(\tilde{x},\tilde{y})}{\partial(u,v)} \right| = \begin{vmatrix} \frac{\partial \tilde{x}}{u} & \frac{\partial \tilde{x}}{v} \\ \frac{\partial \tilde{y}}{u} & \frac{\partial \tilde{y}}{v} \end{vmatrix}$$

with

$\frac{\partial \tilde{x}}{\partial u} = b + vd$; $\frac{\partial \tilde{x}}{\partial v} = c + ud$;

$\frac{\partial \tilde{y}}{\partial u} = f + vh$; $\frac{\partial y}{\partial v} = g + uh$;

In case when the Jacobian determinant is positive, the orientation of the function G is preserved. In contrast, a negative Jacobian flips the orientation of a function G up side down. Use is made about the fact that

$$\iint_R f\, dA = \iint_{-R} -f\, dA$$

It means that the absolute value of the Jacobian determinant is the one must be used. This reflects an expansion or shrinkage about the bond/limit area of the original function G.

Up to this point, the whole procedure to generate a matrix equation of motion of an arbitrary shape floating body in open water sea condition is done completely. The Greens Function matrix is fully obtained (including solution for the singular term) and has been validated based on the boundary equations. A comparison about the computation speed difference between infinite series and integral solution is also provided. If computation speed is not really an issue, one can use the integral solution to conduct the whole analysis, and integrate the terms (G_b) and (G_d) if desired. Considering that originally, the above approach is provided to establish a generic method to integrate any kind of 3-dimensional arbitrarily orientated function, apparently, the solution of Greens Function for ice infested waters is provided in an integral form. There is one integration variable appear in the calculation of an influence function at a point. This issue is exactly the same with the integration of a real part of the wave source term in the open water condition (G_c). Fortunately, it seems that a singular behavior will not occur. It means that the influence function over the whole panel can be approximated by multiplying the influence function at center point by panel area, and there is no need to use the panel integration at all.

5

Further Discussion

This chapter addresses the difference between an integral solution of Greens Function in an open water and the ice-infested waters.

5.1. Comparison of the Integral Solution

Based on the derivation done in chapter 3, the solution of Greens function for ice-infested waters is given by

$$G_{1(x,y,z,\hat{x},\hat{y},\hat{z})} = \frac{1}{2\pi}\int_0^\infty \frac{\left((k^4D - 2h\rho_i g\alpha + g\rho_w)k\cosh(kz) + \rho_w g\alpha\sinh(kz)\right)}{\rho_w g\alpha\left((k^4D - 2h\rho_i g\alpha + g\rho_w)k\tanh(kH) - \rho_w g\alpha\right)}\frac{\cosh(k(H+\hat{z}))}{\cosh(kH)}J_0(kR)dk$$

$$G_{2(x,y,z,\hat{x},\hat{y},\hat{z})} = \frac{1}{2\pi}\int_0^\infty \frac{\left((k^4D - 2h\rho_i g\alpha + g\rho_w)k\sinh(k\hat{z}) + \rho_w g\alpha\cosh(k\hat{z})\right)}{\rho_w g\alpha\left((k^4D - 2h\rho_i g\alpha + g\rho_w)k\tanh(kH) - \rho_w g\alpha\right)}\frac{\cosh(k(H+z))}{\cosh(kH)}J_0(kR)dk$$

On the other hand, the Greens function of the open water case which has been derived by Wehausen and Laitone [20] is given by

$$G_{(x,y,z,\hat{x},\hat{y},\hat{z},t)} = \left[\frac{1}{r} + \frac{1}{r_1} + PV\int_0^\infty \frac{2(\xi+\alpha)e^{-\xi H}.\cosh\xi(H+\hat{z}).\cosh\xi(H+z)}{\xi\sinh\xi H - \alpha\cosh\xi H}.J_0(\xi R)d\xi\right]\cos(\omega t)$$

$$+ i\left[2\pi\frac{(k^2-\alpha^2)}{(k^2-\alpha^2)H+\alpha}.\cosh k(H+\hat{z}).\cosh k(H+z).J_0(kR)\right]\sin(\omega t)$$

To see the difference between above Greens function, the effect of level ice from the ice-infested waters solution is omitted by taking the limit of ice characteristic (D and ρ_i) into zero and apply trigonometric identities. This will give the integral solution become

$$G_{1(x,y,z,\hat{x},\hat{y},\hat{z})} = \frac{1}{2\pi}\int_0^\infty \frac{(k\cosh(kz) + \alpha\sinh(kz))\cosh(k(H+\hat{z}))}{\rho_w g\alpha\,(k\sinh(kH) - \alpha\cosh(kH))}J_0(kR)dk$$

$$G_{2(x,y,z,\hat{x},\hat{y},\hat{z})} = \frac{1}{2\pi}\int_0^\infty \frac{(k\sinh(k\hat{z}) + \alpha\cosh(k\hat{z}))\cosh(k(H+z))}{\rho_w g\alpha\,(k\sinh(kH) - \alpha\cosh(kH))}J_0(kR)dk$$

When the constants ρ_w, g and α are included in the G, it is quite clear that the denominator of above form is exactly the same with the denominator of the wave source term (real part) from open water solution. The fundamental Rankine source term is not present, since the derivation of Greens Function for ice-infested waters, the delta function is plugged in the pressure equation instead of the Laplace equation. It can be concluded that the imaginary line introduced in the derivation of Greens Function for ice-infested waters avoids the presence of this singular term ($1/r$). The image below seabed ($1/r_1$) also vanishes by this procedure. But, since before obtaining the solution (G_2), the assumed solution has been substituted in the seabed boundary condition as well, this condition is automatically satisfied.

However, above forms clearly give an overflow computation as shown in the real part of the wave source term from the Greens function for the open water case due to the presence of hyperbolic terms. Same tech-

nique with the open water case is used to entangle this issue and gives

$$G_{1(x,y,z,\hat{x},\hat{y},\hat{z})} = \frac{1}{4\pi}\int_0^\infty \frac{\left((k+\alpha)e^{kz}+(k-\alpha)e^{-kz}\right)\left(e^{k(H+\hat{z})}+e^{-k(H+\hat{z})}\right)}{(k-\alpha)e^{kH}-(k+\alpha)e^{-kH}} J_0(kR)dk$$

$$G_{2(x,y,z,\hat{x},\hat{y},\hat{z})} = \frac{1}{4\pi}\int_0^\infty \frac{\left((k+\alpha)e^{k\hat{z}}-(k-\alpha)e^{-k\hat{z}}\right)\left(e^{k(H+z)}+e^{-k(H+z)}\right)}{(k-\alpha)e^{kH}-(k+\alpha)e^{-kH}} J_0(kR)dk$$

Based on the acquired forms above, the finite depth issue also re-occurs. Term $(k-\alpha)$ results a zero as soon as the difference between propagating root and an infinite depth wave number cannot be captured. However, since the source and field points are always below the free surface ($\hat{z}$ and z < 0), and the water depth (H) is a positive quantity, some of the exponential terms above still give an overflow computation problem and cannot be evaluated. Another effort to avoid a positive exponent has been done, and the final obtained solution are given as

$$G_{1(x,y,z,\hat{x},\hat{y},\hat{z})} = \frac{1}{4\pi}\int_0^\infty \frac{e^{k(z+\hat{z})}\left(k(1+e^{-2kz})+\alpha(1-e^{-2kz})\right)(1+e^{-2k(H+\hat{z})})}{k(1-e^{-2kH})-\alpha(1+e^{-2kH})} J_0(kR)dk$$

$$G_{2(x,y,z,\hat{x},\hat{y},\hat{z})} = \frac{1}{4\pi}\int_0^\infty \frac{e^{k(z+\hat{z})}\left(k(1-e^{-2k\hat{z}})+\alpha(1+e^{-2k\hat{z}})\right)(1+e^{-2k(H+z)})}{k(1-e^{-2kH})-\alpha(1+e^{-2kH})} J_0(kR)dk$$

Basically, above final forms have been derived in the exactly the same manner as an exponential form of the wave source term of the open water solution. Apparently, some positive exponent terms still occur $(e^{(-2k\hat{z})})$ and $(e^{(-2kz)})$, therefore, the integral still cannot be evaluated into infinity. However, by implementing the same technique of principal value integration, which has been done in open water case, even before reaching $k=\infty$, the nature of this integrand does not seem to be converging. This is most susceptible reason is due to fact that the radiation condition is not satisfied yet. However, further study need to be conducted.

Another thing must be underlined is the fact that at the very end, the final Greens Function only affects the hydrodynamic forces: radiation and diffraction forces. The added mass matrix, damping matrix, and also the diffracted force are highly influenced. The original mass (without added mass) and stiffness matrix remains the same with the open water case since they have nothing to do with hydrodynamic reaction force. Another thing that still become a major concern, is about the wave excitation term. The original wave velocity potential taken from the linear wave theory also must be re-derived by implementing the free surface-level ice interface condition.

6

Conclusion and Future Recommendation

The final conclusion of the whole thesis are presented in this chapter. Research questions stated in the first chapter are answered and the recommendations for future research are also included.

6.1. Conclusion

Possible solution of 3D Greens Function for ice-infested waters

The Green's function for ice-infested waters condition has been derived in this thesis. About the application in a floating body, the formulation is split into 2 solutions based whether the field points are above or below the source point. The obtained formula can be seen in chapter 3.3. *Further Favourable Form*.

Addressing the challenges of numerical hydromechanics analysis for an arbitrary floating body in 3D finite water depth

- Original integral solution of Greens Function (the real wave source term part) need to be rewritten in an exponential form to be computed. The source and field points (center point of the panels) should not be located exactly in the free surface line.
- Alternative form of the Greens Function might improve the computational speed. An infinite series solution with 10^{-6} precision is faster than the integral solution when $R/H \geq 0.05$.
- The convergence rate of the infinite series solution of Greens Function only depends on the ratio of horizontal distance between field and source point (R) and water depth (H).
- Catastrophic cancellation occurs for both solutions in the deep water condition.
- The integral solution fails (singular) for r=0 and R=0 for the infinite series solution. When this is the case, the influence function must be determined based on surface/double integration over the panel.
- Local element and bilinear transformations approaches ensure that any 3-Dimensional function can be integrated over a quadrilateral panel numerically. Without these two transformations, any terms generated in Greens Function for ice-infested waters cannot be calculated when they are singular.

Implementation of Open Water Approach to The Ice-Infested Waters

- There is no singular term present in the solution of Greens Function for ice-infested waters, therefore, the influence of a panel not necessarily need to be integrated over the surface and can be approximated by multiplication with panel area.
- The wave excitation potential need to be re-derived by taking the presence of level ice.

6.2. Future Recommendation

- Further effort to satisfy radiation condition in the formulation of Greens Function for ice-infested waters has to be done.
- Further effort to rewrite the Greens Function in an exponential form might needed to avoid an overflow computation.
- Another alternative form of Greens Function in terms of infinite series solution (or even Chebyshev polynomial/epsilon algorithm) can be derived to improve the computation speed.
- A problem related to finite water depth still occurs. It is wise to derive the Greens Function for the case of infinite water depth as well.

Bibliography

[1] Stegun Irene Abramowitz, Milton , A. *Handbook of Mathematical Functions.*

[2] K. S. Chakrabarti. *The Theory and Practice of Hydrodynamics and Vibration.* .

[3] K. S. Chakrabarti. *Numerical Models in Fluid-Structure Interaction.* .

[4] K. S. Chakrabarti. *Application and Verification of Deepwater Green Function for Water Waves.* Offshore Structure Analysis, Inc., Plainfield, Illinois 60544, 2001.

[5] H.J. de Koning Gans. *Introduction of Numerical Methods in Ship Hydromechanics.* 2012.

[6] H.J. de Koning Gans. *Manual for Experiment of Numerical Methods in Shp Hydromechanics.* 2014.

[7] L. J. Hess and A.M.O. Smith. *Calculation of Non-Lifting Potential Flow About Arbitrary Three-Dimensional Bodies.* Armed Services Technical Information Agency, Arlington 12, Virginia, 1962.

[8] L. J. Hess and A.M.O. Smith. *Calculation of Potential Flow About Arbitrary Bodies.* Progress in Aero. Sci., 1966.

[9] L. J. Hess and A.M.O. Smith. *Calculation of Potential Flow About Arbitrary Three-Dimensional Lifting Bodies.* Douglas Aircraft Company, Long Beach, California, 1972.

[10] F. John. *On The Motion of Floating Bodies, II. Simple Harmonic Motions.*

[11] J.M.J. Journee and W.W. Massie. *Offshore Hydromechanics.* Delft University of Technology, Stevinweg 1, 2628CN, Delft, 2008.

[12] C. Keijdener and A. Metrikine. *Derivation of Green's Function of Infinite, Finite-Depth, Incompressible Fluid Layer Using Cauchy's Theorem.* Delft University of Technology, Stevinweg 1, 2628CN, Delft, 2016.

[13] Sir Horace Lamb. *Hydrodynamics.*

[14] H. Liu, Y. , Iwashita and C. Hu. *A Calculation Method for Finite Depth Free-Surface Green Function.* International Journal Naval Architect and Ocean Engineering, 2015.

[15] N. Newman, J. *Algorithms for the Free-Surface Green Function.* Department of Ocean Engineering, Massachusetts Institute of Technology, Cambridge, MA 02139 USA, 1984.

[16] N. Newman, J. *Distributions of Sources and Normal Dipoles Over a Quadrilateral Panel.* Department of Ocean Engineering, Massachusetts Institute of Technology, Cambridge, MA 02139 USA, 1985.

[17] F. Noblesse. *The Green Function in the Theory of Radiation and Diffraction of Regular Water Waves by a Body.*

[18] C Pozrikidis. *Boundary Integral and Singularity Methods for Linearized Viscous Flow.*

[19] J. Tumblin. *Exact 2-D Integration inside Quadrilateral Boundaries.* Computer Science Department, Northwestern University, Evanston IL 60201.

[20] J.V. Wehausen and E.V. Laitone. *Surface Waves Online.* Regents of the University of California, 2002.

[21] Timothy , Rampal Pierre Williams, D. and Sylvain. Bouillon. *Wave-ice Interaction in the NeXtSIM Sea-Ice Model.*

[22] Ji Xu and Erkan. Oterkus. *A Novel Dynamic Ice-Structure Interaction Model for Ice-Induced Vibration.*

Attachment 1.
EXAMPLE ANSY MECHANICAL APDL COMMAND TO GENERATE THE GEOMETRIC MODEL (RECTANGULAR BARGE)

```
! ansys script file for the ship model
!_____________________________________________________________
FINISH
/clear
/prep7
!_____________________________________________________________
! elements to be used
et,1,shell63                    !used
!_____________________________________________________________
! define ship geometry
*ask,L,ships length,40.0
*ask,B,ships width,15.0
*ask,T,ships draft,6
*ask,thk,plate thickness,0.5
*ask,es,element size,L/20.0
!_____________________________________________________________
! define materials
mp,ex,1,emod                    !linear material property,elastic modulus,call shell, call value
mp,nuxy,1,nxy                   !linear material property,poisson ratio, call shell, call value
!_____________________________________________________________
! set view
/view,all,1,1,1
/vup,all,Z
!_____________________________________________________________
! set up panel
k, 1,L/2,B/2.0,0                !right up front
k, 2,L/2,-B/2.0,0               !left up front
k, 3,-L/2,B/2.0,0               !right up rear
k, 4,-L/2,-B/2.0,0              !left up rear
k, 5,L/2,B/2.0,-T               !right bottom front
k, 6,L/2,-B/2.0,-T              !left bottom front
k, 7,-L/2,B/2.0,-T              !right bottom rear
k, 8,-L/2,-B/2.0,-T             !left bottom rear
!_____________________________________________________________
!  create area's
a,2,1,5,6
aatt,,1                 !associates element attributes,material,set constant
a,1,3,7,5
aatt,,1                 !associates element attributes,material,set constant
a,3,4,8,7
aatt,,1                 !associates element attributes,material,set constant
asel,none               !unselect the full set
a,4,2,6,8
aatt,,1                 !associates element attributes,material,set constant
asel,none                       !unselect the full set
a,6,5,7,8
aatt,,1                 !associates element attributes,material,set constant
asel,none                       !unselect the full set
!_____________________________________________________________
! CREATE MESH
esize,es
!mshape,1,2D
allsel
amesh,all
```

```
!_____________________________________________________________
!  equivalence nodes
nummrg,node,lsp/10000.                    !merge node
NUMMRG,KP,LSP/10000.                      !merge keypoints (will also merge lines, areas, vol)
!_____________________________________________________________
/ESHAPE,1                                 !display elements with shapes determined from the real
constans/section definition
EPLO                                      !Produces an element display of the selected elements
!_____________________________________________________________
CDWRITE,DB,Ship'Model,CDB                 !writes geometry and load database items to a
file, exept solid,Filename,extension
! SET ANALYSIS OPTIONS AND EXECUTE
/OUTPUT,Ship'Model,OUT,,                  !Redirects output file, filename, extension,
location
/OUTPUT,ShipModelOutputNEW,txt
NLIST,,,,COORD
ELIST
KLIST
LLIST
/OUTPUT
! ansys script file for the ship model
!_____________________________________________________________
FINISH
/clear
/prep7
!_____________________________________________________________
! elements to be used
et,1,shell63                              !used
!_____________________________________________________________
! define ship geometry
*ask,L,ships length,40.0
*ask,B,ships width,15.0
*ask,T,ships draft,6
*ask,thk,plate thickness,0.5
*ask,es,element size,L/20.0
!_____________________________________________________________
! define materials
mp,ex,1,emod                              !linear material property,elastic modulus,call shell, call value
mp,nuxy,1,nxy                             !linear material property,poisson ratio, call shell, call value
!_____________________________________________________________
! set view
/view,all,1,1,1
/vup,all,Z
!_____________________________________________________________
! set up panel
k, 1,L/2,B/2.0,0                          !right up front
k, 2,L/2,-B/2.0,0                         !left up front
k, 3,-L/2,B/2.0,0                         !right up rear
k, 4,-L/2,-B/2.0,0                        !left up rear
k, 5,L/2,B/2.0,-T                         !right bottom front
k, 6,L/2,-B/2.0,-T                        !left bottom front
k, 7,-L/2,B/2.0,-T                        !right bottom rear
k, 8,-L/2,-B/2.0,-T                       !left bottom rear
!_____________________________________________________________
!  create area's
a,2,1,5,6
aatt,,1                                   !associates element attributes,material,set constant
```

```
a,1,3,7,5
aatt,,1                          !associates element attributes,material,set constant
a,3,4,8,7
aatt,,1                          !associates element attributes,material,set constant
asel,none                        !unselect the full set
a,4,2,6,8
aatt,,1                          !associates element attributes,material,set constant
asel,none                        !unselect the full set
a,6,5,7,8
aatt,,1                          !associates element attributes,material,set constant
asel,none                        !unselect the full set
!_____________________________________________________________
! CREATE MESH
esize,es
!mshape,1,2D
allsel
amesh,all
!_____________________________________________________________
!  equivalence nodes
nummrg,node,lsp/10000.           !merge node
NUMMRG,KP,LSP/10000.             !merge keypoints (will also merge lines, areas, vol)
!_____________________________________________________________
/ESHAPE,1                        !display elements with shapes determined from the real
constans/section definition
EPLO                             !Produces an element display of the selected elements
!_____________________________________________________________
CDWRITE,DB,Ship'Model,CDB        ! SET ANALYSIS OPTIONS AND EXECUTE
/OUTPUT,ShipModelOutputNEW,txt   !Redirects output file, filename, extension, location
NLIST,,,,COORD
ELIST
KLIST
LLIST
/OUTPUT
```

Attachment 2.
EXAMPLE GEOMETRIC INPUT GENERATED FROM ANSYS (RECTANGULAR BARGE)

LIST ALL SELECTED NODES. DSYS= 0

NODE	X	Y	Z
1	20.0000000000	-7.50000000000	0.00000000000
2	20.0000000000	7.50000000000	0.00000000000
3	20.0000000000	-5.62500000000	0.00000000000
4	20.0000000000	-3.75000000000	0.00000000000
5	20.0000000000	-1.87500000000	0.00000000000
6	20.0000000000	0.00000000000	0.00000000000
7	20.0000000000	1.87500000000	0.00000000000
8	20.0000000000	3.75000000000	0.00000000000
9	20.0000000000	5.62500000000	0.00000000000
10	20.0000000000	7.50000000000	-6.00000000000
11	20.0000000000	7.50000000000	-2.00000000000
12	20.0000000000	7.50000000000	-4.00000000000
13	20.0000000000	-7.50000000000	-6.00000000000
14	20.0000000000	5.62500000000	-6.00000000000
15	20.0000000000	3.75000000000	-6.00000000000
16	20.0000000000	1.87500000000	-6.00000000000
17	20.0000000000	0.00000000000	-6.00000000000
18	20.0000000000	-1.87500000000	-6.00000000000
19	20.0000000000	-3.75000000000	-6.00000000000
20	20.0000000000	-5.62500000000	-6.00000000000

NODE	X	Y	Z
21	20.0000000000	-7.50000000000	-4.00000000000
22	20.0000000000	-7.50000000000	-2.00000000000
23	20.0000000000	-5.62500000000	-2.00000000000
24	20.0000000000	-5.62500000000	-4.00000000000
25	20.0000000000	-3.75000000000	-2.00000000000
26	20.0000000000	-3.75000000000	-4.00000000000
27	20.0000000000	-1.87500000000	-2.00000000000
28	20.0000000000	-1.87500000000	-4.00000000000
29	20.0000000000	0.00000000000	-2.00000000000
30	20.0000000000	0.00000000000	-4.00000000000
31	20.0000000000	1.87500000000	-2.00000000000
32	20.0000000000	1.87500000000	-4.00000000000
33	20.0000000000	3.75000000000	-2.00000000000
34	20.0000000000	3.75000000000	-4.00000000000
35	20.0000000000	5.62500000000	-2.00000000000
36	20.0000000000	5.62500000000	-4.00000000000
37	-20.0000000000	7.50000000000	0.00000000000
38	18.0000000000	7.50000000000	0.00000000000
39	16.0000000000	7.50000000000	0.00000000000
40	14.0000000000	7.50000000000	0.00000000000

NODE	X	Y	Z
41	12.0000000000	7.50000000000	0.00000000000
42	10.0000000000	7.50000000000	0.00000000000
43	8.00000000000	7.50000000000	0.00000000000
44	6.00000000000	7.50000000000	0.00000000000
45	4.00000000000	7.50000000000	0.00000000000
46	2.00000000000	7.50000000000	0.00000000000
47	0.355271367880E-14	7.500000000000	0.00000000000
48	-2.00000000000	7.50000000000	0.00000000000
49	-4.00000000000	7.50000000000	0.00000000000
50	-6.00000000000	7.50000000000	0.00000000000
51	-8.00000000000	7.50000000000	0.00000000000
52	-10.0000000000	7.50000000000	0.00000000000
53	-12.0000000000	7.50000000000	0.00000000000
54	-14.0000000000	7.50000000000	0.00000000000
55	-16.0000000000	7.50000000000	0.00000000000
56	-18.0000000000	7.50000000000	0.00000000000
57	-20.0000000000	7.50000000000	-6.00000000000
58	-20.0000000000	7.50000000000	-2.00000000000
59	-20.0000000000	7.50000000000	-4.00000000000
60	-18.0000000000	7.50000000000	-6.00000000000

NODE	X	Y	Z
61	-16.0000000000	7.50000000000	-6.00000000000
62	-14.0000000000	7.50000000000	-6.00000000000
63	-12.0000000000	7.50000000000	-6.00000000000
64	-10.0000000000	7.50000000000	-6.00000000000
65	-8.00000000000	7.50000000000	-6.00000000000
66	-6.00000000000	7.50000000000	-6.00000000000
67	-4.00000000000	7.50000000000	-6.00000000000
68	-2.00000000000	7.50000000000	-6.00000000000
69	-0.355271367880E-14	7.500000000000	-6.00000000000
70	2.00000000000	7.50000000000	-6.00000000000
71	4.00000000000	7.50000000000	-6.00000000000
72	6.00000000000	7.50000000000	-6.00000000000
73	8.00000000000	7.50000000000	-6.00000000000
74	10.0000000000	7.50000000000	-6.00000000000
75	12.0000000000	7.50000000000	-6.00000000000
76	14.0000000000	7.50000000000	-6.00000000000
77	16.0000000000	7.50000000000	-6.00000000000
78	18.0000000000	7.50000000000	-6.00000000000
79	18.0000000000	7.50000000000	-2.00000000000
80	18.0000000000	7.50000000000	-4.00000000000

NODE	X	Y	Z
81	16.0000000000	7.50000000000	-2.00000000000
82	16.0000000000	7.50000000000	-4.00000000000
83	14.0000000000	7.50000000000	-2.00000000000
84	14.0000000000	7.50000000000	-4.00000000000
85	12.0000000000	7.50000000000	-2.00000000000
86	12.0000000000	7.50000000000	-4.00000000000
87	10.0000000000	7.50000000000	-2.00000000000
88	10.0000000000	7.50000000000	-4.00000000000
89	8.00000000000	7.50000000000	-2.00000000000
90	8.00000000000	7.50000000000	-4.00000000000
91	6.00000000000	7.50000000000	-2.00000000000
92	6.00000000000	7.50000000000	-4.00000000000
93	4.00000000000	7.50000000000	-2.00000000000
94	4.00000000000	7.50000000000	-4.00000000000
95	2.00000000000	7.50000000000	-2.00000000000
96	2.00000000000	7.50000000000	-4.00000000000
97	0.177635683940E-14	7.500000000000	-2.00000000000
98	0.177635683940E-14	7.500000000000	-4.00000000000
99	-2.00000000000	7.50000000000	-2.00000000000
100	-2.00000000000	7.50000000000	-4.00000000000

NODE	X	Y	Z
101	-4.00000000000	7.50000000000	-2.00000000000
102	-4.00000000000	7.50000000000	-4.00000000000
103	-6.00000000000	7.50000000000	-2.00000000000
104	-6.00000000000	7.50000000000	-4.00000000000
105	-8.00000000000	7.50000000000	-2.00000000000
106	-8.00000000000	7.50000000000	-4.00000000000
107	-10.0000000000	7.50000000000	-2.00000000000
108	-10.0000000000	7.50000000000	-4.00000000000
109	-12.0000000000	7.50000000000	-2.00000000000
110	-12.0000000000	7.50000000000	-4.00000000000
111	-14.0000000000	7.50000000000	-2.00000000000
112	-14.0000000000	7.50000000000	-4.00000000000
113	-16.0000000000	7.50000000000	-2.00000000000
114	-16.0000000000	7.50000000000	-4.00000000000
115	-18.0000000000	7.50000000000	-2.00000000000
116	-18.0000000000	7.50000000000	-4.00000000000
117	-20.0000000000	-7.50000000000	0.00000000000
118	-20.0000000000	5.62500000000	0.00000000000
119	-20.0000000000	3.75000000000	0.00000000000
120	-20.0000000000	1.87500000000	0.00000000000

NODE	X	Y	Z
121	-20.0000000000	0.00000000000	0.00000000000
122	-20.0000000000	-1.87500000000	0.00000000000
123	-20.0000000000	-3.75000000000	0.00000000000
124	-20.0000000000	-5.62500000000	0.00000000000
125	-20.0000000000	-7.50000000000	-6.00000000000
126	-20.0000000000	-7.50000000000	-2.00000000000
127	-20.0000000000	-7.50000000000	-4.00000000000
128	-20.0000000000	-5.62500000000	-6.00000000000
129	-20.0000000000	-3.75000000000	-6.00000000000
130	-20.0000000000	-1.87500000000	-6.00000000000
131	-20.0000000000	0.00000000000	-6.00000000000
132	-20.0000000000	1.87500000000	-6.00000000000
133	-20.0000000000	3.75000000000	-6.00000000000
134	-20.0000000000	5.62500000000	-6.00000000000
135	-20.0000000000	5.62500000000	-2.00000000000
136	-20.0000000000	5.62500000000	-4.00000000000
137	-20.0000000000	3.75000000000	-2.00000000000
138	-20.0000000000	3.75000000000	-4.00000000000
139	-20.0000000000	1.87500000000	-2.00000000000
140	-20.0000000000	1.87500000000	-4.00000000000

NODE	X	Y	Z
141	-20.0000000000	0.00000000000	-2.00000000000
142	-20.0000000000	0.00000000000	-4.00000000000
143	-20.0000000000	-1.87500000000	-2.00000000000
144	-20.0000000000	-1.87500000000	-4.00000000000
145	-20.0000000000	-3.75000000000	-2.00000000000

146	-20.0000000000	-3.75000000000	-4.00000000000
147	-20.0000000000	-5.62500000000	-2.00000000000
148	-20.0000000000	-5.62500000000	-4.00000000000
149	-18.0000000000	-7.50000000000	0.00000000000
150	-16.0000000000	-7.50000000000	0.00000000000
151	-14.0000000000	-7.50000000000	0.00000000000
152	-12.0000000000	-7.50000000000	0.00000000000
153	-10.0000000000	-7.50000000000	0.00000000000
154	-8.00000000000	-7.50000000000	0.00000000000
155	-6.00000000000	-7.50000000000	0.00000000000
156	-4.00000000000	-7.50000000000	0.00000000000
157	-2.00000000000	-7.50000000000	0.00000000000
158	-0.355271367880E-14	-7.50000000000	0.00000000000
159	2.00000000000	-7.50000000000	0.00000000000
160	4.00000000000	-7.50000000000	0.00000000000

NODE	X	Y	Z
161	6.00000000000	-7.50000000000	0.00000000000
162	8.00000000000	-7.50000000000	0.00000000000
163	10.0000000000	-7.50000000000	0.00000000000
164	12.0000000000	-7.50000000000	0.00000000000
165	14.0000000000	-7.50000000000	0.00000000000
166	16.0000000000	-7.50000000000	0.00000000000
167	18.0000000000	-7.50000000000	0.00000000000
168	18.0000000000	-7.50000000000	-6.00000000000
169	16.0000000000	-7.50000000000	-6.00000000000
170	14.0000000000	-7.50000000000	-6.00000000000
171	12.0000000000	-7.50000000000	-6.00000000000
172	10.0000000000	-7.50000000000	-6.00000000000
173	8.00000000000	-7.50000000000	-6.00000000000
174	6.00000000000	-7.50000000000	-6.00000000000
175	4.00000000000	-7.50000000000	-6.00000000000
176	2.00000000000	-7.50000000000	-6.00000000000
177	0.355271367880E-14	-7.50000000000	-6.00000000000
178	-2.00000000000	-7.50000000000	-6.00000000000
179	-4.00000000000	-7.50000000000	-6.00000000000
180	-6.00000000000	-7.50000000000	-6.00000000000

NODE	X	Y	Z
181	-8.00000000000	-7.50000000000	-6.00000000000
182	-10.0000000000	-7.50000000000	-6.00000000000
183	-12.0000000000	-7.50000000000	-6.00000000000
184	-14.0000000000	-7.50000000000	-6.00000000000
185	-16.0000000000	-7.50000000000	-6.00000000000
186	-18.0000000000	-7.50000000000	-6.00000000000
187	-18.0000000000	-7.50000000000	-2.00000000000
188	-18.0000000000	-7.50000000000	-4.00000000000
189	-16.0000000000	-7.50000000000	-2.00000000000
190	-16.0000000000	-7.50000000000	-4.00000000000
191	-14.0000000000	-7.50000000000	-2.00000000000
192	-14.0000000000	-7.50000000000	-4.00000000000
193	-12.0000000000	-7.50000000000	-2.00000000000
194	-12.0000000000	-7.50000000000	-4.00000000000
195	-10.0000000000	-7.50000000000	-2.00000000000
196	-10.0000000000	-7.50000000000	-4.00000000000
197	-8.00000000000	-7.50000000000	-2.00000000000
198	-8.00000000000	-7.50000000000	-4.00000000000
199	-6.00000000000	-7.50000000000	-2.00000000000
200	-6.00000000000	-7.50000000000	-4.00000000000

NODE	X	Y	Z
201	-4.00000000000	-7.50000000000	-2.00000000000
202	-4.00000000000	-7.50000000000	-4.00000000000
203	-2.00000000000	-7.50000000000	-2.00000000000
204	-2.00000000000	-7.50000000000	-4.00000000000
205	-0.177635683940E-14	-7.50000000000	-2.00000000000
206	-0.177635683940E-14	-7.50000000000	-4.00000000000
207	2.00000000000	-7.50000000000	-2.00000000000
208	2.00000000000	-7.50000000000	-4.00000000000
209	4.00000000000	-7.50000000000	-2.00000000000
210	4.00000000000	-7.50000000000	-4.00000000000
211	6.00000000000	-7.50000000000	-2.00000000000
212	6.00000000000	-7.50000000000	-4.00000000000
213	8.00000000000	-7.50000000000	-2.00000000000
214	8.00000000000	-7.50000000000	-4.00000000000
215	10.0000000000	-7.50000000000	-2.00000000000
216	10.0000000000	-7.50000000000	-4.00000000000
217	12.0000000000	-7.50000000000	-2.00000000000
218	12.0000000000	-7.50000000000	-4.00000000000
219	14.0000000000	-7.50000000000	-2.00000000000
220	14.0000000000	-7.50000000000	-4.00000000000

NODE	X	Y	Z
221	16.0000000000	-7.50000000000	-2.00000000000
222	16.0000000000	-7.50000000000	-4.00000000000
223	18.0000000000	-7.50000000000	-2.00000000000
224	18.0000000000	-7.50000000000	-4.00000000000
225	18.0000000000	-5.62500000000	-6.00000000000
226	16.0000000000	-5.62500000000	-6.00000000000
227	14.0000000000	-5.62500000000	-6.00000000000
228	12.0000000000	-5.62500000000	-6.00000000000
229	10.0000000000	-5.62500000000	-6.00000000000
230	8.00000000000	-5.62500000000	-6.00000000000
231	6.00000000000	-5.62500000000	-6.00000000000
232	4.00000000000	-5.62500000000	-6.00000000000
233	2.00000000000	-5.62500000000	-6.00000000000
234	0.333066907388E-14	-5.62500000000	-6.00000000000
235	-2.00000000000	-5.62500000000	-6.00000000000
236	-4.00000000000	-5.62500000000	-6.00000000000
237	-6.00000000000	-5.62500000000	-6.00000000000
238	-8.00000000000	-5.62500000000	-6.00000000000
239	-10.0000000000	-5.62500000000	-6.00000000000
240	-12.0000000000	-5.62500000000	-6.00000000000

NODE	X	Y	Z
241	-14.0000000000	-5.62500000000	-6.00000000000
242	-16.0000000000	-5.62500000000	-6.00000000000
243	-18.0000000000	-5.62500000000	-6.00000000000
244	18.0000000000	-3.75000000000	-6.00000000000
245	16.0000000000	-3.75000000000	-6.00000000000
246	14.0000000000	-3.75000000000	-6.00000000000
247	12.0000000000	-3.75000000000	-6.00000000000
248	10.0000000000	-3.75000000000	-6.00000000000
249	8.00000000000	-3.75000000000	-6.00000000000
250	6.00000000000	-3.75000000000	-6.00000000000
251	4.00000000000	-3.75000000000	-6.00000000000
252	2.00000000000	-3.75000000000	-6.00000000000
253	0.00000000000	-3.75000000000	-6.00000000000
254	-2.00000000000	-3.75000000000	-6.00000000000
255	-4.00000000000	-3.75000000000	-6.00000000000
256	-6.00000000000	-3.75000000000	-6.00000000000
257	-8.00000000000	-3.75000000000	-6.00000000000
258	-10.0000000000	-3.75000000000	-6.00000000000
259	-12.0000000000	-3.75000000000	-6.00000000000
260	-14.0000000000	-3.75000000000	-6.00000000000

NODE	X	Y	Z
261	-16.0000000000	-3.75000000000	-6.00000000000
262	-18.0000000000	-3.75000000000	-6.00000000000
263	18.0000000000	-1.87500000000	-6.00000000000
264	16.0000000000	-1.87500000000	-6.00000000000
265	14.0000000000	-1.87500000000	-6.00000000000
266	12.0000000000	-1.87500000000	-6.00000000000
267	10.0000000000	-1.87500000000	-6.00000000000
268	8.00000000000	-1.87500000000	-6.00000000000
269	6.00000000000	-1.87500000000	-6.00000000000
270	4.00000000000	-1.87500000000	-6.00000000000
271	2.00000000000	-1.87500000000	-6.00000000000
272	0.00000000000	-1.87500000000	-6.00000000000
273	-2.00000000000	-1.87500000000	-6.00000000000
274	-4.00000000000	-1.87500000000	-6.00000000000
275	-6.00000000000	-1.87500000000	-6.00000000000
276	-8.00000000000	-1.87500000000	-6.00000000000
277	-10.0000000000	-1.87500000000	-6.00000000000
278	-12.0000000000	-1.87500000000	-6.00000000000
279	-14.0000000000	-1.87500000000	-6.00000000000
280	-16.0000000000	-1.87500000000	-6.00000000000

NODE	X	Y	Z
281	-18.0000000000	-1.87500000000	-6.00000000000
282	18.0000000000	0.00000000000	-6.00000000000
283	16.0000000000	0.00000000000	-6.00000000000
284	14.0000000000	0.00000000000	-6.00000000000
285	12.0000000000	0.00000000000	-6.00000000000
286	10.0000000000	0.00000000000	-6.00000000000
287	8.00000000000	0.00000000000	-6.00000000000
288	6.00000000000	0.00000000000	-6.00000000000
289	4.00000000000	0.00000000000	-6.00000000000
290	2.00000000000	0.00000000000	-6.00000000000
291	0.00000000000	0.00000000000	-6.00000000000
292	-2.00000000000	0.00000000000	-6.00000000000
293	-4.00000000000	0.00000000000	-6.00000000000

294	-6.00000000000	0.00000000000	-6.00000000000
295	-8.00000000000	0.00000000000	-6.00000000000
296	-10.0000000000	0.00000000000	-6.00000000000
297	-12.0000000000	0.00000000000	-6.00000000000
298	-14.0000000000	0.00000000000	-6.00000000000
299	-16.0000000000	0.00000000000	-6.00000000000
300	-18.0000000000	0.00000000000	-6.00000000000

NODE	X	Y	Z
301	18.0000000000	1.87500000000	-6.00000000000
302	16.0000000000	1.87500000000	-6.00000000000
303	14.0000000000	1.87500000000	-6.00000000000
304	12.0000000000	1.87500000000	-6.00000000000
305	10.0000000000	1.87500000000	-6.00000000000
306	8.00000000000	1.87500000000	-6.00000000000
307	6.00000000000	1.87500000000	-6.00000000000
308	4.00000000000	1.87500000000	-6.00000000000
309	2.00000000000	1.87500000000	-6.00000000000
310	0.00000000000	1.87500000000	-6.00000000000
311	-2.00000000000	1.87500000000	-6.00000000000
312	-4.00000000000	1.87500000000	-6.00000000000
313	-6.00000000000	1.87500000000	-6.00000000000
314	-8.00000000000	1.87500000000	-6.00000000000
315	-10.0000000000	1.87500000000	-6.00000000000
316	-12.0000000000	1.87500000000	-6.00000000000
317	-14.0000000000	1.87500000000	-6.00000000000
318	-16.0000000000	1.87500000000	-6.00000000000
319	-18.0000000000	1.87500000000	-6.00000000000
320	18.0000000000	3.75000000000	-6.00000000000

NODE	X	Y	Z
321	16.0000000000	3.75000000000	-6.00000000000
322	14.0000000000	3.75000000000	-6.00000000000
323	12.0000000000	3.75000000000	-6.00000000000
324	10.0000000000	3.75000000000	-6.00000000000
325	8.00000000000	3.75000000000	-6.00000000000
326	6.00000000000	3.75000000000	-6.00000000000
327	4.00000000000	3.75000000000	-6.00000000000
328	2.00000000000	3.75000000000	-6.00000000000
329	-0.355271367880E-14	3.75000000000	-6.00000000000
330	-2.00000000000	3.75000000000	-6.00000000000
331	-4.00000000000	3.75000000000	-6.00000000000
332	-6.00000000000	3.75000000000	-6.00000000000
333	-8.00000000000	3.75000000000	-6.00000000000
334	-10.0000000000	3.75000000000	-6.00000000000
335	-12.0000000000	3.75000000000	-6.00000000000
336	-14.0000000000	3.75000000000	-6.00000000000
337	-16.0000000000	3.75000000000	-6.00000000000
338	-18.0000000000	3.75000000000	-6.00000000000
339	18.0000000000	5.62500000000	-6.00000000000
340	16.0000000000	5.62500000000	-6.00000000000

NODE	X	Y	Z
341	14.0000000000	5.62500000000	-6.00000000000
342	12.0000000000	5.62500000000	-6.00000000000
343	10.0000000000	5.62500000000	-6.00000000000
344	8.00000000000	5.62500000000	-6.00000000000
345	6.00000000000	5.62500000000	-6.00000000000
346	4.00000000000	5.62500000000	-6.00000000000
347	2.00000000000	5.62500000000	-6.00000000000
348	-0.355271367880E-14	5.62500000000	-6.00000000000
349	-2.00000000000	5.62500000000	-6.00000000000
350	-4.00000000000	5.62500000000	-6.00000000000
351	-6.00000000000	5.62500000000	-6.00000000000
352	-8.00000000000	5.62500000000	-6.00000000000
353	-10.0000000000	5.62500000000	-6.00000000000
354	-12.0000000000	5.62500000000	-6.00000000000
355	-14.0000000000	5.62500000000	-6.00000000000
356	-16.0000000000	5.62500000000	-6.00000000000
357	-18.0000000000	5.62500000000	-6.00000000000

LIST ALL SELECTED ELEMENTS. (LIST NODES)

ELEM	MAT	TYP	REL	ESY	SEC	NODES			
1	1	1	1	0	1	1	3	23	22
2	1	1	1	0	1	3	4	25	23
3	1	1	1	0	1	4	5	27	25
4	1	1	1	0	1	5	6	29	27
5	1	1	1	0	1	6	7	31	29
6	1	1	1	0	1	7	8	33	31
7	1	1	1	0	1	8	9	35	33
8	1	1	1	0	1	9	2	11	35
9	1	1	1	0	1	22	23	24	21
10	1	1	1	0	1	23	25	26	24
11	1	1	1	0	1	25	27	28	26
12	1	1	1	0	1	27	29	30	28
13	1	1	1	0	1	29	31	32	30
14	1	1	1	0	1	31	33	34	32
15	1	1	1	0	1	33	35	36	34
16	1	1	1	0	1	35	11	12	36
17	1	1	1	0	1	21	24	20	13
18	1	1	1	0	1	24	26	19	20
19	1	1	1	0	1	26	28	18	19
20	1	1	1	0	1	28	30	17	18

ELEM	MAT	TYP	REL	ESY	SEC	NODES			
21	1	1	1	0	1	30	32	16	17
22	1	1	1	0	1	32	34	15	16
23	1	1	1	0	1	34	36	14	15
24	1	1	1	0	1	36	12	10	14
25	1	1	1	0	1	2	38	79	11
26	1	1	1	0	1	38	39	81	79
27	1	1	1	0	1	39	40	83	81
28	1	1	1	0	1	40	41	85	83
29	1	1	1	0	1	41	42	87	85
30	1	1	1	0	1	42	43	89	87
31	1	1	1	0	1	43	44	91	89
32	1	1	1	0	1	44	45	93	91
33	1	1	1	0	1	45	46	95	93
34	1	1	1	0	1	46	47	97	95
35	1	1	1	0	1	47	48	99	97
36	1	1	1	0	1	48	49	101	99
37	1	1	1	0	1	49	50	103	101
38	1	1	1	0	1	50	51	105	103
39	1	1	1	0	1	51	52	107	105
40	1	1	1	0	1	52	53	109	107

ELEM	MAT	TYP	REL	ESY	SEC	NODES			
41	1	1	1	0	1	53	54	111	109
42	1	1	1	0	1	54	55	113	111
43	1	1	1	0	1	55	56	115	113
44	1	1	1	0	1	56	37	58	115
45	1	1	1	0	1	11	79	80	12
46	1	1	1	0	1	79	81	82	80
47	1	1	1	0	1	81	83	84	82
48	1	1	1	0	1	83	85	86	84
49	1	1	1	0	1	85	87	88	86
50	1	1	1	0	1	87	89	90	88
51	1	1	1	0	1	89	91	92	90
52	1	1	1	0	1	91	93	94	92
53	1	1	1	0	1	93	95	96	94
54	1	1	1	0	1	95	97	98	96
55	1	1	1	0	1	97	99	100	98
56	1	1	1	0	1	99	101	102	100
57	1	1	1	0	1	101	103	104	102
58	1	1	1	0	1	103	105	106	104
59	1	1	1	0	1	105	107	108	106
60	1	1	1	0	1	107	109	110	108

ELEM	MAT	TYP	REL	ESY	SEC	NODES			
61	1	1	1	0	1	109	111	112	110
62	1	1	1	0	1	111	113	114	112
63	1	1	1	0	1	113	115	116	114
64	1	1	1	0	1	115	58	59	116
65	1	1	1	0	1	12	80	78	10
66	1	1	1	0	1	80	82	77	78
67	1	1	1	0	1	82	84	76	77
68	1	1	1	0	1	84	86	75	76
69	1	1	1	0	1	86	88	74	75
70	1	1	1	0	1	88	90	73	74
71	1	1	1	0	1	90	92	72	73
72	1	1	1	0	1	92	94	71	72
73	1	1	1	0	1	94	96	70	71
74	1	1	1	0	1	96	98	69	70
75	1	1	1	0	1	98	100	68	69
76	1	1	1	0	1	100	102	67	68
77	1	1	1	0	1	102	104	66	67
78	1	1	1	0	1	104	106	65	66

79	1	1	1	0	1	106	108	64	65
80	1	1	1	0	1	108	110	63	64

ELEM	MAT	TYP	REL	ESY	SEC	NODES			
81	1	1	1	0	1	110	112	62	63
82	1	1	1	0	1	112	114	61	62
83	1	1	1	0	1	114	116	60	61
84	1	1	1	0	1	116	59	57	60
85	1	1	1	0	1	37	118	135	58
86	1	1	1	0	1	118	119	137	135
87	1	1	1	0	1	119	120	139	137
88	1	1	1	0	1	120	121	141	139
89	1	1	1	0	1	121	122	143	141
90	1	1	1	0	1	122	123	145	143
91	1	1	1	0	1	123	124	147	145
92	1	1	1	0	1	124	117	126	147
93	1	1	1	0	1	58	135	136	59
94	1	1	1	0	1	135	137	138	136
95	1	1	1	0	1	137	139	140	138
96	1	1	1	0	1	139	141	142	140
97	1	1	1	0	1	141	143	144	142
98	1	1	1	0	1	143	145	146	144
99	1	1	1	0	1	145	147	148	146
100	1	1	1	0	1	147	126	127	148

ELEM	MAT	TYP	REL	ESY	SEC	NODES			
101	1	1	1	0	1	59	136	134	57
102	1	1	1	0	1	136	138	133	134
103	1	1	1	0	1	138	140	132	133
104	1	1	1	0	1	140	142	131	132
105	1	1	1	0	1	142	144	130	131
106	1	1	1	0	1	144	146	129	130
107	1	1	1	0	1	146	148	128	129
108	1	1	1	0	1	148	127	125	128
109	1	1	1	0	1	117	149	187	126
110	1	1	1	0	1	149	150	189	187
111	1	1	1	0	1	150	151	191	189
112	1	1	1	0	1	151	152	193	191
113	1	1	1	0	1	152	153	195	193
114	1	1	1	0	1	153	154	197	195
115	1	1	1	0	1	154	155	199	197
116	1	1	1	0	1	155	156	201	199
117	1	1	1	0	1	156	157	203	201
118	1	1	1	0	1	157	158	205	203
119	1	1	1	0	1	158	159	207	205
120	1	1	1	0	1	159	160	209	207

ELEM	MAT	TYP	REL	ESY	SEC	NODES			
121	1	1	1	0	1	160	161	211	209
122	1	1	1	0	1	161	162	213	211
123	1	1	1	0	1	162	163	215	213
124	1	1	1	0	1	163	164	217	215
125	1	1	1	0	1	164	165	219	217
126	1	1	1	0	1	165	166	221	219
127	1	1	1	0	1	166	167	223	221
128	1	1	1	0	1	167	1	22	223
129	1	1	1	0	1	126	187	188	127
130	1	1	1	0	1	187	189	190	188
131	1	1	1	0	1	189	191	192	190
132	1	1	1	0	1	191	193	194	192
133	1	1	1	0	1	193	195	196	194
134	1	1	1	0	1	195	197	198	196
135	1	1	1	0	1	197	199	200	198
136	1	1	1	0	1	199	201	202	200
137	1	1	1	0	1	201	203	204	202
138	1	1	1	0	1	203	205	206	204
139	1	1	1	0	1	205	207	208	206
140	1	1	1	0	1	207	209	210	208

ELEM	MAT	TYP	REL	ESY	SEC	NODES			
141	1	1	1	0	1	209	211	212	210
142	1	1	1	0	1	211	213	214	212
143	1	1	1	0	1	213	215	216	214
144	1	1	1	0	1	215	217	218	216
145	1	1	1	0	1	217	219	220	218
146	1	1	1	0	1	219	221	222	220
147	1	1	1	0	1	221	223	224	222
148	1	1	1	0	1	223	22	21	224
149	1	1	1	0	1	127	188	186	125
150	1	1	1	0	1	188	190	185	186
151	1	1	1	0	1	190	192	184	185
152	1	1	1	0	1	192	194	183	184
153	1	1	1	0	1	194	196	182	183
154	1	1	1	0	1	196	198	181	182
155	1	1	1	0	1	198	200	180	181
156	1	1	1	0	1	200	202	179	180
157	1	1	1	0	1	202	204	178	179
158	1	1	1	0	1	204	206	177	178
159	1	1	1	0	1	206	208	176	177
160	1	1	1	0	1	208	210	175	176

ELEM	MAT	TYP	REL	ESY	SEC	NODES			
161	1	1	1	0	1	210	212	174	175
162	1	1	1	0	1	212	214	173	174
163	1	1	1	0	1	214	216	172	173
164	1	1	1	0	1	216	218	171	172
165	1	1	1	0	1	218	220	170	171
166	1	1	1	0	1	220	222	169	170
167	1	1	1	0	1	222	224	168	169
168	1	1	1	0	1	224	21	13	168
169	1	1	1	0	1	13	20	225	168
170	1	1	1	0	1	20	19	244	225
171	1	1	1	0	1	19	18	263	244
172	1	1	1	0	1	18	17	282	263
173	1	1	1	0	1	17	16	301	282
174	1	1	1	0	1	16	15	320	301
175	1	1	1	0	1	15	14	339	320
176	1	1	1	0	1	14	10	78	339
177	1	1	1	0	1	168	225	226	169
178	1	1	1	0	1	225	244	245	226
179	1	1	1	0	1	244	263	264	245
180	1	1	1	0	1	263	282	283	264

ELEM	MAT	TYP	REL	ESY	SEC	NODES			
181	1	1	1	0	1	282	301	302	283
182	1	1	1	0	1	301	320	321	302
183	1	1	1	0	1	320	339	340	321
184	1	1	1	0	1	339	78	77	340
185	1	1	1	0	1	169	226	227	170
186	1	1	1	0	1	226	245	246	227
187	1	1	1	0	1	245	264	265	246
188	1	1	1	0	1	264	283	284	265
189	1	1	1	0	1	283	302	303	284
190	1	1	1	0	1	302	321	322	303
191	1	1	1	0	1	321	340	341	322
192	1	1	1	0	1	340	77	76	341
193	1	1	1	0	1	170	227	228	171
194	1	1	1	0	1	227	246	247	228
195	1	1	1	0	1	246	265	266	247
196	1	1	1	0	1	265	284	285	266
197	1	1	1	0	1	284	303	304	285
198	1	1	1	0	1	303	322	323	304
199	1	1	1	0	1	322	341	342	323
200	1	1	1	0	1	341	76	75	342

ELEM	MAT	TYP	REL	ESY	SEC	NODES			
201	1	1	1	0	1	171	228	229	172
202	1	1	1	0	1	228	247	248	229
203	1	1	1	0	1	247	266	267	248
204	1	1	1	0	1	266	285	286	267
205	1	1	1	0	1	285	304	305	286
206	1	1	1	0	1	304	323	324	305
207	1	1	1	0	1	323	342	343	324
208	1	1	1	0	1	342	75	74	343
209	1	1	1	0	1	172	229	230	173
210	1	1	1	0	1	229	248	249	230
211	1	1	1	0	1	248	267	268	249
212	1	1	1	0	1	267	286	287	268
213	1	1	1	0	1	286	305	306	287
214	1	1	1	0	1	305	324	325	306
215	1	1	1	0	1	324	343	344	325
216	1	1	1	0	1	343	74	73	344
217	1	1	1	0	1	173	230	231	174
218	1	1	1	0	1	230	249	250	231
219	1	1	1	0	1	249	268	269	250

```
 220  1  1  1  0  1   268  287  288  269

ELEM MAT TYP REL ESY SEC       NODES

 221  1  1  1  0  1   287  306  307  288
 222  1  1  1  0  1   306  325  326  307
 223  1  1  1  0  1   325  344  345  326
 224  1  1  1  0  1   344   73   72  345
 225  1  1  1  0  1   174  231  232  175
 226  1  1  1  0  1   231  250  251  232
 227  1  1  1  0  1   250  269  270  251
 228  1  1  1  0  1   269  288  289  270
 229  1  1  1  0  1   288  307  308  289
 230  1  1  1  0  1   307  326  327  308
 231  1  1  1  0  1   326  345  346  327
 232  1  1  1  0  1   345   72   71  346
 233  1  1  1  0  1   175  232  233  176
 234  1  1  1  0  1   232  251  252  233
 235  1  1  1  0  1   251  270  271  252
 236  1  1  1  0  1   270  289  290  271
 237  1  1  1  0  1   289  308  309  290
 238  1  1  1  0  1   308  327  328  309
 239  1  1  1  0  1   327  346  347  328
 240  1  1  1  0  1   346   71   70  347

ELEM MAT TYP REL ESY SEC       NODES

 241  1  1  1  0  1   176  233  234  177
 242  1  1  1  0  1   233  252  253  234
 243  1  1  1  0  1   252  271  272  253
 244  1  1  1  0  1   271  290  291  272
 245  1  1  1  0  1   290  309  310  291
 246  1  1  1  0  1   309  328  329  310
 247  1  1  1  0  1   328  347  348  329
 248  1  1  1  0  1   347   70   69  348
 249  1  1  1  0  1   177  234  235  178
 250  1  1  1  0  1   234  253  254  235
 251  1  1  1  0  1   253  272  273  254
 252  1  1  1  0  1   272  291  292  273
 253  1  1  1  0  1   291  310  311  292
 254  1  1  1  0  1   310  329  330  311
 255  1  1  1  0  1   329  348  349  330
 256  1  1  1  0  1   348   69   68  349
 257  1  1  1  0  1   178  235  236  179
 258  1  1  1  0  1   235  254  255  236
 259  1  1  1  0  1   254  273  274  255
 260  1  1  1  0  1   273  292  293  274

ELEM MAT TYP REL ESY SEC       NODES

 261  1  1  1  0  1   292  311  312  293
 262  1  1  1  0  1   311  330  331  312
 263  1  1  1  0  1   330  349  350  331
 264  1  1  1  0  1   349   68   67  350
 265  1  1  1  0  1   179  236  237  180
 266  1  1  1  0  1   236  255  256  237
 267  1  1  1  0  1   255  274  275  256
 268  1  1  1  0  1   274  293  294  275
 269  1  1  1  0  1   293  312  313  294
 270  1  1  1  0  1   312  331  332  313
 271  1  1  1  0  1   331  350  351  332
 272  1  1  1  0  1   350   67   66  351
 273  1  1  1  0  1   180  237  238  181
 274  1  1  1  0  1   237  256  257  238
 275  1  1  1  0  1   256  275  276  257
 276  1  1  1  0  1   275  294  295  276
 277  1  1  1  0  1   294  313  314  295
 278  1  1  1  0  1   313  332  333  314
 279  1  1  1  0  1   332  351  352  333
 280  1  1  1  0  1   351   66   65  352

ELEM MAT TYP REL ESY SEC       NODES

 281  1  1  1  0  1   181  238  239  182
 282  1  1  1  0  1   238  257  258  239
 283  1  1  1  0  1   257  276  277  258
 284  1  1  1  0  1   276  295  296  277
 285  1  1  1  0  1   295  314  315  296
 286  1  1  1  0  1   314  333  334  315
 287  1  1  1  0  1   333  352  353  334
 288  1  1  1  0  1   352   65   64  353
 289  1  1  1  0  1   182  239  240  183
 290  1  1  1  0  1   239  258  259  240
 291  1  1  1  0  1   258  277  278  259
 292  1  1  1  0  1   277  296  297  278
 293  1  1  1  0  1   296  315  316  297
 294  1  1  1  0  1   315  334  335  316
 295  1  1  1  0  1   334  353  354  335
 296  1  1  1  0  1   353   64   63  354
 297  1  1  1  0  1   183  240  241  184
 298  1  1  1  0  1   240  259  260  241
 299  1  1  1  0  1   259  278  279  260
 300  1  1  1  0  1   278  297  298  279

 ELEM MAT TYP REL ESY SEC       NODES

 301  1  1  1  0  1   297  316  317  298
 302  1  1  1  0  1   316  335  336  317
 303  1  1  1  0  1   335  354  355  336
 304  1  1  1  0  1   354   63   62  355
 305  1  1  1  0  1   184  241  242  185
 306  1  1  1  0  1   241  260  261  242
 307  1  1  1  0  1   260  279  280  261
 308  1  1  1  0  1   279  298  299  280
 309  1  1  1  0  1   298  317  318  299
 310  1  1  1  0  1   317  336  337  318
 311  1  1  1  0  1   336  355  356  337
 312  1  1  1  0  1   355   62   61  356
 313  1  1  1  0  1   185  242  243  186
 314  1  1  1  0  1   242  261  262  243
 315  1  1  1  0  1   261  280  281  262
 316  1  1  1  0  1   280  299  300  281
 317  1  1  1  0  1   299  318  319  300
 318  1  1  1  0  1   318  337  338  319
 319  1  1  1  0  1   337  356  357  338
 320  1  1  1  0  1   356   61   60  357

 ELEM MAT TYP REL ESY SEC       NODES

 321  1  1  1  0  1   186  243  128  125
 322  1  1  1  0  1   243  262  129  128
 323  1  1  1  0  1   262  281  130  129
 324  1  1  1  0  1   281  300  131  130
 325  1  1  1  0  1   300  319  132  131
 326  1  1  1  0  1   319  338  133  132
 327  1  1  1  0  1   338  357  134  133
 328  1  1  1  0  1   357   60   57  134

 LIST ALL SELECTED KEYPOINTS.  DSYS=     0

   NO. X,Y,Z LOCATION              KESIZE    NODE  ELEM MAT REAL TYP
ESYS
    1  20.0     7.50     0.00     0.00      2    0  0   0  0   0
    2  20.0    -7.50     0.00     0.00      1    0  0   0  0   0
    3 -20.0     7.50     0.00     0.00     37    0  0   0  0   0
    4 -20.0    -7.50     0.00     0.00    117    0  0   0  0   0
    5  20.0     7.50    -6.00     0.00     10    0  0   0  0   0
    6  20.0    -7.50    -6.00     0.00     13    0  0   0  0   0
    7 -20.0     7.50    -6.00     0.00     57    0  0   0  0   0
    8 -20.0    -7.50    -6.00     0.00    125    0  0   0  0   0

 LIST ALL SELECTED LINES.

 NUMBER    KEYPOINTS    LENGTH   (NDIV)(SPACE) KYND NDIV  SPACE
#NODE #ELEM   MAT  REAL  TYP  ESYS
    1    2    1 15.00       0  1.000   0   8  1.000    7    0    0    0    0    0
    2    1    5  6.000      0  1.000   0   3  1.000    2    0    0    0    0    0
    3    5    6 15.00       0  1.000   0   8  1.000    7    0    0    0    0    0
    4    6    2  6.000      0  1.000   0   3  1.000    2    0    0    0    0    0
    5    1    3 40.00       0  1.000   0  20  1.000   19    0    0    0    0
0
    6    3    7  6.000      0  1.000   0   3  1.000    2    0    0    0    0    0
    7    7    5 40.00       0  1.000   0  20  1.000   19    0    0    0    0
0
    8    3    4 15.00       0  1.000   0   8  1.000    7    0    0    0    0    0
    9    4    8  6.000      0  1.000   0   3  1.000    2    0    0    0    0    0
   10    8    7 15.00       0  1.000   0   8  1.000    7    0    0    0    0    0
   11    4    2 40.00       0  1.000   0  20  1.000   19    0    0    0    0
0
   12    6    8 40.00       0  1.000   0  20  1.000   19    0    0    0    0
0
```

Attachment 3.
EXAMPLE GEOMETRIC INPUT GENERATED IN INTERNATIONAL MARINE SOFTWARE ASSOCIATE FORMAT (SPHERE)

$ENTITY
MESH
$VESSEL NAME
prct_try
$DATA SOURCE
Del*2idf
$DATE
07/08/02
$TIME
13:33:12
$UNITS
SI
$COORDINATE SYSTEM
1,-1,-1
$COMMENTS
TITLE = " project: nmsh "
$GEOMETRY
2
$PART
wet_srf
30, 16
-225,2.7555e-14,-0
-225,2.7404e-14,-2.8802e-15
-225,2.6952e-14,-5.7289e-15
-225,2.6206e-14,-8.5148e-15
-225,2.5172e-14,-1.1207e-14
-225,2.3863e-14,-1.3777e-14
-225,2.2292e-14,-1.6196e-14
-225,2.0477e-14,-1.8438e-14
-225,1.8438e-14,-2.0477e-14
-225,1.6196e-14,-2.2292e-14
-225,1.3777e-14,-2.3863e-14
-225,1.1207e-14,-2.5172e-14
-225,8.5148e-15,-2.6206e-14
-225,5.7289e-15,-2.6952e-14
-225,2.8802e-15,-2.7404e-14
-225,7.8056e-30,-2.7555e-14
-223.68,24.327,-0
-223.68,24.194,-2.5428
-223.68,23.795,-5.0578
-223.68,23.136,-7.5174
-223.68,22.224,-9.8946
-223.68,21.068,-12.163
-223.68,19.681,-14.299
-223.68,18.078,-16.278
-223.68,16.278,-18.078
-223.68,14.299,-19.681
-223.68,12.163,-21.068
-223.68,9.8946,-22.224
-223.68,7.5174,-23.136
-223.68,5.0578,-23.795
-223.68,2.5428,-24.194
-223.68,6.8912e-15,-24.327
-219.74,48.368,-0
-219.74,48.103,-5.0559
-219.74,47.311,-10.056
-219.74,46.001,-14.947
-219.74,44.187,-19.673
-219.74,41.888,-24.184
-219.74,39.131,-28.43
-219.74,35.945,-32.365
-219.74,32.365,-35.945
-219.74,28.43,-39.131
-219.74,24.184,-41.888
-219.74,19.673,-44.187
-219.74,14.947,-46.001
-219.74,10.056,-47.311
-219.74,5.0559,-48.103
-219.74,1.3702e-14,-48.368
-213.22,71.843,-0
-213.22,71.449,-7.5096
-213.22,70.273,-14.937
-213.22,68.327,-22.201
-213.22,65.632,-29.221
-213.22,62.218,-35.921
-213.22,58.122,-42.228
-213.22,53.39,-48.072
-213.22,48.072,-53.39
-213.22,42.228,-58.122
-213.22,35.921,-62.218
-213.22,29.221,-65.632
-213.22,22.201,-68.327
-213.22,14.937,-70.273
-213.22,7.5096,-71.449
-213.22,2.0351e-14,-71.843
-204.2,94.475,-0
-204.2,93.958,-9.8753
-204.2,92.411,-19.642
-204.2,89.851,-29.194
-204.2,86.307,-38.426
-204.2,81.818,-47.238
-204.2,76.432,-55.531
-204.2,70.209,-63.216
-204.2,63.216,-70.209
-204.2,55.531,-76.432
-204.2,47.238,-81.818
-204.2,38.426,-86.307
-204.2,29.194,-89.851
-204.2,19.642,-92.411
-204.2,9.8753,-93.958
-204.2,2.6763e-14,-94.475
-192.79,116,-0
-192.79,115.36,-12.125
-192.79,113.46,-24.118
-192.79,110.32,-35.846
-192.79,105.97,-47.181
-192.79,100.46,-58
-192.79,93.846,-68.183
-192.79,86.205,-77.619
-192.79,77.619,-86.205
-192.79,68.183,-93.846
-192.79,58,-100.46
-192.79,47.181,-105.97
-192.79,35.846,-110.32
-192.79,24.118,-113.46
-192.79,12.125,-115.36
-192.79,3.286e-14,-116
-179.12,136.16,-0
-179.12,135.42,-14.233
-179.12,133.19,-28.31
-179.12,129.5,-42.077
-179.12,124.39,-55.383
-179.12,117.92,-68.082
-179.12,110.16,-80.035
-179.12,101.19,-91.112
-179.12,91.112,-101.19
-179.12,80.035,-110.16
-179.12,68.082,-117.92
-179.12,55.383,-124.39
-179.12,42.077,-129.5
-179.12,28.31,-133.19
-179.12,14.233,-135.42
-179.12,3.8572e-14,-136.16
-163.35,154.73,-0
-163.35,153.88,-16.174
-163.35,151.35,-32.171
-163.35,147.16,-47.815
-163.35,141.36,-62.935
-163.35,134,-77.366
-163.35,125.18,-90.949
-163.35,114.99,-103.54
-163.35,103.54,-114.99
-163.35,90.949,-125.18
-163.35,77.366,-134
-163.35,62.935,-141.36
-163.35,47.815,-147.16
-163.35,32.171,-151.35
-163.35,16.174,-153.88
-163.35,4.3832e-14,-154.73
-145.66,171.49,-0
-145.66,170.55,-17.925
-145.66,167.74,-35.654
-145.66,163.09,-52.992
-145.66,156.66,-69.75
-145.66,148.51,-85.743
-145.66,138.74,-100.8
-145.66,127.44,-114.75
-145.66,114.75,-127.44
-145.66,100.8,-138.74
-145.66,85.743,-148.51
-145.66,69.75,-156.66
-145.66,52.992,-163.09

-145.66,35.654,-167.74
-145.66,17.925,-170.55
-145.66,4.8578e-14,-171.49
-126.27,186.23,-0
-126.27,185.21,-19.466
-126.27,182.16,-38.719
-126.27,177.12,-57.548
-126.27,170.13,-75.747
-126.27,161.28,-93.115
-126.27,150.66,-109.46
-126.27,138.4,-124.61
-126.27,124.61,-138.4
-126.27,109.46,-150.66
-126.27,93.115,-161.28
-126.27,75.747,-170.13
-126.27,57.548,-177.12
-126.27,38.719,-182.16
-126.27,19.466,-185.21
-126.27,5.2755e-14,-186.23
-105.39,198.79,-0
-105.39,197.7,-20.779
-105.39,194.45,-41.331
-105.39,189.06,-61.43
-105.39,181.6,-80.855
-105.39,172.16,-99.395
-105.39,160.82,-116.85
-105.39,147.73,-133.02
-105.39,133.02,-147.73
-105.39,116.85,-160.82
-105.39,99.395,-172.16
-105.39,80.855,-181.6
-105.39,61.43,-189.06
-105.39,41.331,-194.45
-105.39,20.779,-197.7
-105.39,5.6313e-14,-198.79
-83.281,209.02,-0
-83.281,207.87,-21.849
-83.281,204.45,-43.458
-83.281,198.79,-64.591
-83.281,190.95,-85.016
-83.281,181.02,-104.51
-83.281,169.1,-122.86
-83.281,155.33,-139.86
-83.281,139.86,-155.33
-83.281,122.86,-169.1
-83.281,104.51,-181.02
-83.281,85.016,-190.95
-83.281,64.591,-198.79
-83.281,43.458,-204.45
-83.281,21.849,-207.87
-83.281,5.921e-14,-209.02
-60.194,216.8,-0
-60.194,215.61,-22.662
-60.194,212.06,-45.075
-60.194,206.19,-66.994
-60.194,198.06,-88.18
-60.194,187.75,-108.4
-60.194,175.39,-127.43
-60.194,161.11,-145.07
-60.194,145.07,-161.11
-60.194,127.43,-175.39
-60.194,108.4,-187.75
-60.194,88.18,-198.06
-60.194,66.994,-206.19
-60.194,45.075,-212.06
-60.194,22.662,-215.61
-60.194,6.1414e-14,-216.8
-36.401,222.04,-0
-36.401,220.82,-23.209
-36.401,217.18,-46.164
-36.401,211.17,-68.613
-36.401,202.84,-90.31
-36.401,192.29,-111.02
-36.401,179.63,-130.51
-36.401,165,-148.57
-36.401,148.57,-165
-36.401,130.51,-179.63
-36.401,111.02,-192.29
-36.401,90.31,-202.84
-36.401,68.613,-211.17
-36.401,46.164,-217.18
-36.401,23.209,-220.82
-36.401,6.2898e-14,-222.04
-12.181,224.67,-0
-12.181,223.44,-23.484
-12.181,219.76,-46.712
-12.181,213.67,-69.427
-12.181,205.25,-91.382
-12.181,194.57,-112.34
-12.181,181.76,-132.06
-12.181,166.96,-150.33
-12.181,150.33,-166.96
-12.181,132.06,-181.76
-12.181,112.34,-194.57
-12.181,91.382,-205.25
-12.181,69.427,-213.67
-12.181,46.712,-219.76
-12.181,23.484,-223.44
-12.181,6.3644e-14,-224.67
12.181,224.67,-0
12.181,223.44,-23.484
12.181,219.76,-46.712
12.181,213.67,-69.427
12.181,205.25,-91.382
12.181,194.57,-112.34
12.181,181.76,-132.06
12.181,166.96,-150.33
12.181,150.33,-166.96
12.181,132.06,-181.76
12.181,112.34,-194.57
12.181,91.382,-205.25
12.181,69.427,-213.67
12.181,46.712,-219.76
12.181,23.484,-223.44
12.181,6.3644e-14,-224.67
36.401,222.04,-0
36.401,220.82,-23.209
36.401,217.18,-46.164
36.401,211.17,-68.613
36.401,202.84,-90.31
36.401,192.29,-111.02
36.401,179.63,-130.51
36.401,165,-148.57
36.401,148.57,-165
36.401,130.51,-179.63
36.401,111.02,-192.29
36.401,90.31,-202.84
36.401,68.613,-211.17
36.401,46.164,-217.18
36.401,23.209,-220.82
36.401,6.2898e-14,-222.04
60.194,216.8,-0
60.194,215.61,-22.662
60.194,212.06,-45.075
60.194,206.19,-66.994
60.194,198.06,-88.18
60.194,187.75,-108.4
60.194,175.39,-127.43
60.194,161.11,-145.07
60.194,145.07,-161.11
60.194,127.43,-175.39
60.194,108.4,-187.75
60.194,88.18,-198.06
60.194,66.994,-206.19
60.194,45.075,-212.06
60.194,22.662,-215.61
60.194,6.1414e-14,-216.8
83.281,209.02,-0
83.281,207.87,-21.849
83.281,204.45,-43.458
83.281,198.79,-64.591
83.281,190.95,-85.016
83.281,181.02,-104.51
83.281,169.1,-122.86
83.281,155.33,-139.86
83.281,139.86,-155.33
83.281,122.86,-169.1
83.281,104.51,-181.02
83.281,85.016,-190.95
83.281,64.591,-198.79
83.281,43.458,-204.45
83.281,21.849,-207.87

83.281,5.921e-14,-209.02
105.39,198.79,-0
105.39,197.7,-20.779
105.39,194.45,-41.331
105.39,189.06,-61.43
105.39,181.6,-80.855
105.39,172.16,-99.395
105.39,160.82,-116.85
105.39,147.73,-133.02
105.39,133.02,-147.73
105.39,116.85,-160.82
105.39,99.395,-172.16
105.39,80.855,-181.6
105.39,61.43,-189.06
105.39,41.331,-194.45
105.39,20.779,-197.7
105.39,5.6313e-14,-198.79
126.27,186.23,-0
126.27,185.21,-19.466
126.27,182.16,-38.719
126.27,177.12,-57.548
126.27,170.13,-75.747
126.27,161.28,-93.115
126.27,150.66,-109.46
126.27,138.4,-124.61
126.27,124.61,-138.4
126.27,109.46,-150.66
126.27,93.115,-161.28
126.27,75.747,-170.13
126.27,57.548,-177.12
126.27,38.719,-182.16
126.27,19.466,-185.21
126.27,5.2755e-14,-186.23
145.66,171.49,-0
145.66,170.55,-17.925
145.66,167.74,-35.654
145.66,163.09,-52.992
145.66,156.66,-69.75
145.66,148.51,-85.743
145.66,138.74,-100.8
145.66,127.44,-114.75
145.66,114.75,-127.44
145.66,100.8,-138.74
145.66,85.743,-148.51
145.66,69.75,-156.66
145.66,52.992,-163.09
145.66,35.654,-167.74
145.66,17.925,-170.55
145.66,4.8578e-14,-171.49
163.35,154.73,-0
163.35,153.88,-16.174
163.35,151.35,-32.171
163.35,147.16,-47.815
163.35,141.36,-62.935
163.35,134,-77.366
163.35,125.18,-90.949
163.35,114.99,-103.54
163.35,103.54,-114.99
163.35,90.949,-125.18
163.35,77.366,-134
163.35,62.935,-141.36
163.35,47.815,-147.16
163.35,32.171,-151.35
163.35,16.174,-153.88
163.35,4.3832e-14,-154.73
179.12,136.16,-0
179.12,135.42,-14.233
179.12,133.19,-28.31
179.12,129.5,-42.077
179.12,124.39,-55.383
179.12,117.92,-68.082
179.12,110.16,-80.035
179.12,101.19,-91.112
179.12,91.112,-101.19
179.12,80.035,-110.16
179.12,68.082,-117.92
179.12,55.383,-124.39
179.12,42.077,-129.5
179.12,28.31,-133.19
179.12,14.233,-135.42
179.12,3.8572e-14,-136.16
192.79,116,-0
192.79,115.36,-12.125
192.79,113.46,-24.118
192.79,110.32,-35.846
192.79,105.97,-47.181
192.79,100.46,-58
192.79,93.846,-68.183
192.79,86.205,-77.619
192.79,77.619,-86.205
192.79,68.183,-93.846
192.79,58,-100.46
192.79,47.181,-105.97
192.79,35.846,-110.32
192.79,24.118,-113.46
192.79,12.125,-115.36
192.79,3.286e-14,-116
204.2,94.475,-0
204.2,93.958,-9.8753
204.2,92.411,-19.642
204.2,89.851,-29.194
204.2,86.307,-38.426
204.2,81.818,-47.238
204.2,76.432,-55.531
204.2,70.209,-63.216
204.2,63.216,-70.209
204.2,55.531,-76.432
204.2,47.238,-81.818
204.2,38.426,-86.307
204.2,29.194,-89.851
204.2,19.642,-92.411
204.2,9.8753,-93.958
204.2,2.6763e-14,-94.475
213.22,71.843,-0
213.22,71.449,-7.5096
213.22,70.273,-14.937
213.22,68.327,-22.201
213.22,65.632,-29.221
213.22,62.218,-35.921
213.22,58.122,-42.228
213.22,53.39,-48.072
213.22,48.072,-53.39
213.22,42.228,-58.122
213.22,35.921,-62.218
213.22,29.221,-65.632
213.22,22.201,-68.327
213.22,14.937,-70.273
213.22,7.5096,-71.449
213.22,2.0351e-14,-71.843
219.74,48.368,-0
219.74,48.103,-5.0559
219.74,47.311,-10.056
219.74,46.001,-14.947
219.74,44.187,-19.673
219.74,41.888,-24.184
219.74,39.131,-28.43
219.74,35.945,-32.365
219.74,32.365,-35.945
219.74,28.43,-39.131
219.74,24.184,-41.888
219.74,19.673,-44.187
219.74,14.947,-46.001
219.74,10.056,-47.311
219.74,5.0559,-48.103
219.74,1.3702e-14,-48.368
223.68,24.327,-0
223.68,24.194,-2.5428
223.68,23.795,-5.0578
223.68,23.136,-7.5174
223.68,22.224,-9.8946
223.68,21.068,-12.163
223.68,19.681,-14.299
223.68,18.078,-16.278
223.68,16.278,-18.078
223.68,14.299,-19.681
223.68,12.163,-21.068
223.68,9.8946,-22.224
223.68,7.5174,-23.136
223.68,5.0578,-23.795
223.68,2.5428,-24.194
223.68,6.8912e-15,-24.327
225,2.7555e-14,-0

225,2.7404e-14,-2.8802e-15
225,2.6952e-14,-5.7289e-15
225,2.6206e-14,-8.5148e-15
225,2.5172e-14,-1.1207e-14
225,2.3863e-14,-1.3777e-14
225,2.2292e-14,-1.6196e-14
225,2.0477e-14,-1.8438e-14
225,1.8438e-14,-2.0477e-14
225,1.6196e-14,-2.2292e-14
225,1.3777e-14,-2.3863e-14
225,1.1207e-14,-2.5172e-14
225,8.5148e-15,-2.6206e-14
225,5.7289e-15,-2.6952e-14
225,2.8802e-15,-2.7404e-14
225,7.8056e-30,-2.7555e-14
$END ENTITY